CHEMICAL PETROLOGY OF POLYMETAMORPHIC ULTRAMAFIC ROCKS FROM GALICIA, NW SPAIN

BY

P. MAASKANT

ABSTRACT

The investigated polymetamorphic peridotites occur associated with metabasic rocks in several complexes of probably Precambrian age in the northern part of the Hesperian massif (Iberian peninsula).

Spinel-clinopyroxene-, spinel-pargasite-, spinel-hornblende- and chlorite-amphibole-peridotites, wehrlites, spinel-amphibole- and plagioclase wehrlites are found; most rocks are partly to completely serpentinized. Attention has been paid particularly to the two first-mentioned catazonal types in which bands, veins and lenses of garnet ± spinel pyroxenite and -pargasitite occur, while brown ceylonite orthopyroxenite and spinel-sensu-stricto clinopyroxenite are present in subordinate amounts.

It is contended that these pyroxenites and pargasitites represent partial melting products of a parental ultramafic rock which contention is corroborated by experimental evidence. The partial melt had a picritic composition and crystallized as an aluminous pyroxene assemblage, in which garnet was formed under subsolidus conditions. Comparisons are drawn with peridotites from other occurrences in which garnet-bearing assemblages are also encountered. It is assumed that these peridotites were emplaced as spinel-clinopyroxene peridotites (lherzolites) during a Precambrian orogenic cycle under high-pressure granulite-facies conditions and equilibrated at 1100°–1200 °C under 15–20 kb pressure. Catazonal retrogradation (800°–900 °C, 10–15 kb pressure) gave rise to large-scale development of pargasite. Garnet probably metastably coexisted with pargasite and the zonary character in the garnets was presumably obtained during this phase. Aluminous chlorite was formed during the Hercynian orogeny under mesozonal conditions; a second generation of pyroxenes and amphiboles possesses lower contents of Al_2O_3.

The spinel-hornblende peridotite probably did not undergo high-pressure granulite-facies conditions during the Precambrian orogeny.

The chlorite-amphibole peridotite is supposed to have a lower Paleozoic age.

The wehrlites are considered to be partial melting products of a parental peridotite and crystallized under low pressures. Spinel-amphibole wehrlites are hydrated plagioclase wehrlites.

New whole-rock analyses of 11 peridotites and 14 pyroxenites are given. Contents of some minor and some trace elements have been determined with neutron activation analysis. Electron microprobe analyses are presented of olivines, pyroxenes, amphiboles, garnets, spinels, chlorites, högbomites and ilmenites. The mineral compositions are compared to whole-rock chemistry and distribution coefficients are calculated from which temperature and pressure estimates are derived.

SUMARIO

Las peridotitas polimetamórficas examinadas en ésta investigación se encuentran asociadas con rocas metabásicas en varios complejos de edad probablemente precámbrica en el norte del macizo hespérico (Península Ibérica).

Se encuentran allí peridotitas de espinela y clinopiroxena, de espinela y pargasita, de espinela y hornblenda y de clorita y anfíbol, wehrlitas, wehrlitas de espinela y anfíbol y wehrlitas de plagioclasa. La mayor parte de las rocas están parcialmente o completamente serpentinizadas.

La mayór atención ha sido prestado a los dos primeros tipos catazonales mencionados arriba en los que figuran láminas, venas y lentes de piroxenitas y pargasititas de granate ± espinela; ortopiroxenita de ceylonita marrón y clinopiroxenita de espinela (sensu-stricto) figuran en cantidades subordinadas.

El autor sostiene que, conforme los resultados experimentales, estas piroxenitas y pargasititas representan los productos parcialmente fundidos de una roca ultramáfica del manto. El componente fundido tenía una composición picrítica y se cristalizó como un conjunto de piroxena aluminosa en lo que se formó granate bajo condiciones subsólidas. Se compara estas rocas con peridotitas encontradas en otras regiones en las que se encuentran también conjuntos con granate.

Se supone que estas peridotitas fueron introducidas como peridotitas de espinela y clinopiroxena (lherzolitas) durante un ciclo orogénico precámbrico bajo condiciones de la facies granulítica de alta presión y se equilibraron a 1100°–1200 °C y bajo una presión de 15–20 kb. Una retrogradación catazonal (800°–900 °C, 10–15 kb) provocó un importante desarrollo de pargasita. El granate probablemente coexistió en estado metaestable con pargasita y obtuvó su caracter zonal durante esta fase. Clorita aluminosa se formó durante la orogenia hercínica bajo condiciones mesozonales; una segunda generación de piroxenas y anfíbolas contiene menos Al_2O_3.

La peridotita de espinela y hornblenda probablemente no fué sometida a condiciones de la facies granulítica de alta presión durante la orogenia precámbrica.

Se supone que la peridotita de clorita y anfíbol es de edad paleozóica inferior.

Se consideran las wehrlitas como los productos de la fusión parcial de peridotita del manto que han cristalizado a baja presión. Las wehrlitas de espinela y anfíbol representan wehrlitas de plagioclasa hidratadas.

Se facilitan los análisis químicos de 11 peridotitas y 14 piroxenitas. Se han determinado cantidades de unos elementos menores y escasos con análisis de (neutro) activación. Se proporciona análisis de microsonda de olivinas, piroxenas, anfíbolas, granates, espinelas, cloritas, högbomitas y ilmenitas.
Se comparan las composiciones de algunos de estos minerales con la química de sus rocas y se calculan los coeficientes de distribución que permiten la determinación de la temperatura y la presión de (re)cristalización.

CONTENTS

CHAPTER I

INTRODUCTION

SCOPE

In this study the chemical approach has been applied to the petrology of the polymetamorphic ultramafic rocks of the Galician basement. With the aid of many analyses minerals and rocks are mutually compared, distribution coefficients between coexisting phases are calculated in order to use them as geothermometers, stability ranges of some minerals are suggested and

events noted in the rocks are compared with those in the country rocks. A model for the evolution of the ultramafic rocks is proposed.

GEOLOGICAL SETTING

The polymetamorphic ultramafic rocks belong to the crystalline basement of Western Galicia. Here, in the axial geanticlinal zone of the Hercynian orogen of the Iberian peninsula, Precambrian formations comprising graywackes and apparently ophiolitic rock suites occur as distinct tectonic units, probably upthrusted through their Paleozoic cover. These rock complexes were subjected to a pre-Hercynian high-pressure type of regional metamorphism quite distinct from its Hercynian low to intermediate counterpart. They occur as massifs of rounded or elliptical outline, more or less aligned in a sinuous belt surrounding the so-called Ordenes basin, and – separated from this by a fundamental fault – also at Cabo Ortegal (Parga-Pondal, 1956; Koning, 1966; den Tex, 1966; Vogel, 1967; Warnaars, 1967; van Zuuren, 1969).

The samples studied are derived from Cabo Ortegal and from several parts in the periphery of the Ordenes basin. These parts, for convenience, will be named the Mellid, Santiago and Castriz areas (Fig. I-1). The rocks occur in terrain studied by staff and graduate students of the Department of Petrology, Leyden University, and the reader is referred to their work for more detailed regional data. Only the most important features of the country rocks will be briefly reviewed here.

Cabo Ortegal (cf. Vogel, 1967)

Three large and several small ultramafic outcrops – probably all part of an originally single flat-lenticular body – occur in a recycled Precambrian, predominantly mafic rock complex. The ultramafites are conformably situated below predominantly felsic gneisses and granulites and above a massive body of banded mafic rocks which during a Precambrian orogenic phase underwent high-pressure granulite facies metamorphism yielding garnet + clinopyroxene + plagioclase assemblages (Vogel's (plagio) pyrigarnites). Partial anatexis occurred in catazonally metamorphosed felsic and mafic rocks while kyanite + zoisite + almandine ± biotite associations segregated in the restites. In the eastern part of the complex eclogites are found in a strongly tectonized and migmatic banded gneiss formation. Evidence of large-scale recumbent folding is available in all Precambrian rock types. In the upper parts of the sequence mesozonal conditions prevailed: staurolite-almandine associations are found in felsic gneisses while their mafic inclusions have been changed into amphibolites. According to Vogel catazonal retrogradation in the hornblende-clinopyroxene-almandine subfacies occurred during a second Precambrian phase, closely related to the injection of pegmatoid matter. Evidence of this phase is found in the appearance of greenish-brown hornblende in mafic assemblages.

Almandine-amphibolite-facies conditions (kyanite-almandine-muscovite subfacies) prevailed during the Hercynian orogeny, by which the mafic rocks were locally amphibolitized. Apart from renewed folding the most intense tectonization occurred along the western and eastern contacts of the complex where it has been thrust upon lower metamorphic Paleozoic rocks with the development of amphibolite to greenschist facies mylonites.

At the close of the Hercynian orogeny abundant hydrothermal activity occurred.

Mellid area (van Scherpenzeel, 1969; Hubregtse, 1970)

In the southeastern periphery of the Ordenes basin a predominantly mafic and ultramafic rock complex is found, which may be divided into a catazonal and a mesozonal part.

In the catazonal sector – the western part of the complex, nearest to the village of Mellid – a thin sheet of ultramafites lies upon pyrigarnites which underwent possibly catazonal and mesozonal retrogradation resulting in amphibolization of clinopyroxene, breakdown of garnet and formation of, e.g., plagioclase and chlorite. In some hornblende plagiopyrigarnites clinopyroxene and garnet stably coexist, while brownish amphibole also belongs to the primary catazonal assemblage, in which higher water pressures and probably lower temperatures prevailed. In paragranulites, found in minor amounts below the pyrigarnites, the catazonal character may be deduced from the alkalifeldspar + garnet ± kyanite association. Biotite, enclosed in garnet and kyanite, forms an integral part of the paragenesis and points to relatively high water pressures during crystallization.

In the meso-epizonal part of the complex chlorite-amphibole peridotites lie upon mafic albite-epidote-amphibolite-facies rocks. Epidote and zoisite amphibolites, amphibolitized metagabbros and younger porphyritic metadolerites are found. The instability of plagioclase and the development of chlorite are epizonal phenomena.

Recumbent folding is found only in the catazonal part of the complex (Plate Ib), while steep open folding is encountered in both parts, having been superimposed on the recumbent folds of the catazonal rocks. Catazonal metamorphic conditions prevailed during a Precambrian orogenic cycle and epi- and mesozonal conditions during a Hercynian cycle. The meso-epizonal part of the complex probably represents an ophiolitic suite of lower Paleozoic age.

Santiago area (van Zuuren, 1969)

In the southwestern rim of the Ordenes basin partially migmatized metasediments (kyanite-almandine- muscovite subfacies) are encountered. In the mafic rocks of this complex – the lower parts of the sequence – one small ultramafic body occurs. Evidence of granulite-facies conditions (hornblende-clinopyroxene-almandine subfacies) is only sparsely found in retrograded plagiopyrigarnites. The majority of the mafic rocks probably underwent no more than almandine-amphi-
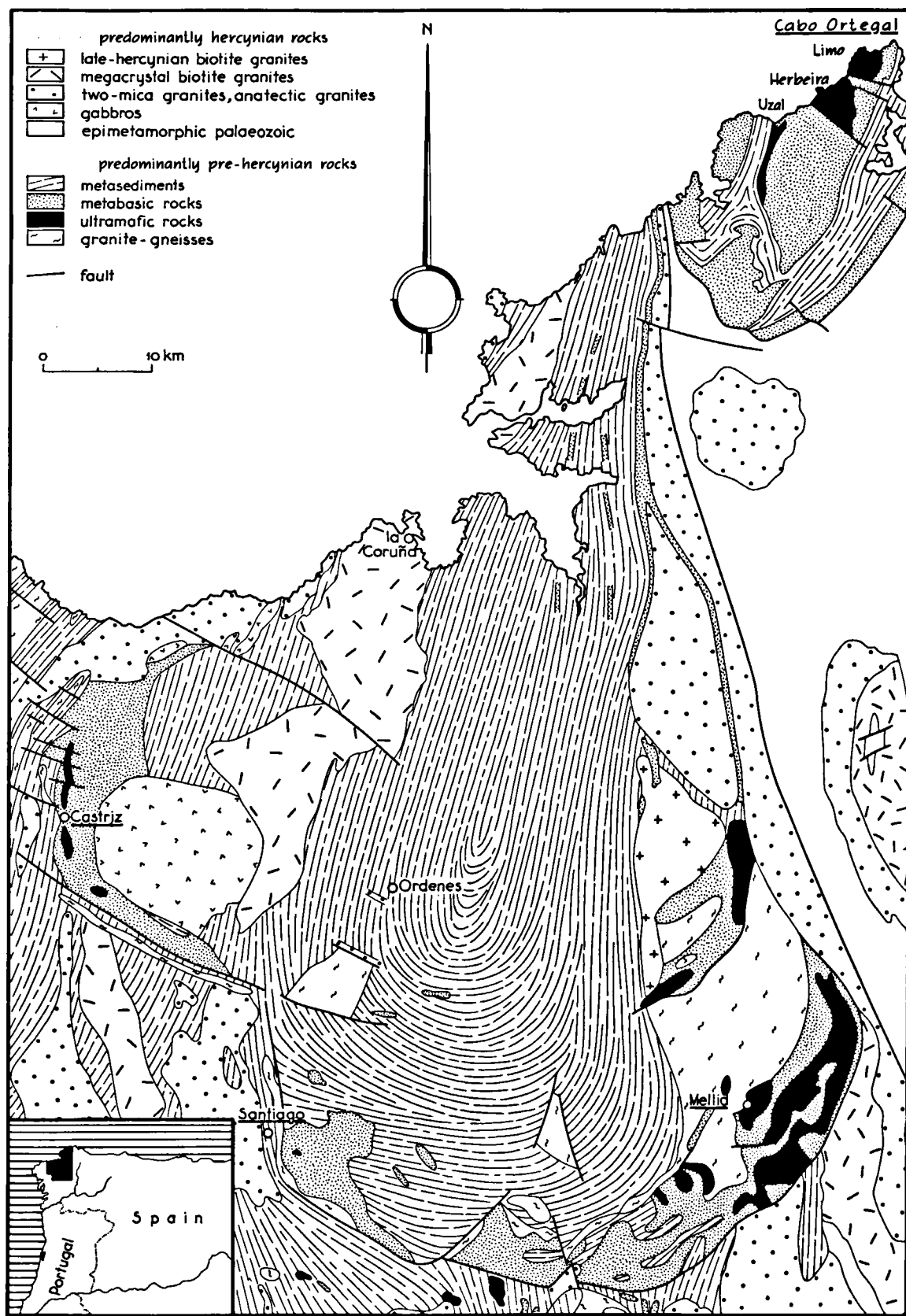
Fig. I-1. Simplified geological map of NW Galicia, after Carte géologique du NO de la péninsule ibérique (1967). The areas from which ultramafic samples have been investigated are underlined.

bolite-facies conditions during the Precambrian orogenic cycle according to van Zuuren (1969).

Albite-epidote-amphibolite- and greenschist-facies-conditions prevailed during two Hercynian phases of metamorphism.

Castriz area (Warnaars, 1967; van Tongeren, 1970)

In the western extremity of the Ordenes basin several small, lenticular, ultramafic bodies of variable composition are found in polymetamorphic, mafic rocks of magmatic descent, presumably of Precambrian age. The mafic rocks include various types of metagabbros and amphibolites. Garnet-bearing assemblages are occasionally found in the metagabbros and the amphibolites, particularly in the northern part, from which the occurrence of eclogitic rocks has also been reported. Hornblende-clinopyroxene-almandine-subfacies conditions prevailed during a Precambrian orogenic cycle, followed by Hercynian mesozonal retrogradation.

A simplified scheme of the regional metamorphic phases in the mafic rock complexes occurring in the various areas according to the authors quoted is given in Table I-1.

NOMENCLATURE

According to Streckeisen (1967) ultramafic rocks may be divided into dunites, peridotites and pyroxenites, based on the amount of olivine present: 90–100, 30–90 and 0–30%, respectively. Subdivisions can be made by taking the proportion of orthopyroxene to clinopyroxene into account. Other minerals may be present in minor amounts in addition to these three minerals, while they also may replace them. The presence of one or other of these minerals – mainly Al_2O_3 rich phases such as plagioclase, spinel, garnet, amphibole and chlorite – is strongly dependent on PT-conditions and has led several authors to the development of a facies classification of peridotites which is indicative for the prevailing PT-conditions.

In the classification used in this paper the name of the Al_2O_3 rich phase(s) is placed as a prefix before the name peridotite.

Peridotites in which primary spinel and clinopyroxene are present are called spinel-clinopyroxene peridotites. Although the presence of clinopyroxene may be already inferred from the name peridotite, it is added to underline the anhydrous character of the

Table I-1. Regional metamorphic phases in the mafic rock complexes occurring in the various areas according to the authors quoted.

P   Precambrian phase

H   Hercynian phase

LH   late-Hercynian activities

P—P   not distinguished as two phases

p   probably present

The classification of Winkler (1967) has been used, although the albite-epidote amphibolite facies has been re-introduced.

metamorphic facies	Cabo Ortegal	Mellid catazonal section	Mellid meso-epizonal section	Santiago	Castriz southern part	Castriz northern part
greenschist facies	LH	H	H	H	H	H
albite-epidote amphibolite facies		H	H	H	H	H
almandine-amphibolite facies — staur. alm. subf.						
kyan. alm. musc. subf.	H			P	p	
sill. alm. orth. subf.						
granulite facies — low P — hbl. opx. plag. subf.						
opx. plag. subf.						
granulite facies — high P — hbl. cpx. alm. subf.	P	P		p	P	P
cpx. alm. subf.	P	p				P
eclogite facies	P					p

rock, contrary to spinel-amphibole peridotites in which clinopyroxene is being replaced by amphibole.

Although this classification is generally applied to all peridotites – without regard to their orthopyroxene/clinopyroxene ratio – its application should be restricted to peridotites in which CaO and Al_2O_3 are present only in minor amounts (most peridotites are indeed lherzolitic peridotites) as is recommended by O'Hara (1967a). Olivine-clinopyroxene rocks are called wehrlites; amphibole wehrlites when clinopyroxene is being replaced by amphibole and plagioclase wehrlites when additional plagioclase is present.

When dealing with experimental investigations, the classification used by the authors concerned is generally maintained.

PETROGRAPHY OF THE VARIOUS ULTRAMAFIC ROCKS

INTRODUCTION

In this chapter a brief review will be given of the common types of ultramafic and associated rocks occurring in the different areas. Attention will be focussed on rock types and phenomena which may furnish possible explanations of their genesis, metamorphism and emplacement.

The process of serpentinization, which affected particularly the Cabo Ortegal ultramafites and the large ultramafic body northeast of Mellid, often obliterating previous mineral parageneses and changing whole-rock chemistry, will not be discussed in detail, as it is considered to be mainly a post-emplacement phenomenon.

ULTRAMAFIC ROCKS AT CABO ORTEGAL

The dominant type of ultramafic rock is a partly serpentinized spinel-pargasite peridotite, usually containing an aluminous chlorite. Macroscopically visible, dark-green amphiboles and black spinels may give a planar or, less often, a linear fabric to the rocks due to a preferred orientation of these minerals, while also lens-shaped amphibole-spinel aggregates contribute to this texture. Orthopyroxenes or bastites – in samples

which are serpentinized to a higher degree – are also clearly visible with the naked eye, especially on weathered surfaces; chlorite is occasionally found, i.e., at the Uzal.

Small occurrences are usually far more serpentinized, which can immediately be seen from their grey or blackish colours (large amounts of magnetite), while less altered ultramafites always show a greenish tint. Sparsely, rocks without amphibole were encountered. Banding is parallel to the planar fabric and, as visible at the Uzal, to the basal plane; it is not a general phenomenon and is only observed at the larger occurrences, where pyroxenite and pargasitite ($\pm$ pink garnet) bands can be followed over several metres. Bands are usually 0.5–5 cm wide, sometimes microfolded with boudins of garnet, and very conspicuous in the field by their selective weathering and lighter colours. Discordant veins have the same characteristics as the bands, although their mineralogical character is quite different, at least where pyroxenites are concerned: garnet and spinel are usually present. The majority of these veins, well exposed at the Limo, preponderantly consists of garnet and amphibole ($\pm$ spinel and pyroxenes) and is about 0.5–2 cm wide (Plates Ia and IIIa). Isoclinal folding has occasionally been observed in these veins.

Mineralogy of the spinel-pargasite peridotite

Olivine, amphibole and orthopyroxene are the main minerals in the peridotite; clinopyroxene and chlorite occur less frequently, while greenish brown to brownish green spinel is a very common accessory. Serpentine minerals (chrysotile and antigorite) and magnetite are clearly products of serpentinization, while brown to opaque rims around spinels (Fe and Cr enrichments) are also due to alteration processes. Pentlandite, pyrrhotite, heazlewoodite and millerite are commonly encountered sulphides.

Olivine (usually 0.5 mm $\varnothing$) is colourless in thin section, completely anhedral – although sometimes, when enclosed in orthopyroxene, a hypidiomorphic habit can be seen –, without inclusions and often partly to completely serpentinized. During serpentinization an olivine grain is divided into several more or less rounded fragments, between which chrysotile develops with central stringers of magnetite and, occasionally, needles of millerite. These fragments nearly always show similar extinction positions and apparently are not rotated; further serpentinization changes olivine remnants into antigorite, often crowded with magnetite dust, imparting a bluish grey colour to this serpentine mineral.

Chemical analyses, presented in Table III–6 (Appendix 1), give compositions varying between $Fo_{89.5}$ and $Fo_{90.5}$ in accordance with a mean optic axial angle $2V_z = 88°$. Even in the case of complete alteration the former presence of olivine can often be deduced from the overall character of the mesh structure and the ore distribution. In this way, altered olivines can be distinguished from serpentinized pyroxenes.

Amphibole (up to several cm $\varnothing$, generally 1 mm $\varnothing$) is slightly pleochroic in thin section (γ' faintly greenish, α' nearly colourless). The author can neither confirm Vogel's statement (1967) to the effect that newly formed amphiboles are colourless, nor did he find marked differences in other optical properties ($2V_z = 80°–90°$ with c/z of $13°–16°$ for older amphiboles vs. $2V_z = 87°$ with c/z of $21°$ in newly formed ones). Usually older amphiboles form corroded, strained, bent or broken grains with included blebs, spindles and wormlets of brownish green spinel parallel to the crystallographic c-axis. Secondary amphiboles generally possess a hypidiomorphic habit, showing prisms and rhombs without any spinel inclusions. They replace the older generation of amphibole and also clinopyroxene, into which they intrude along exsolution lamellae and cleavage planes. Both amphiboles, individually or as aggregates with or without spinel, impart a distinct foliation to the host rock. It is tempting to conceive of the close association of amphibole with spinel as an indicator of former presence of garnet, as has been done by Vogel (1967). Garnet, however, has never been found in these aggregates, although it is always present in nearly pure pargasitite veins, even as small relics.

Following the nomenclature of Phillips (1966) and Whittaker (1968), peridotite amphiboles are inter-mediate between pargasite and common hornblende and may be called common hornblendic pargasites. Older amphiboles are more pargasitic (higher contents of alumina and alkalies) than newly formed specimens. The first mentioned generally have lower positive optic axial angles ($80°–82°$) than secondary amphiboles ($86°–90°$), while in both c/z ranges from $18°$ to $22°$.

Orthopyroxene (0.5 mm $\varnothing$, large porphyroclasts several mm $\varnothing$) is colourless in thin section, although thick sections occasionally reveal a faint pleochroism (γ' pink, α' colourless). Often, as with amphiboles, a clear distinction can be made between primary and secondary orthopyroxenes. Primary orthopyroxenes are mostly strained, often bent or broken; spindles and rods of green to brownish green spinel parallel to the crystallographic c-axis and blades parallel to (010) are frequently included, while blade-like spinel exsolution occurs along the boundary of kinkbands, parallel to (001). Clinopyroxene exsolution lamellae parallel to (010) occasionally occur, often in close association with exsolved spinel.

Recrystallized, secondary orthopyroxenes do not exhibit these phenomena: they often surround and partly intrude the older generation as small anhedral grains along cleavage planes, while older pyroxenes may sometimes be seen with recrystallized, spinel free borders. Individual grains of spinel often lie in this rim of new pyroxenes.

As could be deduced from the foregoing, chemical analyses show lower contents of Al_2O_3 in the newly formed orthopyroxenes, while Mg/Fe ratios are slightly higher in secondary orthopyroxenes (Table III-7, Appendix 1). Both pyroxenes are enstatites with $En_{89.3}$ to $En_{90.4}$ and $2V_z$ varying between $80°$ and $88°$; alumina rich orthopyroxenes tend to have lower positive optic axial angles than Al-poor specimens.

Clinopyroxene (0.5 mm $\varnothing$) is present in minor amounts as very corroded, dentated grains without spinel inclusions and exsolution lamellae of orthopyroxene. Its mean composition is $En_{48.5}Wo_{48.5}Fs_{3.0}$ with an Al_2O_3 content of $1.2–2.0\%$. Amphibole replaces clinopyroxene, although the latter is usually directly altered into serpentine; $2V_z = 54°–58°$ with c/z = $39°–43°$.

Chlorite (0.5–1 mm $\varnothing$, large booklets up to several cm $\varnothing$) frequently occurs in more serpentinized samples as sometimes swollen and bent booklets with often a rim of magnetite and carbonate between the booklets. Chlorite usually surrounds brown to opaque spinels (magnetite-chromite), indicating impoverishment in Mg and Al of the originally brownish green spinel necessary to form these chlorites with, of course, a supply of silica and water. Chlorites, thus formed, generally neither possess magnetite rims nor carbonate included.

In thin section chlorite is colourless; in thick sections a slightly greenish colour is observed. Twinning according (001) often occurs. X-ray determinations and chemical analyses indicate this chlorite to be a 14 Å-clinochlore with a negative elongation and $2V_z = 25°–28°$. Chromium (derived from spinel) is

occasionally incorporated in these chlorites: a wet-chemical analysis (Cardoso & Parga-Pondal, 1951) showed 1.88% Cr_2O_3, while an electron microprobe analysis of a chlorite (sample BU 2) revealed 1.0% Cr_2O_3.

Spinel (porphyroblasts up to 5 mm ⌀, in close association with amphibole and orthopyroxene considerably smaller) has brownish green to greenish brown colours; in heavily serpentinized samples the colour turns brown to opaque due to significant increases in magnetite and chromite molecules. Serpentinization usually starts with the development of magnetite in cracks and along rims, ending in magnetite (± chromite) and serpentine (by supply of silica), while chlorite also develops around brown to opaque spinels. Within one sample spinel colours may range from green (spinel exsolved from pyroxenes, in association with amphibole) via brownish green (large porphyroblasts) to brown and opaque: nomenclature (Winchell & Winchell, 1959) mentions this as a transition from ceylonite via picotite to chromite/magnetite.

Chemical analyses show decreasing Mg/Fe ratios and increasing Cr/Al ratios, corresponding to the above-mentioned trend.

Alteration products are serpentine minerals and magnetite; talc occurs only occasionally. The principal opaque minerals are pentlandite, pyrrhotite and magnetite; occasionally heazlewoodite, millerite, rutile, hematite and various Fe-hydroxides are found.

Pyroxenites and garnet-bearing rocks

Regional metamorphism accompanied by deformation hampers an unambiguous distinction between bands and veins (see also Vogel, 1967). If bodies lying parallel to the planar texture are called bands, and discordant rocks are classed as veins, veins occur more frequently than bands. A mineralogical differentiation is possible:

1) spinel-free pyroxenites (± olivine ± amphibole) are found only as bands (up to 5 cm wide); spinel- and garnet-bearing bands are an exception;
2) spinel ± garnet are always present in the veins (serpentine veins not included): the majority of the veins contains garnet + amphibole; locally spinel pyroxenites occur.

A useful subdivision of the various rocks may be:

1) spinel-free pyroxenites;
2) spinel pyroxenites:
a) brown ceylonite orthopyroxenites,
b) spinel sensu stricto clinopyroxenites;
3) garnet-bearing veins, in which all transitions from garnet-spinel pyroxenites via garnet ± amphibole veins to amphibole ± garnet veins are possible.

Spinel-free pyroxenites (R 153, R 173, MP 18, MP 20 and MP 21)

– Orthopyroxene (sometimes slightly pleochroic), clinopyroxene and greenish amphibole are the main constituents of these medium- to fine-grained panxenomorphic rocks. Clearly recrystallized samples (MP 20) are fine-grained. Preponderance of amphibole over clinopyroxene usually occurs, MP 21 consists almost entirely of amphibole. Non-recrystallized pyroxenes are often strained and bent and surrounded by recrystallized pyroxenes; orthopyroxenes contain exsolution lamellae of clinopyroxene. Ortho- and clinopyroxene do not have exsolved spinel, while electron microprobe analysis of both pyroxenes shows distinctly lower Al_2O_3 contents than in all other pyroxenes analysed. Intercalations or alternating laminations (R 173) of olivine and orthopyroxene (usually surrounded by magnetite dust) occur, while abundant carbonate is present interstitially (R 153 and R 173). In recrystallized samples dark-brown to opaque laths and rods of Cr-rich magnetite are encountered parallel to the crystallographic c-axis in both pyroxenes; opaque dendrites and wormlets of the same mineral frequently occur in clinopyroxene, particularly near the contact with amphibole, by which clinopyroxene is being replaced. Cr-rich magnetite is ubiquitously present as small subrounded grains; other opaque accessories are pentlandite and pyrrhotite.

Sample MP 18 represents a composite band (3 cm wide) with an external zone of chlorite orthopyroxenite and a central core consisting mainly of greenish amphibole, strained and bent orthopyroxene, remnants of clinopyroxene and minor amounts of chlorite.

Microscopical observations (absence of aluminous spinel and garnet), chemical evidence of mineral compositions (low alumina pyroxenes, common hornblende instead of more aluminous pargasite) and whole-rock analyses reveal that all these pyroxenites (or rather amphibolized pyroxenites) are completely different from the spinel pyroxenites and garnet-bearing veins, described below: the essential difference is reflected in the clearly higher Al/Si ratios in the latter.

Brown ceylonite orthopyroxenites (R 67, V 1403b, V 1404).

– These orthopyroxenites contain far more pyroxenes and much less (to none at all) olivine than peridotitic rocks, while spinel usually displays browner colours, indicating higher contents of Cr.

Large, primary orthopyroxenes (up to 5 mm ⌀) are often strained and bent; they contain abundant exsolution lamellae of clinopyroxene and are crowded with brownish green spinel inclusions. Around large grains recrystallized, unstrained and clear orthopyroxenes occur with individual spinel grains.

Clinopyroxene, present in subordinate amounts, also contains exsolution lamellae of orthopyroxene and numerous inclusions of spinel; it has been extensively replaced by greenish amphibole. Olivine occurs interstitially between pyroxenes as completely anhedral grains; it has generally not been serpentinized in this "protecting" pyroxenic environment. Brown spinel occurs interstitially and as large individual grains,

while sometimes accumulates of spinel are found (V 1404).

In two olivine-free samples (V 1404 and R 67) garnet occurs; locally in the first sample as large anhedral grains in a greenish amphibole environment; in R 67 as small, interstitial grains surrounding orthopyroxene and next to spinel, giving the impression of having been formed at the expense of orthopyroxene and spinel.

Spinel sensu stricto clinopyroxenite (R 378). – Spinel sensu stricto clinopyroxenite is found only in the sample mentioned as several discordant veins (maximum thickness 1 cm). Differences with the previously described orthopyroxenites are conspicuous: (1) bright-green to olive-green spinel instead of brown ceylonite; (2) preponderance of clinopyroxene over orthopyroxene (ratio 3:1); (3) absence of olivine and garnet; (4) interstitial pale-brown amphibole instead of the usual greenish coloured amphibole.

Spinel, bright-green in the centre of the vein and olive-green near its borders, mostly occurs wedge-shaped, filling up interstices, although large porphyroblasts (up to several mm $\varnothing$) are found. Both pyroxenes are usually strained and contain abundant exsolution lamellae of pyroxenes. Pale-brown amphibole is often associated with spinel; its brownish colour is probably due to higher contents of Ti; higher amounts of Al and Na mark this amphibole as a true pargasite. Alumina contents in both pyroxenes are high (6.5% Al_2O_3), while the content of Na_2O remains comparatively low (0.9%) in clinopyroxene; Mg/Fe ratios in both pyroxenes are distinctly lower than in all other pyroxenes from the Cabo Ortegal area (see next chapter).

Garnet-bearing veins and bands. – The first appearance of garnet is as small, interstitial grains around orthopyroxene and brownish spinel. In a further stage of this "garnetization" process orthopyroxene is being consumed or left behind, impoverished in its Al_2O_3 content, as small remnants within or around garnet. Clusters of small garnet grains, often accompanied by subrounded ilmenite, develop amidst the pyroxenes. Coronas consisting of an aggregate of small garnet grains surround green spinel porphyroblasts. Mg-rich ilmenite and högbomite are found in close association with these cores of green spinel. Ilmenite usually is the only opaque mineral in these rocks, in only one sample (V 1405) rutile occurs as the dominant Ti-mineral between chlorite flakes. X-ray diffraction and a microprobe analysis of högbomite confirmed its tentative identification by Vogel (1967).

The first rim immediately around large spinel often consists of colourless chlorite flakes (with, except for a lower content of Cr, approximately the same composition as those in the host peridotite). From the spinel core outward, the garnet corona initially is sometimes interspersed with small spinel grains, the colour of which changes outward from green to brownish. Mg-bearing carbonate is often present. In

the centre of the coronas a generally pure garnet zone exists, while at the rims greenish amphibole ± spinel develops, sometimes in a kelyphitic texture and partly at the expense of garnet but, in the opinion of the author, probably often independent of garnet. The development of amphibole (a common hornblendic pargasite as in the host peridotite) is not restricted to the garnet corona, but occurs everywhere in these rocks: in stress-shadows of boudin-shaped garnet aggregates, as a rim of small, recrystallized grains between garnet and neighbouring peridotite, and as replacement of clinopyroxene. Amphibole veins with remnants of garnet and green spinel (PC 5 and MP 28) represent amphibolized garnet-bearing veins, although a stable association of amphibole and garnet should be considered possible in ultramafic rocks under certain circumstances, as will be discussed below.

At the very beginning of this so-called garnetization process pyroxenes still contain numerous inclusions of spinel; the inclusions, however, rapidly disappear and exsolution lamellae of pyroxenes become an exception when the amount of garnet increases. Mg/Fe ratios in both pyroxenes are equal to ratios in the peridotite; with decreasing Al a slight increase of this ratio is noted. Further characteristics of both pyroxenes can be found in the description of the peridotite.

Colourless chlorite (slightly greenish in thick sections) occurs around green spinels, amidst garnet aggregates and along their rims as individual, unoriented flakes and clusters. It appears to be younger than amphibole, remnants of which are often present in chlorite aggregates. With regard to the paragenetic relation with spinel, textural evidence pleads in favour of formation of chlorite from spinel, added silica (derived from orthopyroxene?) and water. Apatite is a very common accessory: it often forms clouded, euhedral crystals (up to 100 micron $\varnothing$) with abundant rutile needles included parallel to {001} (L 1). Zircon is mainly present as idiomorphic grains in more amphibole-rich veins.

The pyrope content of garnet varies between 54 and 62%, although largely homogeneous garnet rims show enrichments in almandine and spessartine molecules. For chemical details the reader is referred to chapter III.

Contacts of the veins with the wall-rock are generally sharp, even in thin, microfolded veins: within a few millimetres the garnet-clinopyroxene-amphibole assemblage changes into an olivine (serpentine)-amphibole association. A somewhat higher degree of serpentinization of the host peridotite near the veins is often noted: fresh olivine neighbouring garnet is an exception, the more as amphibole usually surrounds garnet. One of the exceptions (in MP 10) shows clinopyroxene between garnet and olivine. Garnet occurs in this sample up to 1 cm outside the vein in the host rock. A microprobe analysis of these garnets shows a higher Cr content, a lower Mg/Fe ratio, more Ca and Mn than the garnet in the centre of the vein. Isolated garnets in serpentinized peridotites or bordering the host rock are often rimmed with a

mineralized kelyphite (amphibole is serpentinized and spinel altered into magnetite), while sometimes a thin rim of bastite (serpentinized orthopyroxene) can be detected around completely altered olivine, indicating that garnet and olivine were not a compatible pair under these conditions.

Apart from the common occurrence of garnet in veins, garnet has also been found in two peridotite samples (FCM 1 and R 313a) that have no clear relation to vein material. Both samples are derived from the Carreiro zone of tectonic movement (Faro de Punta Candelaria and Playa de Córtes, respectively) and show heavily tectonized to mylonitized peridotites which are only slightly serpentinized. In one of the samples (FCM 1 – a 20 cm long boudin) garnet occurs – with a kelyphitic rim of spinel and orthopyroxene – together with chestnut-brown spinel, slightly greenish amphibole, and orthopyroxene as rounded clusters in a largely recrystallized groundmass consisting predominantly of olivine and orthopyroxene. In these clusters garnet is present as large, anhedral grains, in which rows of tiny brown spinel and orthopyroxene are included. The kelyphitic rim reaches a maximum thickness at the border of the clusters; especially when the rim adjoins olivine, around which in that case, secondary orthopyroxene has been developed, probably as a reaction product between garnet and olivine.

Going from garnet towards greenish amphibole (usually present between individual garnet grains) the kelyphitic rim becomes coarser, while individual, brownish green dendrites of spinel develop, and quickly passes into often subhedral, greenish amphibole with abundant reddish brown spinel. Garnet forms embayments into strained orthopyroxene suggesting formation of garnet at the expense of orthopyroxene.

Clinopyroxene is present in subordinate amounts, while carbonate is a conspicuous accessory. The described clusters occur only sparsely in the host rock, although radial concentrations of tiny spinel and kelyphitic textures can be seen more often. The author does not consider these clusters to represent an integral part of the peridotitic host rock; smeared out vein material seems to be a more logical solution. The chemical composition of garnet and amphibole does not deviate essentially from that of the same minerals in the veins: a somewhat higher Cr content of garnet and amphibole could be predicted from the high ratio of Cr in the associated brown spinel.

In the groundmass olivine occurs in two generations: large (up to several mm $\varnothing$), strained and bent grains of olivine lie in a recrystallized mosaic of olivine and orthopyroxene. Greenish amphibole, brown spinel and clinopyroxene in this order form the other constituents.

In the other sample, R 313a, garnet, without showing distinct kelyphitic rims and without brownish spinel, is usually found as anhedral grains in amphibole aggregates. Sometimes solitary garnets occur amidst the groundmass which consists of the same minerals with the same texture as in the above-mentioned sample.

Garnet-bearing amphibole aggregates (sometimes with minor clinopyroxene) appear to represent former banding – probably mylonitized garnet-bearing bands.

ULTRAMAFIC ROCKS NEAR MELLID

Two types of ultramafic rock are found in this part of Galicia: 1) a foliated spinel-pargasite peridotite, moderately serpentinized, with garnet ($\pm$ amphibole) boundins and lenses (Plates II and IIIb), occurring locally near the village of Mellid and nicely exposed in a quarry along the road leading from Mellid to the south; 2) a highly serpentinized peridotite in a N–S zone further to the east of Mellid.

Foliated spinel-pargasite peridotite
This peridotite as a thin, horizontal sheet concordantly overlies basic granulite-facies rocks. A maximum thickness of 50 m is surmised, the planar texture – best visible on weathered surfaces – lying subhorizontally, subparallel to the borders of the sheet of ultramafic rock. West of Mellid a few isolated occurrences of this peridotite were encountered.

Macroscopically only amphibole and olivine are visible as dark grains in a greenish grey rock; parallel to the planar texture, pink to lilac garnets and dark-green amphiboles are easily recognizable with the naked eye in lenses, up to 20 cm long. Mineralogically the host rock is a spinel-pargasite peridotite with subordinate amounts of clinopyroxene and brownish spinel. Olivine, amphibole and orthopyroxene occur as large anhedral grains (up to 3 mm $\varnothing$), often with concave boundaries, usually strained and bent, sometimes broken, in a fine-grained recrystallized matrix consisting of the same minerals with in addition spinel, clinopyroxene and sometimes abundant talc.
Olivine grains often are apparently elongated parallel to the planar fabric. The true dimensional as well as a possible lattice orientation have not been investigated, petrofabric analysis being beyond the scope of this study. The grains mostly show undulatory extinction and deformation lamellae. Alteration into serpentine minerals is rare, although magnetite has been formed in cracks. Optical and chemical data give the same values as for Cabo Ortegal olivines.

Colourless *orthopyroxene*, sometimes with olivine inclusions, very rarely shows spinel exsolution, while very thin clinopyroxene lamellae occasionally occur parallel to (010). Rutile inclusions are sometimes present. Large porphyroclasts of orthopyroxene are sometimes rimmed by a cummingtonitic amphibole. Orthopyroxene compositions do not differ significantly from those of the Cabo Ortegal orthopyroxenes; somewhat higher contents of Al_2O_3 are noted.
Amphibole is pleochroic from brownish to faintly greenish and is present as large, anhedral, often somewhat rounded grains with occasional inclusions of brownish green spinel. Its chemical composition closely resembles amphibole compositions of the above-mentioned spinel sensu stricto clinopyroxenites. These amphiboles also show somewhat higher contents of

titanium than do amphiboles from the Cabo Ortegal peridotite. Small orthopyroxene grains often surround amphibole.

Clinopyroxene is present as small, corroded grains.

Brownish *spinel* occurs as anhedral grains with a size smaller than the above-mentioned porphyroclasts (maximal 1 mm ∅, usually less). Small rows of spinel, torn off from larger ones, and elongated individual grains are also responsible for the planar fabric of the rock. The groundmass (20 micron ∅) consists mainly of talc, carbonate, brownish green spinel and opaque minerals (mostly magnetite) in minor amounts. Fragments of olivine, amphibole and orthopyroxene with an average diameter of 300 micron are present in this groundmass. In less planar, i.e., less deformed samples, in which talc is mainly present in shear planes, the distinction between porphyroclasts and groundmass is less clear.

Garnet, kelyphitization of garnet and its coexistence with pargasite

Garnet occurs in lenses – often smeared out in the same plane – amidst the host peridotite. Cores of spinel are lacking, although individual spinel grains, often light-brownish unlike the green variety encountered in the Cabo Ortegal veins, occur haphazardly. Chlorite has not been found in or near the garnet. Garnet is usually present as large, somewhat rounded, anhedral grains (several mm ∅), although in some instances (sample 4 M 10) crystal faces seem to have developed. Rounded orthopyroxenes are common inclusions: sometimes they are surrounded by a feathery, kelyphitic rim consisting of orthopyroxene, threads and wormlets of spinel and minor clinopyroxene, suggesting a reaction between aluminous orthopyroxene and garnet (Plate IIIcd). Trails of tiny inclusions, probably rutile, are common, while carbonate is also present. Dirty, subhedral apatite with included rods of rutile is frequently found in both garnet and amphibole. Hypidiomorphic, nematoblastic, slightly brownish amphibole often occurs inside the garnets: situated amidst garnet individual parts of one grain usually show equal extinction positions, which suggests that amphibole did not form later than garnet, but probably in stable association with it.

Around garnet a coarse kelyphitic rim, often 1 mm wide of orthopyroxene, amphibole, green spinel and minor clinopyroxene is generally present. Immediately next to garnet orthopyroxene occurs, crowded with wormlets and threads of spinel which lie perpendicular to the garnet border, while often clinopyroxene is present with the same orientation. Amphibole with spinel inclusions, followed by pure amphibole, are found further away from the garnet. Spinel shows the tendency of getting more brownish outward, in which it corresponds to spinel features observed in the Cabo Ortegal garnets, although here the phenomenon occurs amidst amphiboles.

A reaction relationship between garnet and olivine has been found in a few samples (5 M 2 and 96–C3–10).

An orthopyroxene border around olivine abruptly passes into a spinel-orthopyroxene kelyphite with additional clinopyroxene and amphibole (Plates IV and Va). All orthopyroxene (in kelyphite and rim) and clinopyroxene between garnet and olivine has the same orientation. Amphibole grains, mainly present near garnet, do not show a preferred orientation and probably have been formed later.

The complexity of the kelyphite – coarse, radially arranged spinel next to clear orthopyroxene and finer-grained, not dimensionally oriented spinel next to garnet – might be due to the fact that only the outer part of this kelyphite recrystallized. In the opinion of the author, however, a recrystallization in this radial pattern is unlikely.

Two processes were probably involved. First, a reaction between garnet and olivine in which orthopyroxene was formed at the expense of olivine and the radially arranged kelyphite at the expense of garnet (see Möckel, 1969); further, kelyphitization of the remaining garnet due to instability of the garnet itself. Olivine is not a common constituent of the garnet-bearing veins and bands and definitely belongs to the host peridotite assemblage. Only occasionally, at the margins of veins and bands and during deformation phases, does it come into contact with garnet. Aluminous orthopyroxene is not a stable phase in the garnet-bearing assemblage as garnet developed at the expense of it.

It is tentatively concluded that both reactions (aluminous orthopyroxene + garnet and olivine + garnet) proceeded to the right under PT-conditions which may be related to high-pressure granulite-facies-conditions for the crustal rocks. The alteration of garnet proper probably started during catazonal retrogradation. Overall alteration of garnet, however, did not occur: garnet and amphibole are often found in stable association without any signs of kelyphitization. Electron microprobe analysis reveals a distinct enrichment of Mn and Fe in the garnet against included amphibole and in the garnet rims (Fig. III-2 and Plate VIb). Interpretation of this phenomenon is difficult. The zonary character might be obtained primarily during the growth of the garnet, although, in the opinion of the author, a fractional crystallization is not likely. The gradual increases in Mn and Fe contents toward the garnet borders do not plead in favour of a later accretion of Mn- and Fe-rich rims. It may, however, also be envisaged that the zonary character is due to a later redistribution within the garnet and represents a readjustment to changed PT-conditions. Although of a rather speculative nature – the possibility of diffusion processes taken into consideration –, it may be suggested that, during a catazonal retrogressive phase, the originally homogeneous garnet is armoured against amphibolization by the development of Mn- and Fe-richer rims. This hypothesis warrants the assumption that garnets with higher contents of Mn and Fe are in stable association with amphibole, whereas garnets richer in pyrope are not stable. Higher contents of Mn in the garnet rims

may also preserve the garnets from large-scale amphibolization as Mn is only slightly incorporated in the amphibole molecule.

With respect to the coexistence of garnet and amphibole in these garnet-bearing assemblages, the results of the experiments of Gilbert (1968) are quoted. He investigated the stability of some amphibole end members at high pressures under hydrous conditions. As the chemical composition of the garnet-bearing assemblages (Table III-2) shows similarities with these amphibole compositions – some of the veins consists predominantly of pargasite – conclusions drawn from these results may be applied to the veins under consideration. These results are presented in Fig. II-1.

the Mellid area. In dense, radially textured kelyphites pyroxenes are present in subordinate amounts and individual spinel grains are observed only occasionally. Ca and Al X-ray emission pictures may stress the isochemical nature of this alteration process (Plate Vbcd).

The conclusion seems warranted that the close connection between orthopyroxene rims around olivine and a spinel-amphibole kelyphite around garnet is only, at least in these rocks, a spatial connection (see Möckel, 1969).

Chlorite-amphibole peridotite of Mellid

Most samples show largely to entirely serpentinized rocks, in which only serpentine minerals and opaque
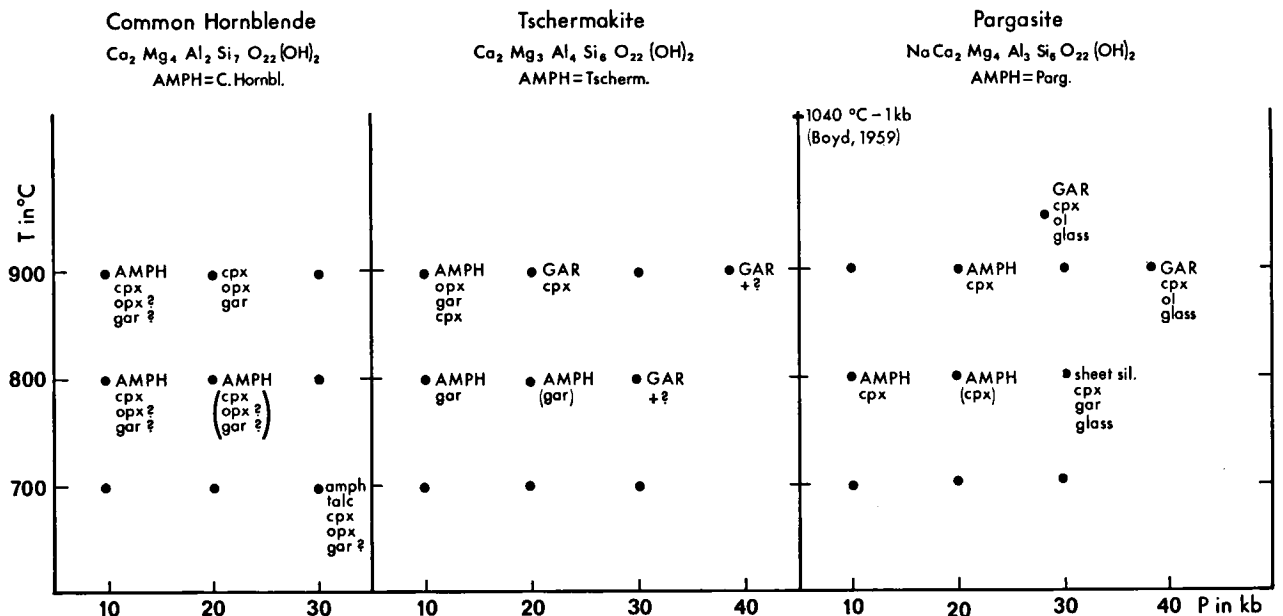
Fig. II-1. Some results of high-pressure hydrothermal runs for amphibole end members (after Gilbert, 1968). Abbreviations: cpx = clinopyroxene; opx = orthopyroxene; gar = garnet; ol = olivine; sheet sil. = sheet silicate; ? = presence not confirmed or unidentified phase or phases; ( ) = metastable phase(s); capitals indicate dominant phase.

Generally speaking, it may be said that garnet and amphibole (meta) stably coexist at temperatures of 800°–900 °C under pressures of 10–20 kb in garnet-bearing assemblages that are poor in sodium. The higher stability limit of pargasite causes an earlier disappearance of garnet in rocks which contain higher amounts of sodium. However, garnet being absent in the host peridotite, the spinel to garnet peridotite transition is not crossed and PT-conditions should be restricted to 800°–900 °C under 10–15 kb pressure (cf. O'Hara, 1967a, and Lambert & Wyllie, 1968).

The large-scale development of spinel-amphibole kelyphite is related to the second generation of amphibole and took place during a second retrogressive phase. Garnet was severely attacked in this phase and only small remnants of garnet were left in amphibole-rich samples. These remnants have significantly lower pyrope contents than large garnets from

material (mostly magnetite) are found with flakes of chlorite, carbonate and talc in minor amounts. Around magnetite aggregates (presumably with appreciable amounts of the chromite molecule) clusters of chlorite are often encountered. In two less serpentinized samples (96–D2–5 and 96–D2–73) olivine in large crystals (up to 5 mm ∅), anhedral amphibole and abundant chlorite (often concentrated in streaks and clusters) are the principal constituents. Olivine is sometimes strained and broken into fragments with approximately the same orientation. Its forsterite content is surprisingly low compared with the olivines described above: 85.0%. Colourless amphibole is usually crowded with tiny, opaque particles (probably magnetite) and often rimmed by turbid, brownish masses of tremolite. Complete replacement by tremolite and newly formed tremolite fibres also occur. Feathery fibres, slightly brownish coloured and

free of Ca, showing oblique extinction, point to a cummingtonitic amphibole, which may have been derived from orthopyroxene, although distinct bastites, proof of a former presence of orthopyroxene, are not found. Indications in favour of a former presence of clinopyroxene are completely lacking: clinopyroxene, if it has been present at all, probably has been amphibolized entirely prior to attack by serpentinization. Chlorite shows the same features (optically and chemically) as mentioned above. Amphibole has a common hornblendic composition.

SPINEL-HORNBLENDE PERIDOTITE OF THE SANTIAGO AREA

The only fresh hand-specimen available (96–A4–51) shows a highly recrystallized, spinel-hornblende peridotite, only slightly serpentinized with minor amounts of serpentine (in cracks of olivine) and talc.

Olivine (1–3 mm $\varnothing$) usually contains dark-green inclusions of spinel and ilmenite has occasionally been found enclosed. Olivine porphyroclasts lie in a fine-grained, cataclastic groundmass (150 micron $\varnothing$) consisting mainly of greenish amphibole, dark-green spinel and distinctly pleochroic orthopyroxene (pink to nearly colourless); Mg-rich ilmenite abundantly occurs as mostly subrounded grainlets, while also small olivine grains are present. Droplets, needles and rods of spinel are present in amphibole and orthopyroxene; amphibole also contains ilmenite inclusions. Chlorite and (?) rutile are encountered as accessories in subordinate amounts.

Lower forsterite contents in olivine and lower enstatite contents in orthopyroxene (corresponding nicely to the observed pleochroism and the measured optic axial angle of 70°–80° (van Zuuren, 1969)) distinguish this small body from the peridotites described above; Mg/Fe ratios in spinel are also conspicuously lower. The amphibole has a common hornblendic character.

ULTRAMAFIC AND ASSOCIATED ROCKS OF THE CASTRIZ AREA

Warnaars (1967) made an extensive study of the ultramafic and related rocks in this area. It may, for comparative reasons, serve a useful purpose to give a cursory review of his work.

A large variety of rock types with great chemical and textural differences is found. The various rock types can be schematically subdivided into the following groups: (1) peridotites and their serpentinized equivalents, (2) wehrlites and (3) gabbros and pyroxenites. Transitional compositions occur also.

1) *spinel-clinopyroxene peridotite* (FW 928) – restricted occurrence E of Ferreira (northern part of the area) –: fragmented and recrystallized, fine-grained matrix consisting of olivine and minor ortho- and clino-pyroxene, cut by veinlets of serpentine with magnetite. Bent remnants of primary pyroxenes with exsolution lamellae of each other occur. Streaks and broken grains of greenish brown spinel with opaque rims and cracks (members of the magnetite-chromite series) are encountered. In a pyroxenitic part of the same sample an incipient stage of uralitization is characterized by cloudy, turbid masses in both pyroxenes; interstitial light-green spinel is present in this equigranular pyroxenite (400 micron $\varnothing$) and almost certainly released from primary more aluminous pyroxenes, for the composition of which the reader is referred to Tables III-7 and III-8. Olivines and pyroxenes in this peridotite have compositions similar to those from Cabo Ortegal and Mellid. The Al_2O_3 contents of primary pyroxenes, however, are somewhat higher.

Bands of *spinel-garnet pyroxenite* (up to several cm wide) occur locally within this peridotite. Garnet has developed around light-green porphyroblasts of spinel, which often have a greyish green core due to the presence of numerous tiny, opaque inclusions. The predominant mineral is clinopyroxene, often highly cataclastic, without pyroxene or spinel exsolution and with a chemical composition which markedly differs from analysed clinopyroxenes found in garnet-bearing assemblages from Cabo Ortegal and Mellid. The proportions of Al, Ti and Na are significantly higher (see Table III-8). Small grains of garnet and spinel are also encountered in the groundmass. The absence of chlorite and a pargasitic amphibole is noteworthy. Uralitization of clinopyroxene is observed and serpentine and vesuvianite may be considered breakdown products of garnet.

Along the margins of the ultramafic bodies near Castriz more or less serpentinized peridotites are found: sample FW 894 represents a *chlorite-amphibole peridotite*, in which olivine and slightly brownish to colourless amphibole (common hornblende, see Table III-10) are the main constituents. Slightly greenish chlorite, often associated with a member of the magnetite-chromite series, is frequently encountered, often in clusters. Clinopyroxene occurs in minor amounts, all orthopyroxene has disappeared. Sample FW 770 is an example of a completely serpentinized rock in which only serpentine minerals, chromite and magnetite are present.

2) *Wehrlites* – the most common rock type according to Warnaars – are clinopyroxene-olivine rocks. Samples FW 898, FW 769 and 32, all partly serpentinized, show large (1 cm $\varnothing$) poikilitic clinopyroxenes, colourless and crowded with exsolved blades of Fe-Ti oxides (probably magnetite and ilmenite), with many, usually subrounded olivines, in which primary, hypidiomorphic, dark-green or brown spinel is enclosed. Clinopyroxene is sometimes altered into tremolite. Orange-brownish to nearly opaque kaersutite is present as poikiloblasts and as smaller grains, often in clear association with greenish brown spinel. In serpentinized parts clusters of chlorite are encountered around members of the magnetite-chromite series. In other wehrlites, such as FW 769°, a poikilitic texture is absent: colourless, subhedral clinopyroxenes (4 mm $\varnothing$) with orthopyroxene lamellae and abundant

exsolution of brownish green spinel and blades of ilmenite, and recrystallized, smeared out, more or less interstitial olivine form more than 95% of the rock. Small grains of orange-brownish amphibole, recrystallized clinopyroxene, spinel and minor orthopyroxene form narrow coronas around large clinopyroxenes. In FW 897 both textures can be detected: poikilitic clinopyroxene, with olivine included, both with hypidiomorphic spinel enclosed, and recrystallized assemblages (average grain size 300–700 micron ∅).

A rapid decline of the clinopyroxene-olivine component is found in *spinel-amphibole wehrlites* (FW 753 and FW 808), which are generally encountered at the margins of ultramafic rocks. Remnants of poikilitic clinopyroxene are still present, but the mineral usually recrystallized in intricate replacement textures crowded with abundant, brownish green spinel and partly altered into nearly colourless amphibole (probably a tremolitic amphibole). An earlier replacement of clinopyroxene forms orange-brownish amphibole. Olivine, with included olive-green to brown-green spinel, is rimmed by orthopyroxene and a fibrous, colourless amphibole, successively. Rims of orthopyroxene are occasionally encountered around spinel included in olivine. Alteration of orthopyroxene is common. Poikilitic amphibole, slightly orange-brownish and crowded with ilmenite and minor magnetite, is present.

The most remarkable difference with the plain wehrlites mentioned above is the occurrence of fine-grained (generally less than 100 micron ∅) aggregates of slightly greenish amphibole (common hornblende), often with cores of light-green spinel with occasionally corundum in its centre. The aggregates are sometimes entirely enclosed by clinopyroxene and olivine with their respective reaction rims. The aggregates show gradual transitions with these rims, i.e., from slightly brownish to slightly greenish amphibole. Generally, however, the amount of this spinel-amphibole aggregate is so high (about 50%) that primarily crystallized olivine and clinopyroxene seem to "float" in an amphibole groundmass. Sometimes plagioclase and its alteration products (saussurite, zoisite and carbonate) are present between olivine and clinopyroxene. Plagioclase does not occur within the spinel-amphibole masses, but always in individual pockets.

More plagioclase – in pockets, with a distinct mosaic texture – is found in *plagioclase wehrlites* (FW 768, FW 809b and FW 921), in which the further constituents are formed by a recrystallized granoblastic assemblage (0.5–1 mm ∅) of olivine, thinly rimmed by orthopyroxene and an orthopyroxene-spinel sym-

plektite when in contact with plagioclase, and hypidiomorphic clinopyroxene. Some large olivine and clinopyroxene grains, however, have remained. Olive-green spinel and orange-brownish amphibole are present in minor amounts. In a coarse-grained sample (FW 809b) interstitial (? hydro) grossular was found.

3) Real *gabbroic compositions* – gabbros haphazardly occur within the ultramafic rocks – are reached in coarse-grained (up to 1 cm ∅) samples (i.a., FW 848, FW 850a), in which subhedral clinopyroxene, plagioclase (labradorite, hardly zoned) and olivine are the predominant minerals. Olivine-free samples are also present. Olivine, when in contact with plagioclase, is invariably rimmed by orthopyroxene and a coarse orthopyroxene-spinel symplektite with minor clinopyroxene, successively. Threads of spinel are often arranged perpendicular to a central line in the host orthopyroxene; this central line may indicate the former contact olivine-plagioclase (see Möckel, 1969). Wormlets of spinel also occur in clinopyroxene when bordering plagioclase. Sometimes spinel is altered into diaspore. Orange-brown amphibole is often found between these reactions rims of clinopyroxene and plagioclase; amphibole has grown around clinopyroxene and replaced it. Clinopyroxene, due to its Ti content, is sometimes coloured slightly purplish. Blades of ilmenite are present. Orthopyroxene shows a distinct pleochroism (γ' faintly greenish, α' pink), especially in olivine-free samples. According to Warnaars, who found veins of olivine-free gabbro cutting pyroxenites and vice versa, coarse- and fine-grained pyroxenites occur together with fine-grained gabbros in some places.

In these medium- to coarse-grained *pyroxenites* (clinopyroxenites to websterites) clinopyroxene is distinctly pleochroic (γ' brownish violet, α' colourless) and contains orthopyroxene lamellae and blades of exsolved ilmenite. Orthopyroxene, having an Fe-rich bronzitic composition, also shows distinct pleochroism (γ' light-green, α' pink). Exsolution of clinopyroxene is encountered occasionally. Alteration of orthopyroxene into talc may be observed in both gabbros and pyroxenites, especially when bordering plagioclase. In fine-grained gabbros, usually olivine-free, brownish amphibole is frequently present. If the amount of amphibole increases the amount of plagioclase, often saussuritized, decreases resulting in amphibole- pyroxene rocks (Warnaars' pyribolites) – occurring at the periphery of some ultramafic outcrops – in which the constituent minerals display characteristics as described above.

CHEMISTRY OF ROCKS AND MINERALS

INTRODUCTION

Employing the rapid-rock-analysis methods of Shapiro & Brannock (1962) and Shapiro (1967) several ultramafic and associated rocks from Cabo Ortegal and the Mellid area were analysed by Miss M. van Wijk and Mr. K. F. M. Belfroid (Petrochemical Laboratory, Institute of Geology and Mineralogy, University of Leyden). Analyses from the Castriz area and additional analyses from Cabo Ortegal are already quoted by Warnaars (1967) and Vogel (1967), respectively.

Tables and Figures of chapter III are presented in Appendices 1 and 2.

Serpentinization of the majority of the ultramafic rocks analysed notably reduces MgO and SiO_2 contents. Several attempts have been made to calculate pre-serpentinization compositions of ultramafic rocks (Thayer, 1966, and Carswell, 1968a) to afford better comparison with the various pyrolite models. If the constant-composition-principle is held to obtain, with only introduction of H_2O assumed, recalculation on a water-free basis with reduction of ferric to ferrous iron is easily achieved.

Thayer (1966) considers serpentinization mainly as a constant volume reaction, with addition of H_2O and leaching of SiO_2, MgO and FeO, although Hostetler et al. (1966) strongly questioned abundant migration of MgO and on thermodynamic grounds considered removal of SiO_2 very improbable.

With regard to the ultramafic rocks under study, indications for a marked increase of volume could neither be detected in the field, nor in thin section. Significant migration of elements, however, is wholly absent, although locally small-scale migration certainly exists. The author is under the impression that a considerable volume increase will generally be very difficult, if not impossible, to prove in tectonically emplaced and metamorphosed peridotites; consequently, he prefers a constant composition reaction – peridotite acting as a more or less elastic sponge – over a constant volume reaction implying large-scale migration.

Recalculation on a H_2O- and CO_2-free basis with reduction of ferric to ferrous iron (this procedure is commonly used when pre-serpentinization compositions are calculated) renders analysis directly comparable with already H_2O-poor samples, such as FCM 1 and 1 M 9.

As the analysis of Cr and Ni did not belong to the routine analytical procedure followed in the petrochemical laboratory, these elements were not analysed; although Cr has been determined by neutron activation analysis (see Table III-5), these results have not been incorporated in the whole-rock analysis.

Chemical analysis of vein and band material is seriously hampered by the difficulties experienced in sampling: the thickness of the veins, which have a limited extension, mostly does not exceed 3 cm, and tiny dilatation veins of serpentine nearly always intersect the veins of interest.

Furthermore, garnet-bearing veins are very inhomogeneous: cores of green spinel, surrounded by garnet, in a matrix of pyroxenes and amphiboles; grain-size varying from medium to coarse; highly variable mineral modal compositions from garnet-clinopyroxene to nearly pure amphibole assemblages. Consequently, cleaned samples often did not weigh more than 30–40 gr: an amount far too low to get a reliable idea of the mean composition of a vein, although the 10 individual analyses, admittedly, display great similarities.

Calculation on a H_2O-free basis is impossible in this case because of intersecting serpentine veins, the substance of which must be subtracted from the true vein material. Estimation of the serpentine content present in the analysed rock sample can be evaluated from 1) modal analyses, although in these inhomogeneous samples these cannot be considered to be thrustworthy at all; 2) the volume of serpentine visible in the analysed hand-specimen and 3) the amount of water present after subtraction of a specific percentage, assumed to be present in amphibole.

An average of about 10–15% of serpentine is thought to be present, reducing MgO contents by a few percents, but not essentially changing vein compositions. Mineral analyses combined with incidentally performed point-counter analyses already easily show that MgO contents should be lower. Although serpentine-free analyses can be produced in this way, only the original analyses are presented, while only the mean vein composition is "deserpentinized".

NEUTRON ACTIVATION ANALYSIS

Determination of some minor and some trace elements has been carried out at the Department of Chemistry, Reactor Centrum Nederland at Petten (N.H.); for the techniques of this method the reader is referred to Oosterom & Das (1969). The main object of these analyses is to see whether significant differences are present between peridotites and the various pyroxenites. The results are presented in Table III-5.

With regard to Co and Sc contents a distinct difference is noted between peridotites and pyroxenites (see also Stueber & Goles, 1967): average values of 11 and 36 ppm Sc and 142 and 76 ppm Co were found in peridotites and pyroxenites, respectively. Marked differences in the contents of these elements between garnet-bearing and garnet-free assemblages are not encountered.

Na and Mn contents generally are in agreement with "wet-chemical" determinations; both values are given for comparative reasons.

Cr contents in the garnet-bearing veins and bands are conspicuously lower than those of garnets from peridotites. Relatively high Cr contents are recorded from

two amphibolized pyroxenite samples and the brown ceylonite orthopyroxenite.

According to the investigations of Frey (1969) on rare earth contents of minerals in primary peridotites from the Lizard, Eu contents in clinopyroxene are markedly higher than in olivine, orthopyroxene and spinel, while Ce is mainly concentrated in spinels. The abundances of these elements in garnets and amphiboles are not known. The only conclusions that may be drawn are that peridotites show lower relative contents of Eu than pyroxenites, while the high amount of Ce in the pargasitite sample PC 5 is probably due to the presence of grains of zircon. There appears to be no relation between Eu and Ce contents.

ELECTRON MICROPROBE ANALYSIS

In the last decade electron microprobe analysis of rock-forming minerals increased tremendously. For techniques of the method the reader is referred to review papers by Smith (1965), Keil (1967), Long (1967) and Sweatman & Long (1969). Compared with wet-chemical analysis the great advantage of this method mainly consists of its ready applicability and its, usually non-destructive, analysis in situ. Time-consuming rock-crushing and mineral concentration is no longer imperative. Standard-size, rectangular, polished thin sections can be used in some apparatus, although in most apparatus only round specimens can be accomodated, due to the geometry of the sample-holder.

Usually spot analyses are made on clean, flat surfaces (without inclusions, exsolution lamellae, alteration products, cracks and pits) of the unknown minerals, resulting in a quantitative analysis of a volume of about 20 cubic microns, depending on analytical conditions.

It is evident that more grains should be analysed to obtain a statistically reliable analysis of a mineral in a rock, supposing the mineral is homogeneous and any clean spot on its surface can be chosen for analysis. This is really a disadvantage of the method; a wet-chemical analysis of a pure, or nearly pure, mineral concentrate is far more representative of the composition of a mineral than the average of a few electron microprobe spot analyses, the analysed volume being infinitely small compared to the chemically analysed volume. When the minerals have crystallized or completely recrystallized under equilibrium conditions or otherwise have homogeneous compositions, no compositional differences between the chemical analysis of a pure mineral concentrate and an electron microprobe analysis should be obtained if systematic errors are neglected. Only the much larger population gives statistically more reliable results, while microprobe spot analyses represent a few grab samples only. Limitations of this working hypothesis relate to the purity of the mineral concentrate, the uniform distribution of elements over the grains even under equilibrium conditions, and the randomness of sampling the analysed grains. Mineral concentrates are never 100%

pure, even when inclusions, exsolutions and alteration products are disregarded. When it is impossible, as it usually is, to get rid of included and exsolved phases present within the host mineral (orthopyroxene lamellae in clinopyroxene and vice versa, blades of spinel in pyroxenes, rutile in amphibole and garnets) wet-chemical analyses represent at their best solid solution compositions. With electron microprobe analysis a similar overall composition can also be measured with area analysis instead of spot analysis, although it is not done customarily. Microscopical estimation of the amount of exsolved material should be carried out very carefully, as the three-dimensional aspect of thin sections should also be taken into consideration: usually amounts of exsolved phases tend to be highly overestimated.

Uniform distribution of elements over grains of the same mineral species under equilibrium conditions may not be a correct postulate, yet it is inherently assumed to apply in bulk analyses of mineral concentrates. Electron microprobe analysis, however, may directly reveal compositional variations between various grains, even in the content of major elements and even when equilibrium conditions undoubtedly prevailed.

If these variations are reproducible, a certain deviation from uniform distribution must be taken for granted and calculated distribution coefficients should be handled very carefully. These considerations invariably lead to the question how many and which grains should be analysed (i.e., how many spot analyses should be carried out) in order to get a reliable picture of the mean composition of a homogeneous, unzoned mineral. For economic reasons the number of grains selected for analysis is usually limited from 3 to 5. Although this selection should be completely arbitrary, in practice, the largest and "cleanest" grains are commonly chosen for analytical convenience. It should, however, be born in mind that small recrystallized grains may well have compositions different from those of megacrystals and phenocrysts different compositions from groundmass grains.

Crystallographic orientation does not seem to have any effect on the amount of X-ray generation in rock-forming minerals, although Smith (1965) noted different X-ray yields from different crystal planes of one sphalerite crystal.

In hydrous silicates (e.g., sheet silicates, zeolites), however, evaporation of structural water may be expected to occur at different rates parallel or perpendicular to the basal cleavage, influencing the reliability of the analyses, although so far no indications of this have been detected by the author.

When measurements are carried out under stable instrumental conditions, a precision of 1% relative is usually obtained, at least when counting statistics are taken into consideration and, of course, the same areas are re-examined. By taking always two or even more standards for the same elements (e.g., corundum and kyanite for Al, quartz and wollastonite for Si) this precision and instrumental stability can always be checked.

In aphanitic samples electron microprobe whole-rock analyses can be made by continuous area-scanning (the sample continually moves under a scanning electron beam). The method may successfully be applied when the amount of rock is too low for a chemical analysis or when small-scale chemical variations – e.g., in contact zones – have to be investigated. For comparative reasons two analyses are given, together with the chemical analyses in Table III-4.

Mineral analyses have been carried out with a Cambridge Scientific Instruments Geoscan; the most important instrumental data are mentioned and the pertinent correction procedure briefly discussed.

Polished thin sections and standards were coated with a film of approximately 200 Å of carbon obtained by vacuum evaporation from a carbon arc. Only major and minor elements were analysed. An investigation of the trace elements present in the various minerals lies beyond the scope of this study: contents less than 0.1 % are not indicated in the Tables. Usually the elements Na, Mg, Al, Si, K, Ca, Ti, Cr, Mn, Fe and Ni have been measured, unless some of these elements manifestly were absent or present below the 0.1 % level in certain minerals, e.g., Na and K in olivine and garnet.

Most elements have been analysed using an accelerating potential of 15 kV, while 20 kV was commonly applied for the analysis of the relatively heavy elements Cr, Mn, Fe and Ni. To facilitate the choice of a clean area of measurement all analyses have been carried out with a highly focussed electron beam, giving a resolution of the backscattered electron image of about 1 micron on the fluorescent screen of the cathode-ray tube. An electron spot with a diameter of about 1 micron results in a mean X-ray excitation volume of about 20 cubic microns, varying with the used characteristic wavelength of the analysed element, the applied kilovoltage and mineral density. Counting times were 50 seconds per grain (usually 3–5 grains were selected for a mineral analysis), while sometimes after every 10 seconds the specimen or the beam was shifted over a few microns in order to check homogeneity. Contamination and/or surface damage does not occur in the analysed minerals after an electron bombardment period of 50 seconds. In analysing feldspars, however, defocussed spots and/or continuous sample-shifting must be applied to prevent large-scale evaporation of sodium.

Sample-currents generally have been chosen so that a calculated precision of about 1% at the 10% level is obtained; this roughly corresponds to 80–100 pulses/sec./percentage of analysed element in standard. Following a suggestion by Ziebold (1967), the author is of the opinion that actual standard deviations in the individual measurements are about twice as high as standard deviations due solely to X-ray counting statistics. Uniform corrections for background (characteristic lines are superimposed upon the continuous spectrum) and dead-time of counters and electronic circuitry having been applied, different bulk chemistry of standard and analysed mineral necessitates corrections for mass-absorption, atomic number effect, characteristic and continuous fluorescence.

The contribution of both fluorescence corrections to the overall correction factor is usually small in silicates (generally less than 2%), while the high take-off angle of the instrument (i.e., 75°) substantially decreases mass-absorption corrections.

Large corrections can of course be avoided or at least very much reduced, if chemically analysed mineral standards that are homogeneous on micronscale with more or less equal composition and structure can be used. However, any attempt to realize this is doomed to fail as a tremendous set of mineral standards would be required: for the simple olivine solid solution series at least 4 different members (e.g., Fo_{20}, Fo_{40}, Fo_{60} and Fo_{80}) are necessary to establish a reliable correction calibration curve. Furthermore, it is rather difficult to get hold of accurately analysed, homogeneous mineral standards without admixtures of other mineral phases!

The use of simple oxides or silicates (several oxides cannot be used because of their physical properties) and pure elements, as propagated i.a., by Long (1967) and Sweatman & Long (1969), necessitates the evaluation of a rigid correction procedure, which, however, once established, can be universally applied.

The standards used are: albite (Na), periclase and olivine (Mg), corundum and kyanite (Al), quartz and wollastonite (Si), orthoclase (K), wollastonite and diopside (Ca), synthetic TiO (Ti), Cr metal (Cr), rhodonite (Mn), Fe metal and olivine (Fe), Ni metal (Ni).

Apparent concentrations have been corrected with a universal computer program – strongly modified after Springer (1967a) – in which the following correction procedures are applied: *mass-absorption correction* – expression of Philibert (1963) with $h = 1.2\ A/Z^2$, mass-absorption coefficients from Heinrich (1966), *a*) Heinrich σ (1967) or *b*) Duncumb & Shields σ (1966); *generation factor* – *c*) stopping power formula of Bethe (1930) in simplified form (Reed, 1964) with backscatter factor from Bishop (1968) $(R = f(\bar{Z}))$, or *d*) Bethe formula with variable J (Duncumb & Reed, 1968) in combination with

$$\bar{R} = \sum_{i=1}^{n} c_i R_i$$

from Bishop (1968), or *e*) Bethe formula with variable J (Springer, 1967b) and backscatter factor

$$\bar{R} = \sum_{i=1}^{n} c_i R_i$$

from Bishop (1968); *characteristic fluorescence* – formula given by Reed (1965); *continuous fluorescence* – formula given by Springer (1967c). The various methods applied lead toward 6 combinations (*ac, ad, ae, bc, bd, be*), which are all printed out. The correction code *ad* proves to give best results when the lighter elements are analysed with 15 kV – Sweatman & Long (1969) also

propagate this method – while for the correction of the lighter elements analysed at 20 kV the combination *bc* seems to be favourable (Kieft & Maaskant, 1969).

Peridotite compositions (Table III-1)
Comparing chemical analyses of peridotitic rocks from the various areas, extreme care should be taken, as different degrees of serpentinization prohibit a direct comparison between the original analyses: analyses should first be recalculated. Original and recalculated, H_2O-free analyses are presented in Table III-1. Three almost completely serpentinized samples (V 3, 2 M 2 and 6 M 2) show relatively low contents of CaO and alkalies, and higher MgO percentages. They might represent more dunitic compositions, although a possible loss of CaO and alkalies with advanced serpentinization (more than 90%) leading towards approximately monomineralic serpentine compositions with some magnetite and chromite added, should not be ruled out (Page, 1966; Paraskevopoulos, 1969).

Leaving these samples out of consideration, the presented nine analyses (6 from Cabo Ortegal, 2 from the foliated Mellid peridotite and 1 of a peridotite from the Castriz area) do not show essential differences: variations in MgO and SiO_2 are small (bearing in mind the rigid method of recalculation), Mg/Fe ratios show minor fluctuations, amounts of CaO and Al_2O_3 are rather constant, while low contents of alkalies and TiO_2 are conspicuous.

The analyses resemble peridotite analyses from the Lizard (Green, 1964), Southern Norway (i.a., Carswell, 1968a) and Morocco (Kornprobst, 1969). When comparisons are made with the various pyrolite models proposed (Ringwood et al., 1964; Green & Ringwood, 1967a), pyroxene and garnet pyrolites are best fitted, while assumed mantle compositions as well as model pyrolites contain higher amounts of TiO_2 and alkalies (see Table III-1).

Garnet-bearing veins and bands (Table III-2)
Chemical fluctuations in the composition of these veins distinctly reflect mineralogical variations: if analyses are given in the order of increasing SiO_2 contents it is visible that CaO and Na_2O vary in sympathy with SiO_2 corresponding to increasing ratios of clinopyroxene/garnet or, in the majority of the cases, of amphibole/garnet.

Amphibole-rich veins, or rather amphibole-rich samples (as the often small amount of material cannot be considered representative for the whole vein) generally show higher amounts of alkalies, higher Fe_2O_3/FeO ratios and lower amounts of MnO. The main effect of the unavoidable presence of serpentine veinlets concerns enhancement of MgO contents by about 1–2%. The analysis of a garnet-spinel pyroxenite (Vogel, 1967) with 19.8% MgO and a low percentage of water might be an indication of this general MgO increase.

On the whole, analyses still show a surprisingly uniform character: MgO … 21.5–23.3%; CaO … 7.3–10.2%, with sample L 3, which consists almost

entirely of garnet, as an exception; FeO + Fe_2O_3 … 6.1–9.6%, (PC 5, with only 4.5%, is a pargasitite vein) Al_2O_3 … 10.4–15.4% and SiO_2 … 38.7–44.5%.

The mean composition of these veins displays a picritic character, a few analyses revealing the presence of normative nepheline. This resemblance is even more pronounced when 10% of serpentine is subtracted. The picrite that Green & Ringwood (1967a) used for experimental investigations has been selected for these comparative purposes (fig. IV-1).

Analyses from the Cabo Ortegal spinel clinopyroxenite (R 378) and amphibole wehrlites from the Castriz area (FW 753) closely match the composition of the garnet-bearing veins, although in R 378 the Mg + Fe/Ca ratio is definitely lower.

Other veins and bands and some rocks of the Castriz area (Table III-3)
The chemical compositions of the brown ceylonite orthopyroxenite (V 1403b) and a wehrlite from the Castriz area (FW 769) show an intermediate character – relative to either MgO, CaO or Al_2O_3 contents – between peridotitic host rock and garnet-bearing veins. A marked difference, however, is a higher SiO_2 amount in both samples. Two amphibolized pyroxenitic bands, samples MP 20 and MP 21, exhibit the same chemical phenomena as the garnet-bearing veins, except for higher SiO_2 and CaO and lower Al_2O_3 contents. The composition of the composite vein, MP 18 (central part as MP 20 and MP 21, external zones consisting of chlorite orthopyroxenite), predictably displays higher Mg/Ca ratios. In a coarse-grained olivine gabbro, FW 848, from the Castriz area, the lowest Mg/Ca ratio of all rocks analysed is obtained.

Olivines (Table III-6)
Olivine analyses in various samples from Cabo Ortegal all show nearly equal Mg/Fe ratios: fresh or partly serpentinized, all have 100 Mg/Mg + Fe ratios of about 90%. In a spinel-free amphibolized pyroxenite (MP 20), however, the forsterite content is markedly less: 87%. The foliated Mellid peridotite contains olivines with the same forsterite content as the Cabo Ortegal peridotites, although in one sample, 5 M 2, with lenses of garnet and abundant amphibole, a forsterite content of 87.9% has been measured.

The chlorite-amphibole peridotite NE of Mellid contains olivines with still lower amounts of the forsterite molecule: 85.9%.

Forsterite contents of the olivines in the Castriz ultramafic and related rocks decrease from spinel-clinopyroxene peridotite, via amphibole peridotite and wehrlite to olivine-gabbro. The analyses nicely correspond to analyses given by Warnaars (1967), although he found higher forsterite contents in a recrystallized spinel-clinopyroxene peridotite (FW 928) than in olivines occurring in the pyroxenitic part of this sample. Olivines in the spinel-amphibole peridotite from the Santiago area are approximately

similar to those from the gabbros in the Castriz area. All olivines analysed are homogeneous.

A distinct positive correlation can be seen between Mg/Fe ratios in olivines and whole-rock, giving an idea about this ratio in the rock when no whole-rock analysis is available.

Significant differences in composition between primary and recrystallized olivine have not been detected.

Orthopyroxenes (Table III-7)

Variations in the composition of the orthopyroxenes from the Cabo Ortegal peridotite are small: Al_2O_3 contents fluctuate between 3.1 and 4.3%, CaO contents are low and Mg/Fe ratios are relatively constant.

Differences between primary and recrystallized orthopyroxenes consist of lower Al_2O_3 contents and a somewhat higher Mg/Fe ratio in the latter. Conspicuously higher amounts of Al_2O_3 are measured in a brown ceylonite orthopyroxenite, V 1403b, in which large phenoclasts of both orthopyroxene and clinopyroxene occur, while abundant exsolved spinel indicates still higher original values; higher contents of Cr_2O_3 correspond to these higher Al_2O_3 percentages.

Orthopyroxenes in the spinel sensu stricto clinopyroxenite, R 378, also possess high amounts of Al_2O_3 in combination with lower Mg/Fe ratios and higher CaO values. A recrystallized amphibolized pyroxenite, MP 20, has orthopyroxenes with the lowest Al_2O_3 content of all Cabo Ortegal orthopyroxenes analysed, while Mg/Fe ratios are equal to those in the host peridotite orthopyroxenes.

In the foliated Mellid spinel-pargasite peridotite partial analyses of orthopyroxenes were specifically directed to differences between primary and recrystallized orthopyroxenes. Core, recrystallized rim and surrounding kelyphite of orthopyroxene occurring within garnet show a steady decrease of Al_2O_3 contents (4.0–3.2–2.7%) and CaO contents (0.4–0.2%) against a small increase of the Mg/Fe ratio. In garnet-free environments the same characteristics were encountered.

The increase of this Mg/Fe ratio can readily be explained by the exsolution of spinel, which, having Mg/Fe ratios that vary between 2 and 3, automatically increases Mg/Fe ratios in its host orthopyroxenes.

The same trend has been detected in a pyroxenitic part of the spinel-clinopyroxene peridotite sample FW 928 from the Castriz area: Al_2O_3 6.4–5.8–4.6%, MgO 30.2–31.0–32.1%, FeO 9.7–9.3–8.4%.

Orthopyroxene analyses from wehrlitic and gabbroic rocks from the Castriz area distinctly reflect the lower Mg/Fe ratios of their host rocks in their compositions, with Al_2O_3 contents ranging from 3.0 to 4.0%.

Summarizing, the following remarks can be made:

1) Mg/Fe ratios in orthopyroxenes are dependent on rock chemistry;
2) within any one sample an increase of this ratio corresponds to lower contents of Al_2O_3, Cr_2O_3 and CaO (exsolved spinel and clinopyroxene);

3) orthopyroxenes having highest Al_2O_3 contents within one sample, represent the best approximations of a primary orthopyroxene composition;
4) distinctly varying Al_2O_3 contents with a more or less constant base level indicate a transition from primary towards recrystallized orthopyroxene, possibly under re-equilibrated conditions;
5) no significant differences between orthopyroxene compositions in peridotite and garnet-bearing veins or bands, neither at Cabo Ortegal nor at Mellid, could be detected. This may be explained by assuming that the liquid, from which both orthopyroxene and clinopyroxene crystallized, was saturated in these phases.

Clinopyroxenes (Table III-8)

Clinopyroxenes from Cabo Ortegal peridotite and garnet-bearing veins display great similarities: high Mg/Fe ratios, generally small amounts of sesquioxides and very low jadeite contents. It should be noted, however, that with electron microprobe analysis no distinction can be made between ferrous and ferric iron, at least not in these relatively Fe-poor minerals. Variations between different samples and within the same sample are small, Al_2O_3 fluctuating between 1.2 and 2.7%. Distinctly recrystallized grains give the lowest Al_2O_3 values. Phenoclasts of clinopyroxene in the brown ceylonite orthopyroxenite, V 1403b, contain higher Al_2O_3 contents (up to 5.5%) and, with decreasing Al_2O_3, show a corresponding decrease of TiO_2, Cr_2O_3, NiO and MgO against a distinct increase of CaO. The behaviour of Fe is not clear, mainly because of its low concentration level.

Clinopyroxenes in the spinel sensu stricto clinopyroxenite, R 378, exhibit similar phenomena as do orthopyroxenes in this sample: high amounts of Al_2O_3 (6.5%), a distinctly lower Mg/Fe ratio, while Na_2O and TiO_2 contents are higher than in other Cabo Ortegal clinopyroxenes.

Lowest Al_2O_3 values (0.4%) have been encountered in the recrystallized amphibolized pyroxenite, MP 20, while Mg/Fe ratios are more or less equal to those in the peridotite clinopyroxenes.

Clinopyroxenes from the foliated Mellid peridotite differ from those from the Cabo Ortegal peridotite in that they have somewhat lower Mg/Fe ratios, lower CaO contents, and higher Al_2O_3 and Na_2O percentages. In the spinel-clinopyroxene peridotite from the Castriz area, FW 928, Warnaars (1967) notes a primary and a recrystallized assemblage. Clinopyroxene in the latter assembly contains less Al_2O_3 and more CaO, corresponding to the above-mentioned trends. Clinopyroxenes occurring in a pyroxenitic part of the same sample, however, show an increase of MgO with decreasing Al_2O_3 contents. In wehrlitic and gabbroic rocks from the Castriz area a marked increase of Na_2O and TiO_2 is found in clinopyroxenes, while, resembling the common trend from diopside towards more augitic pyroxenes, Mg/Fe ratios are lower and CaO decreases.

Finally, regard should be had to the totally different

character of a clinopyroxene occurring in a spinel-garnet clinopyroxenite band (B 439a).

Unlike low contents of Al_2O_3, TiO_2 and Na_2O usually found in garnet-bearing veins (see above), percentages of these elements in this clinopyroxene are distinctly higher, while amounts of MgO, FeO and CaO are approximately equal to the amounts encountered in gabbroic clinopyroxenes from the same area. With respect to clinopyroxenes mentioned above, some general remarks may be made:

1) jadeite contents are very low. Even in wehrlitic and gabbroic rocks the maximum value of 1.3% Na_2O is by no means high;
2) Mg/Fe ratios in clinopyroxenes are dependent on rock chemistry;
3) remarks 3), 4) and 5) mentioned under orthopyroxenes also apply to clinopyroxenes;
4) a decrease of Al_2O_3 in clinopyroxenes within one sample corresponds to a notable increase of CaO (due to exsolved spinel). In the pyroxenitic part of peridotite FW 928 the Al_2O_3 content remains approximately constant, while MgO increases: this divergent phenomenon can be ascribed to exsolution of the Tschermakite molecule $CaAl_2SiO_6$;
5) a clear trend of Mg/Fe ratios with decreasing Al_2O_3 contents is not visible: MgO decreases or increases (see above) while the low level of FeO also hampers a clear insight in the chemical behaviour of this oxide;
6) large variations in clinopyroxene compositions in a composite dyke occurring in the lherzolite of Lers (Avé Lallemant, 1967) are shown in Figure III-1).

Garnets (Table III-9)

Pyrope-rich garnets occur in veins, lenses or eyes in the peridotitic rocks of Cabo Ortegal and the ultramafic rocks around Mellid, while this mineral has also been found in a few bands in the spinel-clinopyroxene peridotite from the Castriz area. Compositions are rather uniform, as was to be expected from vein analyses, and variations are mainly dependent on their mode of occurrence: 1) remnants in a mainly pargasitic groundmass show lower pyrope contents and higher amounts of almandine and spessartine molecules, CaO being rather indifferent; 2) garnets enclosed in host peridotite (FCM 1) or at the borders of the veins (MP 10) have higher contents of Cr_2O_3 than garnets in the centre of the veins.

The first feature mentioned can readily be explained by the inhomogeneous character of the mineral: although being largely homogeneous, large grains always show a decrease of the pyrope content both near their borders (kelyphitic rims or amphiboles) and against included amphibole. Figure III-2 shows several step-scanning profiles of Mn and Fe radiation across garnet boundaries in a Mellid garnet (1 cm $\varnothing$). Fe and Mn contents generally increase very slowly; steeper increases, particularly of Mn, are found only in the last 25 micron from the border. Near included minerals these increases are significantly less.

Step-scanning profiles of Mg, Fe, Ca and Mn

radiation across a small remnant of garnet (65 micron $\varnothing$) in a pargasite vein, MP 28, show a small homogeneous core with less pyrope-bearing rims, while CaO remains constant (Plate VIb). Within the same vein higher Cr_2O_3 percentages seem to correspond to somewhat higher pyrope contents.

The colour of usually associated spinel often gives an indication of the Cr content in the garnet; e.g., brown, Cr-rich spinel accompanies garnet with 1.1% Cr_2O_3 in sample FCM 1.

As in electron microprobe analysis no distinction can be made between ferrous and ferric iron, andradite contents are not known. Cation ratios, however, reveal that this amount should be very low, as was postulated for high-pressure garnets by Smulikowski (1964).

Comparisons with garnets from garnet peridotites (i.a., Bohemian massif, Fiala, 1966; Southwestern Norway, O'Hara & Mercy, 1963) show distinctly lower pyrope contents and Cr_2O_3 percentages in the Galician garnet-bearing assemblages, as can be seen in fig. III-3 (after Carswell, 1968a).

Kornprobst (1969) also notes a positive correlation between MgO contents of garnet and host rock up to a certain "saturation level" of the garnet, attained in peridotites and Mg-rich pyroxenites.

To verify this statement the author analysed garnets from two garnet peridotites with enclosed layers of garnet clinopyroxenite: samples AR 30a (Alpe Arami, Ticino, Switzerland; for reference, see Möckel (1969) and O'Hara & Mercy (1966)) and SA 8 (Zöblitz, Erzgebirge, E Germany; for reference, see Behr et al., (1965) and Rost (1961)). Pyrope contents in both peridotite and pyroxenite garnets are approximately equal; calculated on a basis of Mg + Ca + Fe + Mn = 3.00 compositions are $Mg_{1.97}Ca_{.39}Fe_{.61}Mn_{.03}$ and $Mg_{1.96}Ca_{.37}Fe_{.64}Mn_{.03}$ for AR 30a and $Mg_{2.13}Ca_{.30}Fe_{.55}Mn_{.02}$ and $Mg_{2.14}Ca_{.28}Fe_{.56}Mn_{.02}$ for SA 8 in peridotites and pyroxenites, respectively. Cr contents, however, markedly differ: 1.5 and 0.5, 1.6 and 0.3 wt. % Cr_2O_3 in peridotite and pyroxenite garnets from AR 30a and SA 8, respectively.

The relation between a_0, n_D and the chemical composition of garnets has already been investigated frequently. Generally, pyrope-rich garnets possess, compared with other garnets, relatively low refractive indices and small unit cell sizes (Frietsch, 1957, and Winchell, 1958). A reliable estimate of the pyrope content on the basis of these physical properties – to which the specific gravity may be added – is, however, not possible when appreciable amounts of Cr are present. Fiala (1965) noted a positive correlation between the refractive index and the Cr content in garnets from Bohemian garnet peridotites: n_D from 1.740 to 1.765 and wt.% Cr_2O_3 from 0.85 to 6.85% with approximately equal contents of pyrope (69.9–73.6 mol. %).

Vogel (1967) already gave some a_0 and n_D values for garnets from Cabo Ortegal garnet pyroxenites: 11.537/1.737, 11.55/1.741 and 11.57/1.742 for a_0

(± 0.006) and n_D (± 0.002) in samples R 70, R 312 and R 348, respectively. The author determined the refractive index for two Mellid garnets (M 1 and 5 M 2): $1.732 < N < 1.738$. Unit cell sizes varying from 11.536 to 11.543 ± 0.005 were determined for two Mellid garnets (5 M 2 and M 1) and two Cabo Ortegal garnets (L 1 and V 1403a).

The relation between refractive index and Cr content, noted by Fiala (1965), was also found in garnets from sample SA 8: N 1.745 ± 0.002 and N 1.740 ± 0.002 for garnets in garnet peridotite and garnet clinopyroxenite, respectively. Small differences in the a_0 values were also encountered: 11.522 and 11.517 ± 0.005, 11.536 and 11.531 ± 0.005 in perido- tite and pyroxenite garnets of SA 8 and AR 30a, respectively.

Interstitial (? hydro) grossular – total of oxides 98.5% – is present in a plagioclase wehrlite (FW 809b) from the Castriz area, while small, hypidiomorphic grains of hydroandradite are abundantly present in a com- pletely serpentinized peridotitic rock from Cabo Ortegal (R 72). Analyses of these minerals are not given.

Several garnets from the composite dyke in the lherzolite of Lers have been analysed (see fig. III-1). When going from the host lherzolite toward the centre of the dyke, the first garnets appear as small blebs in clinopyroxenes, directly followed by interstitial garnets in close association with green spinel. The blebs of garnet and the cores of the interstitial garnets possess approximately equal compositions.

When calculated on a basis of $Mg + Ca + Fe + Mn = 3.00$, their composition is $Mg_{1.94}Ca_{.42}Fe_{.61}Mn_{.03}$, while the rims of the inter- stitial garnets have different compositions: $Mg_{1.71}Ca_{.44}Fe_{.79}Mn_{.06}$. In the central parts of the dyke large, possibly primary garnets are found; their composition (core and utmost rims, respectively) is $Mg_{1.79}Ca_{.49}Fe_{.70}Mn_{.02}$ and $Mg_{1.51}Ca_{.50}Fe_{.93}Mn_{06}$ The same trend as noted in the Galician garnets is observed in these samples: an increase of Fe and Mn toward the rims of the garnet. Lower pyrope contents in the garnets of the central parts of the dyke are, in all probability, due to lower MgO contents in this central rock assemblage. The position within the dyke of these analysed garnets is given in Fig. III-1.

Amphiboles (Table III-10)
The major difference in chemical composition between the two generations of amphiboles found at Cabo Ortegal lies in the amount of Al substitution in the four coordinated Z position. The older generation contains less SiO_2 and more Al_2O_3; sympathetically with Al an increase of alkalies and TiO_2 is found, while Mg/Fe ratios are slightly lower.

Cr_2O_3 percentages depend mainly on the local availability of this element (see Table III-10, nr 2). The relation between colour and chemical composition is obscure: although one might distinguish between

slightly greenish, older amphiboles and nearly colour- less, secondary ones within one sample, this character- istic generally does not hold.

In the opinion of the author the colour seems to vary mainly with TiO_2: greenish specimens – less than 1.0%, slightly brownish specimens – 1.0–2.0%, and distinctly brownish amphiboles – more than 2.0% TiO_2. Light-brownish amphibole from the spinel sensu stricto clinopyroxenite, R 378, is an example of a still larger Al substitution with increased amounts of alkalies and TiO_2.

Amphiboles from the amphibolized pyroxenite (MP 20), the chlorite-amphibole peridotite E of Mellid (96–D2–5) and the peridotite sample from the Santiago area (95–A4–51) closely resemble each other in that they contain much less Al_2O_3 (7.0, 5.7 and 8.3%, respectively) than the above-mentioned am- phiboles.

The foliated Mellid peridotite and its garnet- bearing assemblages contain, dependent on the sample chosen, brownish as well as greenish amphiboles. Differences with Cabo Ortegal amphiboles mainly consist of somewhat higher amounts of alkalies and TiO_2 in the former amphiboles.

Brownish amphiboles from Castriz wehrlitic and gabbroic rocks are characterized by high amounts of TiO_2 and lower Mg/Fe ratios.

Abundantly exsolved ilmenite and white clouds (in reflected light) of a probably leucoxenic nature often turn these amphiboles (especially in wehrlitic rocks) nearly opaque and suggest a still higher primary content of titanium.

Limitations of electron microprobe analysis are severely felt when structural formulae of these am- phiboles are established, especially while also the water content remains unknown. In these cases there is no satisfying method to present a structural formula $A_{0-1}X_2Y_5Z_8O_{22}(OH, F)_2$.

Two methods of recalculation are given: both are based on the procedure followed by Phillips (1963, 1966) and Whittaker (1968). Vacant sites, however, have not been created.

1) All Fe is taken as FeO. Indeed, most pargasite analyses listed in Deer, Howie & Zussman (1963, Vol. 2, pp. 286–287) show a majority of ferrous iron. The excess of Mg, Fe, Mn and Ni in the Y site is brought to the X site and subtracted as cummingtonite molecule because this amphibole end member cannot be placed in the amphibole compositional space of Phillips (1966). The remainder is recalculated on a cumming- tonite-free basis. Equal Mg/Fe ratios are calculated for cummingtonite and calcic amphibole.
2) The cummingtonite molecule is subtracted in the first method; in the second method it is eliminated by the assumption that all Mg, Fe, Mn and Ni is present in the Y site and only Ca and Na fill the X site. Ferric iron is calculated on the basis $Y + Z = 13$.

It should always be kept in mind that more or less artificial formulae are drawn up: the calculated

amounts of FeO and Fe_2O_3 depend entirely on the accuracy with which all other elements were analysed, while also the amount of water influences these contents. The reproducibility of appreciable amounts of calculated ferric iron in the investigated amphiboles of Cabo Ortegal, however, forms a strong argument in favour of the presence of this ion in the formula, although systematic, analytical errors might be involved. On the other hand, comparison with whole-rock compositions of nearly pure pargasite veins strongly suggests an overestimation of ferric iron in the structural formula of the average Cabo Ortegal amphibole.

The water content is not known; as totals of other oxides vary between 96 and 98% an amount of 3% should be present (leaving other minor components out of consideration), which, in view of the results of chemical analyses, does not sound implausible. A semiquantitative analysis of F and Cl in a pargasite from the Mellid spinel-pargasite peridotite revealed that both elements are not present above the 0.2% level.

An unknown or inaccurately known water content makes a calculation on a basis of 23 O preferential to calculation on a basis of 24 O, as has been argued by Borg (1967) and Leake (1969).

Calculations have been performed in the following order (second method):

1) numbers of cations are calculated on a basis of 23 O (all Fe still taken as FeO);
2) Y + Z is reduced to 13.00, all numbers of cations are multiplied with this reduction factor;
3) sum of valencies is calculated (always less than 46.00 because of the Y + Z reduction) and the difference with 46.00 represents the number of ferric iron cations;
4) weight percentages of FeO and Fe_2O_3 are calculated.

In Fig. III-4 amphibole analyses are plotted in terms of their yzcoordinates (Whittaker, 1968): y = number of Al^{VI} + Fe^{3+} + Cr + 2 Ti and z = number of Si in excess of 6. The amount of cummingtonite molecule is given in molecular percentages. The real structural formula probably lies in between the two formulae that are obtained in this way: a calcic amphibole with minor amounts of cummingtonite molecule and ferric iron. The author is fully aware of the shortcomings of the methods applied, but is of the opinion – also based on the analytical results and recalculations of other amphiboles analysed in our laboratory – that they represent useful approximations.

Four main groups of calcic amphiboles may be distinguished:

1) Ti-rich pargasites (kaersutitic pargasites) from wehrlitic rocks in the Castriz area: orange-brown to nearly opaque; large, negative 2V;

2) pargasites:
a) brownish pargasites from spinel sensu stricto clinopyroxenite, from the Mellid spinel-pargasite peridotite and Castriz gabbroic rocks;
b) common hornblendic pargasites from Cabo Ortegal and Mellid spinel-pargasite peridotite: usually slightly greenish to nearly colourless;
3) common hornblendes, often with edenitic affinities, in the other occurrences;
4) tremolite as a secondary product.

The Ti-rich pargasites closely resemble the kaersutites from wehrlites from San Carlos, Arizona (Prinz & Nehru, 1969), and the pargasites may be compared with those from the Lizard complex (Green, 1964).

Some remarks about the amphibole compositions may be made:

1) Mg/Fe ratios vary in sympathy with whole-rock compositions: highest values are obtained in peridotitic rocks and lowest in the gabbroic rocks from the Castriz area;
2) High contents of Ti in the host rock may be reflected in higher amounts of Ti in amphibole. However, the garnet-bearing veins are also relatively Ti-rich because of the frequent occurrence of ilmenite and the occasional presence of högbomite. The poikilitic texture – often visible in the Castriz wehrlites – and the interstitial character of brownish pargasite – in the spinel sensu stricto clinopyroxenite vein from Cabo Ortegal – distinctly point to an igneous origin of these amphiboles. Relative to this, the small amounts of calculated ferric iron in these amphiboles are noted. The amphibole from the spinel sensu stricto clinopyroxenite vein is an exception, although the very low amount of Si atoms in the structural formula might be an indication that the analysis is not reliable. If any value may be attached to these calculated amounts of ferric iron and if higher amounts of ferric iron are indicative of higher water pressures, it might be concluded that the kaersutitic amphiboles crystallized under lower water pressures than pargasites less rich in Ti. It may be inferred from the absence of these kaersutitic pargasites in the garnet-bearing veins that they are probably not a stable phase under catazonal conditions (hornblende-clinopyroxene-almandine subfacies). The main conditional differences between kaersutitic pargasites and Ti-poor pargasites might thus be higher temperatures, lower load and water pressures in the production of the former minerals.
3) Second generation pargasites from Cabo Ortegal peridotites possess lower Al/Si ratios than first generation amphiboles, while in chlorite-amphibole peridotites from the Mellid area common hornblendes are found with lower amounts of alkalies than pargasites.

With regard to these data and the experimental investigations of Boyd (1959) and Gilbert (1968) – see Fig. II-1 – it is suggested that higher amounts of alumina and alkalies in calcic Ti-poor amphiboles

reflect higher PT-conditions: pargasites are stable under high-pressure granulite-facies conditions, while common hornblendes may only occur under low-pressure granulite-facies to almandine-amphibolite-facies conditions.

Spinels (Fig. III-5)

In the analysed spinels the main elements are Mg, Fe, Al and Cr; percentages of other components (Mn, Ni and Ti) are generally low: MnO 0.0–0.4% (maximum in brown spinels), NiO 0.1–0.5% (maximum in green spinels) and TiO_2 0.0–0.3% varying arbitrarily. Only four elements being of significant importance, plotting of varying ratios (Mg/Mg + Fe vs. Cr/Cr + Al) is more illustrative than tabelled analyses. The impossibility of distinguishing between ferrous and ferric iron with electron microprobe analysis necessitates a calculation, based on the spinel structural formula, of the amount of this ion present. Generally the $Fe^{3+}/Fe^{2+} + Fe^{3+}$ ratios are less than 10%. In this way also Mg/Mg + Fe^{2+} and Cr + Fe^{3+}/Cr + Fe^3 + Al have been calculated and plotted in Figure III-5, so that a full line represents one single analysis. Opaque spinels were not analysed quantitatively. The general trend towards lower Mg/Fe and Al/Cr ratios, visualized in Figure III-5, is, however, distinctly pursued resulting in spinels of magnetite-chromite compositions.

Within one sample several types of spinel may occur, as described in the previous chapter. When compositions of individual grains were found to lie close to each other, an average has been calculated.

A correlation between colour and composition may be inferred, when a uniform thickness of the thin sections can be assumed:

	100 Mg/Mg + Fe	100 Cr/Cr + Al
light-green	70–80%	less than 5%
dark-green	55–65%	less than 5%
olive-green tints indicate small Cr admixtures		
light brown	about 75%	about 10%

brownish green to greenish brown spinels are found in the Fe-Cr-part of the ceylonite field
brown spinels, having 100 Cr/Cr + Al ratios between 25 and 50%, are situated mainly in the picotite field. The classification of Winchell & Winchell (1959) has been followed.

Large, light-green spinels in the garnet-bearing veins of Cabo Ortegal, in the garnet-bearing band in the Castriz area and in the spinel sensu stricto clinopyroxenite (R 378) prove to fall in the spinel sensu stricto field mainly. This applies only to nearly pure garnet or garnet-pargasite veins, as in veins containing considerable amounts of clinopyroxene (R 302b and V 1403a) brownish green to brownish spinels are always encountered. The light-brown spinel, occasionally encountered within garnets occurring in the

Mellid spinel-pargasite peridotite, also turns to be a spinel sensu stricto with somewhat more Cr present.

Brown spinels closely associated with garnet clusters in sample FCM 1 show conspicuous differences from brown spinels occurring in the host peridotite. Generally, peridotitic and wehrlitic spinels (analyses from Warnaars are added) are Cr-rich ceylonites or picotites.

Gabbroic spinels as well as spinels from the spinel-amphibole aggregates occurring in some wehrlitic rocks have distinctly lower Mg/Fe ratios than spinels from garnet-bearing veins; also the spinels from the peridotite sample from the Santiago area come into this area.

Variations in spinel composition in a composite dyke in the lherzolite of Lers show a clear trend, when going from the outer parts of the dyke (brown ceylonite orthopyroxenite) towards the centre (clinopyroxene and garnet).

A relation between Mg/Fe ratios in the whole-rock and spinel composition is clear, at least as far as garnet-bearing veins and gabbroic rocks are concerned.

Other minerals (Table III-11)

Several minerals have been partly or qualitatively analysed or checked: e.g., tremolite (Ca, Al), cummingtonitic amphibole (Ca, Mg, Fe and Al), vesuvianite and diaspore.

Others have been quantavely analysed for various reasons: chlorite because of its petrogenetic significance, högbomite for its unusual occurrence and badly known structural formula and ilmenite for the amount of geikielite molecule.

Chlorites derived from garnet-bearing veins (R 139 and MP 14) have compositions equal to chlorites from the peridotitic host rocks (BU 2 and HK 18), except that in peridotite chlorites higher Cr contents may be present. X-ray diffraction analysis of two of them (BU 2 and HK 18) revealed that 14 Å-chlorites are concerned here: $d_{001} = 14.24 \pm .04$ Å and $d_{060} = 1.540 \pm .002$ Å. When chlorite compositions are taken as $(Mg_{6-x-y}Fe^{2+}{}_yAl_x)(Si_{4-x}Al_x)O_{10}(OH)_8$ found d-values correspond to $x = 1.0 \pm .2$ and $y = 1.0 \pm .5$, according to Brown (1961). Electron microprobe analyses show a good fit to these data, although y is rather low (.30).

Brown högbomite, encountered in clear association with green spinel in the garnet-bearing veins of Cabo Ortegal (Plate VIa), shows a good agreement with a formula given by McKie (1963): $R^{2+}{}_{1.0-1.6}Ti^{4+}{}_{.2-.4}R^{3+}{}_{3.7-4.3}O_{7.6-8.0}(OH)_{0-0.4}$. Petrographical evidence distinctly pleads in favour of a formation of högbomite at the expense of spinel. It might be suggested that this spinel originally contained large amounts of Ti – its clear association with ilmenite is also noteworthy in this respect –, although Ti contents in spinels are rather low (see above). Titanium is probably derived from clinopyroxenes which reacted with spinel to give garnet.

The stability relations of högbomite are poorly known: "under hydrothermal conditions at 825 °C,

p(H_2O) 2000 bars, partial decomposition to spinel, aluminous pseudobrookite, and rutile has been observed" (McKie, 1963). In these samples, however, it was formed at the expense of spinel; in an other garnet-bearing vein, sample V 1405^B, rutile was found in close association with chlorite. It is tentatively conceived that högbomite alters into rutile and chlorite with added silica.

Ilmenites prove to be magnesium-rich as is often found to be the case in gabbroic rocks.

PETROGENESIS OF THE VARIOUS ULTRAMAFIC ROCKS

INTRODUCTION

With the aid of the petrographical and chemical data an attempt will be made to unravel the geological history of the ultramafic rocks under study. Of course, evidence from neighbouring rocks – which are often far better suited to indicate the sequence of endured events – cannot be disregarded. However, before proceeding to interprete these data in the light of results derived from the country rocks, these data will be investigated on their proper merits.

In the first paragraph the distribution of elements over coexisting phases will be discussed and the merits of derived equilibrium temperatures will be evaluated. Experimental investigations on peridotites are briefly mentioned. Much attention has been paid to the genesis and origin of the garnet-bearing veins and bands. This may, in view of the negligibly small volume they possess, seem irrelevant, but given their calco-aluminous character, generally implying more variations of mineralogical species, their role should not be underestimated. With the knowledge of mineral stability ranges and the data available from other localities, a genetic scheme for the peridotites will be established. A few remarks will be made about the peridotite sample from the Santiago area and the chlorite-amphibole peridotite from Mellid, while, with regard to the Castriz rocks, some of Warnaars' hypotheses will be critically reviewed.

Comparisons with the studies of Vogel (1967), Warnaars (1967), van Zuuren (1969), Hubregtse (1970) and van Scherpenzeel (1969) are made and conclusions about the general use of this specific approach of the petrogenetic problems of the various area will be drawn.

DISTRIBUTION OF ELEMENTS IN COEXISTING MINERALS (Table IV-2)

Introduction
The wide stability ranges of olivine and pyroxenes may be seen as one of the main reasons for the extensive use of distribution coefficients to establish equilibrium temperatures in ultramafic rocks.

It should be noted that the desire to present tangible facts and figures instead of having to choose more or less objectively between several hypotheses, which often have to be interpolated, is a good human characteristic.

Extensive simplifications, predominantly consisting of assumed constancy, nonvariance or minor role of several factors involved, have to be applied when a genetic interpretation is given to calculated distribution coefficients. Consequently, it was unavoidable and logical that their applicability, as postulated by several authors, underwent much criticism, usually dealing with the validity of the simplifications used.

This resulted in modifications of existing distribution coefficients (Mg/Fe in olivine vs. orthopyroxene), the laying down of more refined approaches (clinopyroxene grid of O'Hara (1967b)), while other methods became more or less discredited (Ca/Ca+Mg in clinopyroxene).

Although the author fully concurs in the general understanding that many problems are involved in the procedures pursued, yet he considers that it is always worthwhile to calculate distribution coefficients, and this for the following reasons: 1) with more available data a better picture is statistically obtained of the "right or wrong" of the applied method; 2) if the data do not yield the proper equilibrium conditions, at least they may indicate different evolutionary trends when comparisons with similar rocks are made.

Mg/Fe distribution between coexisting pyroxenes
Kretz (1961, 1963) and Bartholomé (1962), in the assumption that pyroxenes form ideal solid solutions reacting under equilibrium conditions, derived a distribution coefficient K_D (or the inverse $1/K_p$).

$$K_D = \frac{(Mg/Mg + Fe^{2+})\ opx}{(Fe^{2+}/Mg + Fe^{2+})\ opx} \times \frac{(Fe^{2+}/Mg + Fe^{2+})\ cpx}{(Mg/Mg + Fe^{2+})\ cpx}$$

$$= \frac{(Fe^{2+}/Mg)\ cpx}{(Fe^{2+}/Mg)\ opx} = 1/K_p$$

in which opx = orthopyroxene (generally, Ca-poor pyroxene) and cpx = clinopyroxene (generally, Ca-rich pyroxene).

This distribution coefficient should be mainly dependent on temperature, as other factors (pressure, whole-rock composition and minor elements) only play a subordinate role according to these authors.

O'Hara & Mercy (1963) demonstrated on theoretical grounds that distribution coefficients are also dependent on pressure and compositional differences and

suggested that "the distribution coefficient may be expected to be a function of Al_2O_3 content unless Al_2O_3 saturated pyroxenes are considered, and even then may still be a function of $Cr_2O_3:Fe_2O_3:Al_2O_3$ ratios, and the jadeite and aegirine contents of the pyroxene" (O'Hara, 1967b).

Binns (1962) and Naldrett & Kullerud (1967) found lower K_D values with decreasing Mg/Fe ratio in the host rock.

Relative to this the method of analysis should also be mentioned again. As has been argued above (see Chapter III), "plain" analyses (i.e., without exsolved phases) are usually obtained with electron microprobe analysis. This invariably leads to the conclusion that no primary equilibrium temperatures are obtained when distribution coefficients – calculated on this basis – are interpreted, because the analysed pyroxene compositions are not primary. Instead, recrystallized assemblages, when reequilibrated, may give a secondary K_D while intermediate values represent "frozen in", "fossilized" indicators of original higher temperatures. Of course, it is possible, in case reliable estimates about the amount of exsolved phases can be made, to reconstruct primary compositions, to calculate original distribution coefficients and thus to find the originally higher temperatures.

The exsolved phases in the studied pyroxenes are mainly spinel and pyroxenes. From petrographical evidence it may safely be concluded that more spinel than pyroxene was exsolved. Furthermore, Mg/Fe ratios in ortho- and clinopyroxene being only slightly different as compared with the significantly smaller Mg/Fe ratios in spinel, the amount of spinel can be

regarded as the main factor determining possible K_D differences between primary and secondary pyroxenes.

Based on the observed Mg/Fe ratios in ortho- and clinopyroxenes and spinel (100 Mg/Mg + Fe = 90, 94 and 70, respectively) from Cabo Ortegal peridotites and on the assumption that equal amounts of spinel are present in both ortho- and clinopyroxene and exsolution rates are more or less equal, the following Table clearly shows the different K_D's that are obtained (Table IV-I).

The impossibility of discriminating between ferrous and ferric iron with electron microprobe analysis is a real disadvantage when distribution coefficients have to be calculated. The addition of ferric to ferrous iron is unjustified and confusing (Bartholomé, 1961) and usually leads to somewhat higher temperatures (Fiala, 1966; Carswell, 1968a).

Considering the generally low amounts of sodium and a usually good electrostatic balance in the analysed pyroxenes, the content of ferric iron must be small, so that only small errors will be introduced.

Mg/Fe distribution between coexisting olivine and orthopyroxene

Distribution coefficients have been calculated with the formula given by Bartholomé (1962):

$$K_{ol-opx} = \frac{(Fe^{2+}/Mg) \quad ol,}{(Fe^{2+}/Mg)^2 opx}$$

while also the modification proposed by Monchoux & Besson (1969) – in which the Fa/Fo ratio is raised to the power 1.65 – has been applied. The differences

Table IV-1. Spinel admixtures in ortho- and clinopyroxenes.

wt.%	orthopyroxenes				clinopyroxenes			
	1	2	3	4	5	6	7	8
SiO_2	58.02	55.87	53.65	51.38	55.00	53.07	51.07	49.00
MgO	35.04	34.43	33.80	33.16	17.35	17.39	17.44	17.48
FeO	6.93	7.21	7.49	7.77	1.97	2.40	2.85	3.30
CaO	–	–	–	–	25.67	24.77	23.83	22.87
Al_2O_3	–	2.49	5.06	7.69	–	2.37	4.81	7.34
	99.99	100.00	100.00	100.00	99.99	100.00	100.00	99.99
$\frac{100\ Mg}{Mg + Fe}$	90.00	89.49	88.95	88.38	94.00	92.80	91.60	90.40

	K_D	K_p	T in °C
1–5	.574	1.74	730°
2–6	.661	1.51	920°
3–7	.738	1.36	1160°
4–8	.808	1.24	1400°

1 = $(Mg_{1.8}Fe_{0.2}) Si_2O_6$
5 = $Ca(Mg_{0.94}Fe_{0.06}) Si_2O_6$
spinel = $(Mg_{0.7}Fe_{0.3}) Al_2O_4$
2–6, 3–7 and 4–8 have spinel admixtures of 5, 10 and 15 mol.%, respectively

Notes
1) This is only a schematic table for illustrative purposes!
2) Other combinations can be applied instead of the listed ones.

3) When clinopyroxene analyses (5–8) are plotted in the clinopyroxene grid of O'Hara (1967b) equilibrium temperatures are found varying between 500° and 1200 °C from 5 to 8.

Table IV-2. Distribution coefficients and derived temperatures and pressures

	K_D opx-cpx	K_D ol-opx (Fa/Fo)[1]	K_D ol-opx (Fa/Fo)[1.65]	100 Ca / (Ca+Mg) in cpx	100 Ca / (Ca+Mg+Fe) in cpx	a_c cpx	β_c
spinel-pargasite peridotite Cabo Ortegal	0.58	9.18	2.21	50.3	48.7	52.1	1.95
spinel orthopyroxenite V 1403b	0.69			48.4	46.8	50.4	5.65
		↓		49.7	47.9	51.6	4.30
				51.1	49.4	53.0	3.89
decreasing Al₂O₃	0.59			50.2	48.6	52.4	1.91
spinel clinopyroxenite R 378	0.78			52.1	49.7		
amphibolized pyroxenite MP 20	0.56	8.35	2.44	50.3	48.4		
spinel-pargasite peridotite Mellid area	0.72	8.47	2.02	50.5	48.7	51.9	3.60
spinel-clinopyroxene peridotite Castriz area	0.82	8.48	2.04	49.3	47.1	51.0	4.52
				50.8	48.4		
Castriz wehrlite	0.73	5.04	1.76	51.5	48.3		
				52.3	49.2		
Castriz gabbro	0.76	4.18	1.93	54.2	49.3		
				53.4	48.8		
spinel-hornblende peridotite Santiago area		4.50	2.04				
COLUMN	I	IIa	IIb	IIIa	IIIb	IV	

that are obtained by using the two methods are obvious. The latter, more recent, method seems to give more sensitive results.

Ca-Mg-distribution in clinopyroxene
Boyd & Schairer (1964) and Davis & Boyd (1966) studied the system $CaMgSi_2O_6$–$Mg_2Si_2O_6$ at 1 and 30 atm., respectively; they argue that solid solution of $MgSiO_3$ in clinopyroxene varies mainly with temperature, the influence of pressure being relatively small.

The usefulness of plotting Ca/Ca + Mg ratios of clinopyroxenes into this phase diagram, however, is greatly reduced by the fact that natural clinopyroxenes largely deviate from this ideal system: although other bivalent cations (Fe, Mn and Ni) might be taken together with Mg resulting in Ca/Ca + Mg + Fe + Mn + Ni ratios, the role of Al is far less clear. Jadeite and/ or aegirine contents being low, most alumina in the analysed clinopyroxenes is incorporated as Tschermakite-molecule or may be just spinel. Higher amounts of Tschermakite molecule $CaAl_2SiO_6$ point to higher crystallization temperatures (Kushiro, 1962, 1965a) but also give higher Ca/Ca + Mg ratios in clinopyroxenes, which ratios, according to the above-mentioned authors, indicate lower equilibrium temperatures. A

sympathetic relation between Al_2O_3 contents and Ca/Ca + Mg ratios is mentioned by Peters (1968). It is highly questionable, however, whether this relation accounts for anything, as whole-rock compositions vary largely in this trend. In this respect also corresponding ratios in Beni Bouchera rocks (Kornprobst, 1969) and the composite dyke from the lherzolite of Lers (Fig. III-1) are mentioned.

Within one sample increasing Ca/Ca + Mg as well as Ca/Ca + Mg + Fe + Mn ratios generally correspond to decreasing Al_2O_3 contents (see Table III-8).

Clinopyroxene grid of O'Hara (1967b)
Taking the importance of Al_2O_3 into consideration, O'Hara plots clinopyroxene compositions into the triangle $CaSiO_3$–$MgSiO_3$–Al_2O_3 (CS-MS-A) of the four component system CaO–MgO–Al_2O_3–SiO_2 (CMAS).

At fixed temperatures and pressures pyroxenes, coexisting with olivine and an Al-rich phase, should possess unique compositions in this triangle, according to O'Hara who states that the usually small variations in the generally low wollastonite component in orthopyroxene make this mineral less suited for the procedure. It should be stressed that O'Hara's grid should

n °C	T	T	T	T	T	p in kb / P
0	1250	900	850	900	750	8–12
0			900	950	1150	15–20
			850	900	1050	10–15
			800	850	900	10–15
0			850	900	700	8–12
0			750	850		
0	1200	800	850	900		
0	1200	1000	800	900	950	15–20
0	1200	1000	850	950	1100	15–20
			800	900	800	10–15
50	1100	1200	750	900		
			750	850		
00	1100	1100	600	850		
			700	850		
	1100	1100				
	IIa	IIb	IIIa	IIIb	IV	

only be used for four-phase peridotites: there is evidently no place for Green & Ringwood's aluminous pyroxene pyrolite (1967), in which all Al is present in pyroxenes, while also the transition from spinel- to garnet-bearing assemblages may take place at higher PT-conditions. The adjective "provisional" (O'Hara, 1967b) is certainly not superfluous for this clinopyroxene PT-projection!

It must be admitted that the pursuance of this procedure is very tempting as it gives information about temperature as well as pressure.

Two parameters of the composition of the clinopyroxene are calculated:

$$\alpha_c = \frac{\text{wt. \% } CaSiO_3 \times 100}{\text{wt. \% } (CaSiO_3 + MgSiO_3)}$$

and

$$\beta_c = \frac{\text{wt. \% } Al_2O_3 \times 100}{\text{wt. \% } (CaSiO_3 + MgSiO_3 + Al_2O_3)},$$

in which $CaSiO_3 =$ wt. $CaSiO_3$ equivalent to all CaO present in the analysis; $MgSiO =$ wt. $MgSiO_3$ equivalent to all MgO, MnO and NiO; $Al_2O_3 =$ wt. Al_2O_3 equivalent to all Al_2O_3, Cr_2O_3 and Fe_2O_3 present less an amount equivalent to Na_2O and K_2O present.

The combinations of these parameters, however, may quite easily give the wrong results or no results at all when these two functions do not intersect.

Consequently, the author proposes a less strict use of this grid: first, the mineralogical character of the Al-rich phase – determining the character of the whole assemblage – should be established from petrographical evidence. Secondly, general indications about α_c and β_c should be used in order to evaluate reasonable PT-conditions within this restricted field. Further, the occurrence of garnet in basic assemblages (i.e., the garnet-bearing veins and bands) should restrict possible $\alpha_c\beta_c$ combinations to the high-pressure part of the spinel lherzolite facies (the ariegite subfacies of O'Hara (1967a), characterized by the diopside + enstatite + garnet + spinel associations).

The role of Al-rich amphibole is not clear in this scheme, but the presence in significant amounts of a fifth and hydrous phase is bound to obliterate higher PT-indications.

Conclusions from temperature and pressure estimates
As stated in the introduction to this paragraph, calculated temperatures may not be right but distinct differences within one-rock type should be of some significance in themselves.

Values derived from olivine/orthopyroxene distribution coefficients indicate high crystallization temperatures of 1100°–1250°C, and are lowest in wehrlites and gabbros (column IIa). Values in column IIb are usually somewhat lower and to a slight degree show an inverse trend compared with data in column IIa. With the mineralogical composition of the peridotites in mind it may be concluded that the method IIb is more sensitive to changing PT-conditions than the method IIa, the values of which correspond to values calculated by means of other methods (see below).

Temperature estimates based on the diagrams of Boyd & Schairer (1964) and Davis & Boyd (1966) show relatively narrow temperature ranges (column III): low values of 600°–700 °C for the Castriz gabbroic rocks – which have a higher Ca/Mg ratio – already indicate that Al and Fe cannot be disregarded. When Fe is taken together with Mg all values are more or less equal (850°–950°C). By taking exsolved spinel into account Warnaars (1967) calculated a 100 Ca/Ca + Mg + Fe ratio of 42.7 (corresponding to 1100°C) against an analysed ratio of 49.1 in clinopyroxenes from a wehrlitic sample.

Obvious differences between the data of the two spinel-pargasite peridotites and the spinel-clinopyroxene peridotite are found in columns I and IV. High temperatures, noted in the Mellid and Ferreira samples, recur in the spinel clinopyroxenite vein, R 378, and a trend from high to moderate temperatures is visible in the brown ceylonite orthopyroxenite vein, V 1403b, rocks occurring in the "750 °C" Cabo Ortegal spinel-pargasite peridotite. This peridotite probably lost all evidence of a former high temperature stage at this level, while in some pyroxene-rich veins these

indications are still preserved and only adjustments to this lower temperature level are achieved. The abundant occurrence of spinel exsolution lamellae in the latter samples indicates even higher temperatures of 1300°–1400 °C, comparable with the "artifical" pyroxenes mentioned in Table IV-1. The Al-rich, Na- and Ti-bearing clinopyroxene in the spinel-garnet clinopyroxenite band from the area around Ferreira, when compared with clinopyroxenes from the Cabo Ortegal garnet-bearing veins, may also serve as an indicator of primary high temperatures.

In conclusion, primary, high equilibration temperatures (1100°–1200 °C) and pressures (15–20 kb) are assumed for these three peridotites. These values neatly correspond to values established for the Pyrenean and Beni Bouchera lherzolites (see O'Hara (1967b), Fig. 12.6). The low values calculated for the Cabo Ortegal peridotite (700°–750 °C at 8–12 kb pressure) indicate the presence of a second stage in the history of this peridotite. The answer to the question why the 750 °C-level is not found in the other peridotites might be that these rocks did not or to a lesser extent undergo these PT-conditions.

With regard to the calculated temperatures of Castriz wehrlites and gabbros (1150°–1200 °C) and the absence of garnet, an original place near the solidus at pressures of about 10 kb – in the low pressure part of the spinel lherzolite facies of O'Hara (1967a) – seems warranted.

Summarizing, it may be stated that temperature and pressure estimates derived from the various distribution coefficients, when supported by petrographical evidence, form a useful aid in surmising the general pattern and history of PT-conditions, although it should be realized that actual temperature and pressure values are open to considerable doubt.

The question if equilibrium was attained remains crucial. In view of the observed compositional variations, the remnants of prior PT-conditions and adjustments to later conditions, including serpentinization processes, it is difficult to say if equilibrium was ever established or re-established in the Galician peridotites.

Concerning the validity of the procedures used, a possible presence of primary spinel – with regard to the Al_2O_3 saturation of orthopyroxene – should be considered. If it is reasonable to assume that primary spinels in peridotitic rocks should display a hypidiomorphic to idiomorphic habit and possess high contents of Cr, then primary spinel was not present. Only in one sample, FCM 1, brown and sometimes hypidiomorphic spinels were found. In gabbroic and wehrlitic rocks from the Castriz area primary spinel was probably present. Conclusions about the Al_2O_3 saturation of orthopyroxene cannot be drawn from these scanty data.

EXPERIMENTAL DATA ON LHERZOLITIC ROCKS

Classification and composition

Regarding the geological setting of the peridotites under consideration, their place within the alpine-type

peridotite-serpentinite association is obvious (Wyllie, 1969); also their association with granulite facies metagabbros and metabasalts is noted.

Their lower Mg/Fe ratio might serve as a secondary characteristic to distinguish them from stratiform ultramafites (Miyashiro, 1966). Within this association (group 4 of Wyllie, 1969) five subdivisions have been established, three of which are based on the different metamorphic conditions, while high-temperature peridotites (i.a., Lizard, Green (1964) and Tinaquillo, Mackenzie (1960)) with distinct contact metamorphic aureoles and ultramafic rocks formed by metamorphic differentation and metasomatic processes (Sørensen, 1967) form the remaining two categories.

Recent hypotheses, based on seismic and geological evidence, concerning the chemical nature of the upper mantle favour peridotitic rather than eclogitic compositions (Ringwood, 1969). Furthermore, if the origin of basalts is sought in a parental peridotite or garnet peridotite (O'Hara, 1965), these upper mantle source rocks should be capable of delivering basaltic magmas by partial fusion processes, leaving behind a refractory ultramafic residuum, highly or completely depleted in the basaltic component (Ringwood et al., 1964). Most alpine-type peridotites appear to have undergone at least some fractionation and do not resemble supposed pyrolite models in that they contain too low amounts of minor elements (particularly alkalies and titanium), even when a few percents of CaO and Al_2O_3 are still present. The Galician peridotitic rocks with mean values of CaO: 2.67%, Al_2O_3: 3.59%, Na_2O: 0.24%, K_2O: 0.03% and TiO_2: 0.10% (see Table III-1) display similar characteristics.

Phase equilibria studies on whole-rock systems

In experimental petrology ultramafic rocks are commonly described in terms of their major components SiO_2, Al_2O_3, MgO, FeO and CaO and, under hydrous conditions, H_2O. Since experiments including FeO as an individual component are scarce and as in most ultramafic silicates MgO and FeO may be regarded as isomorphous substitutes (MacGregor, 1967), these mafic oxides are usually taken as one component, resulting in a quaternary system, abbreviated CMAS(H), in which, however, the role of Fe and minor elements is by no means clear.

Peridotitic rocks, in which small, but significant amounts of CaO and Al_2O_3 are present, occur in three different and easily recognizable assemblages, mainly due to the varying mineralogical character of the Al-rich phase: plagioclase, spinel and garnet, as the other major mineral components – olivines and pyroxenes – possess wide stability ranges, although the Al_2O_3 content in pyroxenes is also significant in this connection (Ringwood et al., 1964; Green & Ringwood, 1967b).

Under hydrous conditions Al-rich amphibole (pargasite) assemblages and at lower pressures hornblende-to-tremolite- and chlorite-bearing assemblages may be added. Many mineral facies – both anhydrous and hydrous – have thus been established (O'Hara, 1967a),

while others (e.g., Rost, 1968) restricted the number to only three main types (chlorite-, spinel- and garnet peridotites). In rocks with pyrolitic compositions four mineral assemblages are commonly envisaged (Green & Ringwood, 1967b): amphibole-, plagioclase-, pyroxene- and garnetpyrolite.

The pyroxene-bearing assemblage is subdivided into a higher T-aluminous pyroxene- and a lower T-spinel-pyroxene assemblage.

Significant facies boundaries have been established empirically from several, mostly anhydrous, mineral reactions, in all of which the mineralogical site of Al is essential.

The usefulness of these experimental studies of mineral stability ranges is certainly great, but their significance should not be overestimated as the composition of mineral mixtures used often strongly deviates from natural ultramafic systems with large, and maybe unjustified, simplifications. Unfortunately, only few investigations have been carried out on natural systems resembling alpine-type peridotites. The pyrolite III of Green & Ringwood (1967b) ,however, although an "artificial" system, compositionally shows a good fit to the Galician peridotites.

Momentarily disregarding the abundant presence of an Al-rich amphibole, the absence (either stable or relictic) of plagioclase and garnet evidently places the Galician peridotites into the pyroxene pyrolite "sensu lato" field, corresponding to pressures between 8–10 and 20–25 kb. The presence of aluminous spinel, Al-poor pyroxenes, Al-rich amphibole and finally the development of an aluminous chlorite already give a rough indication of the history of the peridotitic rocks within this field. Temperature and pressure estimates, derived from distribution coefficients between various minerals, of 1100°–1200 °C/15–20 kb and 700°–750 °C/ 8–10 kb may be marked as two stages within this evolutionary path.

GARNET-BEARING VEINS AND BANDS

Introduction

The mode of occurrence of the garnet-bearing veins may be best explained by a process of partial melting. Other possible explanations (e.g., deformation and/or metasomatic processes, penetrating liquids from country rocks) are not supposed to present logical solutions for the fundamentally different chemical and mineralogical character of these rocks. The arguments for an evolution along these lines of these veins (inclusive of possible origins of garnet-free veins and bands) and their host rocks will be further discussed.

Experimental investigations of similar rocks are mentioned and comparisons with rocks from other localities are given.

Partial melting of the upper mantle

Current hypotheses concerning genesis and evolution of basic magmas have a common origin: partial fusion of a parental upper mantle rock.

Physical processes leading towards this type of fusion having been proposed, several parameters control the type of basalt that will develop: degree of partial melting, composition of parental rock, fractionation trends, depth of partial melting and magma segregation, dry or wet melting conditions.

Degree of partial melting. – Although the amount of vein material, which is supposed to represent a partial melt, is very low, (less than 5%), it might be considered that a higher fraction of the parental rock was molten. This suggestion renders two explanations possible for the small amount of vein material visible: 1) small amounts of an initial melt became trapped in veins within the host rock while the bulk of the melt completely separated from the host rock and in deep orogenic zones became metamorphosed to form amphibolites, mafic granulites or eclogites; 2) no segregation took place but the liquid pervasively crystallized within the host rock, probably after having acted as a lubricant during ascent (den Tex, 1969), while only a small portion individualized and became trapped in veins. In this respect the concentration of amphibole in the bottom parts of the Cabo Ortegal ultramafites, as found by Romijn (1959), is mentioned. A study of the associated mafic rocks and their possible derivation from the ultramafic rocks lies beyond the scope of this work. However, strong impoverishment in the basaltic component is not found, at least not in the exposed ultramafic rocks. This aspect will, therefore, not be pursued. The second possibility may be cancelled on textural evidence: more gradual transitions between the host rock, the pervasively crystallized liquid fraction and the squeezed liquid of the same composition should be encountered: i.e., a more hybrid character should be expected.

But the most powerful argument in favour of a small degree of melting lies in the composition of these veins, as will be discussed below.

In addition it may be mentioned that a fairly small degree of melting has also been assumed in other localities from which comparable phenomena have been described.

Composition of parental rock. – The transition from plagioclase- to pyroxene pyrolite being irrelevant in the rocks studied, the occurrence of garnet at the solidus is of vital importance.

This appearance of garnet, however, is also dependent on the chemical composition of the parental upper mantle rock, which is unknown. Some data about the occurrence of garnet at the solidus are: above 23 kb in a natural garnet peridotite (Ito & Kennedy, 1967), above 25 kb in pyrolites I and II (Green & Ringwood, 1967b), above 30 kb in pyrolite III (Green & Ringwood, 1967b).

From this somewhat controversial evidence several conflicting hypotheses have been established concerning the disappearance of minerals by partial melting processes and the mineralogical character of the residuum at high pressures (O'Hara, 1968; Kushiro, 1969; Green & Ringwood, 1969). When the

assumption is warranted that a very low degree of partial melting will not essentially change the composition of the parental rock, the original mineral assemblage of the residuum should not deviate much from the parental rock assemblage and should give information about this assemblage. The early entrance, however, of a hydrous phase, such as amphibole, obscures a clear view of this residual assemblage: the question remains whether garnet was present of not? The possibility of former garnet presence has been rejected by the author on petrographical grounds. If this assumption is right the parental rock should have been a lherzolite too, although the possibility remains for a garnet lherzolite to have recrystallized at lower pressures in the spinel lherzolite stability field subsequent to segregation of a phase rich in the garnet component. The composition of the veins favours the latter hypothesis, which may corroborate with data derived by Green & Ringwood (1969): ..."at depths of around 100 km, a relatively small degree of partial melting causes the disappearance of garnet, and liquids are in equilibrium with olivine and aluminous pyroxenes. Liquids derived in this way ... have chemical compositions approaching picrites with more than 30% normative olivine".

Other possibilities are given by O'Hara (1968) – see below under "liquid B" – and Kushiro (1969).

It should be born in mind that the different conclusions derive from varying starting-points, i.e., from differing compositions of the parental rocks.

Primitive character and composition of liquid. – The garnet-bearing veins show picritic compositions and are comparable with Green & Ringwood's picrite (1967a). They are very rich in normative olivine and are slightly hypersthene normative.

It is unjustified to draw any conclusion concerning fractionation trends within the garnet-bearing veins. This question also involves the primitive character of the liquid, the crystallization of which – under subsolidus conditions – yielded a garnet-bearing assemblage. Some fractionation may have given rise to cumulates of primary precipitates in bands, veins, lenses or pockets. The occasional presence in the Cabo Ortegal area of pyroxenitic bands and veins (V 1403b, MP 18, MP 20 and MP 21), in which clinopyroxene is often replaced by amphibole, should be mentioned in this respect. Distinct field relations with garnet-bearing veins are lacking, although garnet has been encountered in some samples (V 1404, R 67). Elsewhere, the succession orthopyroxenite, websterite, garnet ± spinel pyroxenite has been clearly demonstrated (Beni Bouchera, Totalp, Lers). In this connection relations in the only composite vein (MP 18) are interesting: chlorite orthopyroxenite rims occur around orthopyroxene-clinopyroxene (replaced by amphibole) – rich cores. Consequently, if fractionation has indeed taken place it is evident that orthopyroxene ± Cr-rich spinel should crystallize first and the Al-rich part of the liquid last. The possibility that the orthopyroxenite rim represents a reaction rim between ultramafic host

rock and picritic liquid must be rejected on chemical grounds (cf. Kornprobst, 1969).

Summarizing, it may tentatively be concluded that the composition of the garnet-bearing veins is representative for the primitive liquid when a small amount of a (mainly ortho-) pyroxenitic component is added.

The presence of serpentine in the veins might be interpreted as compensating more or less the deficiency in this component.

Depth of partial melting and magma segregation. – A large reduction in scale should be made when these phenomena are applied to the veins in question: incipient melting ($<5\%$) instead of partial melting ($>5\%$) – a distinction used by Green & Ringwood (1969) – has taken place. Successful magma segregation will occur only when 20–40% of the parental rock is molten, while in this case only a squeezed out, trapped liquid is at stake, of which it is questionable whether it may be regarded as an independent chemical system.

The depth at which melting starts is indicated by the point at which a supposed pyrolitic diapir, following an adiabatic gradient (Green & Ringwood, 1967a), intersects the surface of its dry or wet solidus.

One could imagine that with a further rise of this diapir the amount of liquid may increase and segregate from residual crystals only at depths significantly lower than that at which melting started. This may explain the observed phenomena: the picritic liquid (mainly derived from the melting of garnet ± clinopyroxene) segregates and crystallizes at PT-conditions where garnet is no longer a solidus phase in the picritic assemblage – except perhaps in the lenses at Mellid –, while the lherzolitic or garnet-harzburgitic residuum (according to O'Hara, 1968) recrystallizes within the lherzolite stability field.

The low degree of melting, however, does not warrant the assumption that the differences between depth of melting and depth of magma segregation (i.e., liquid segregation) was large.

Dry or wet melting conditions. – Data about solidus assemblages during melting under hydrous conditions of appropriate upper mantle rock are scarce: Kushiro's lherzolite (1968) possesses a rather low MgO/SiO_2 ratio, the experiments of Bultitude & Green (1968) concern an olivine nephelinite and a picritic nephelinite, while Green (1969) investigated an olivine-rich basanite.

With regard to wet conditions of melting the presence of the Gutenberg low velocity zone is of utmost interest. Some authors are of the opinion that the explanation of this zone in oceanic and orogenically active regions has to be sought in a partial melting process, in which the temperature of incipient melting is lowered by 100°–200 °C when only small amounts of water (0.1%) are present, probably not as a free phase but incorporated in amphibole crystals. Taking the sequence of mineralogical events into account the author favours an initially dry melting, probably in the low velocity zone.

EXPERIMENTAL INVESTIGATIONS

The uncertainty about the composition of the parental rock, which corresponds to the fairly large pressure range (23–30 kb) in pyroxene- to garnet pyrolite transitions and the early presence of a hydrous phase in both residual rock and trapped liquid, obscuring the original mineralogical character, render a satisfactory solution difficult, if not impossible. Upon evaluation of the various parameters comparisons will be made with Green & Ringwood's picrite (1967a), the investigated system diopside-pyrope (O'Hara, 1963; Kushiro, 1965; O'Hara & Yoder, 1967) and the initial liquid B of O'Hara (1968).

Green & Ringwood's picrite (1967a)
The crystallization sequence and possible fractionation trends of this picrite can be deduced from Fig. IV-1, in which its chemical composition is also given.
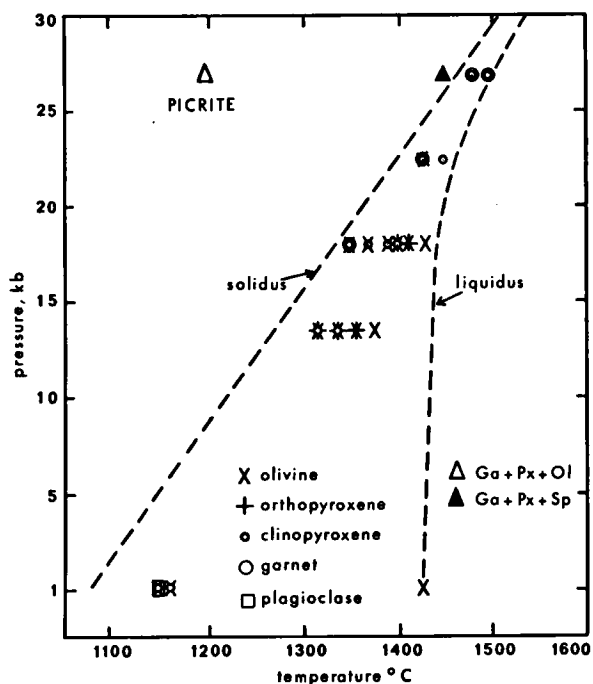
Fig. IV-1. Melting and subsolidus experiments on the picrite of Green & Ringwood (1967a).

Chemical composition:				
		Fe₂O₃	.92	CaO	9.67
SiO₂	45.51 wt.%	FeO	8.67	Na₂O	1.64
TiO₂	1.93	MnO	.15	K₂O	.08
Al₂O₃	12.44	MgO	18.79	P₂O₅	.20

The most remarkable differences with the petrographical evidence from the veins from this and other localities are: the occurrence of garnet as a liquidus phase at 18, 22.5 and 27.5 kb – generally after solidification of pyroxenes – and the relatively small importance of orthopyroxene as a liquidus phase. Regarding the latter phenomenon the occurrence of orthopyroxene as a liquidus phase at 1325 °C, 18 kb, instead of olivine – presumably due to access of water – may be mentioned.

Green & Ringwood further state that at about 35–70 km depth "fractionation is dominated by separation

of aluminous orthopyroxene or orthopyroxene with subcalcic augite"; at higher pressures garnet and clinopyroxene may segregate.

Concerning the occurrence of garnet at the solidus, two sets of data may present a useful working hypothesis. First, from the experiments of Kushiro & Yoder (1966) and MacGregor (1964) it may be deduced that garnet is present at the solidus under lower PT-conditions in less mafic assemblages (lower Fo/An ratios). Secondly, with a fractionation of orthopyroxene (generally the CaO-Al₂O₃-SiO₂ (CAS) component), i.e., a decrease of the Fo/An ratio is found. Consequently, it might be envisaged that in a more external part of a composite vein aluminous clinopyroxene with exsolved blebs, lamellae and rods of garnet is found while in a central part garnet directly crystallized out of the last liquid (see also Kornprobst, 1969). Similar considerations may be applied to unzoned veins. Within the relatively small pressure and temperature interval (the temperature difference between liquidus and solidus of Green & Ringwood's picrite being about 100 °C at 18 kb and 50 °C at 22.5 kb) in which fractional crystallization may take place and transitions between "pyroxenite" and "garnet granulite" occur in gradually less mafic assemblages, garnet may be formed 1) primarily, 2) under subsolidus conditions or 3) not be formed at all. The various possibilities are drawn schematically in Fig. IV-2. Metamorphic processes may, of course, considerably influence the mineralogical character of the subsolidus assemblages.
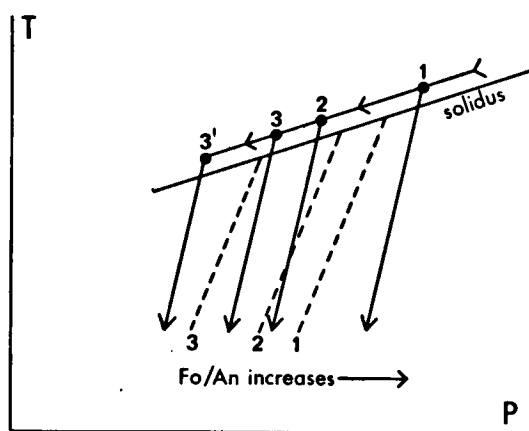
Fig. IV-2. Schematic diagram of the solidus and subsolidus behaviour of initial melting liquids with regard to their Fo/An ratio.
Broken lines (1,2 and 3) indicate garnet transition lines in compositions 1,2 and 3 = 3', respectively.
Composition 1 gives primary garnet; compositions 2 and 3 give subsolidus and primary garnet, respectively (comparable with Beni Bouchera rocks); composition 3' (= 3 under lower pressures) does not give garnet at all (comparable with spinel sensu stricto clinopyroxenite from Cabo Ortegal, R 378).

The system diopside-pyrope
With reference to the appearance of garnet and with the occurrence of orthopyroxenites in mind it is useful

to cast a glance at this system, although it was investigated at 30 kb (Fig. IV-3) and for the composition
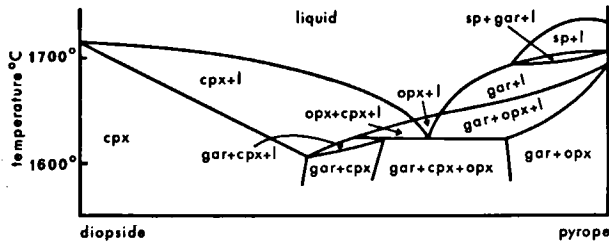
Fig. IV-3. The system diopside-pyrope at 30 kb, after O'Hara (1963) and O'Hara & Yoder (1967).

diopside: pyrope = 1:1 (Fig. IV-4) only, in the absence of iron. Possibilities mentioned by Kornprobst (1969) are also applicable to the rocks under consideration: a primary field of orthopyroxenite at high pressures (about 30 kb, Fig. IV-4) and at certain compositions may be present; both solidus and sub-
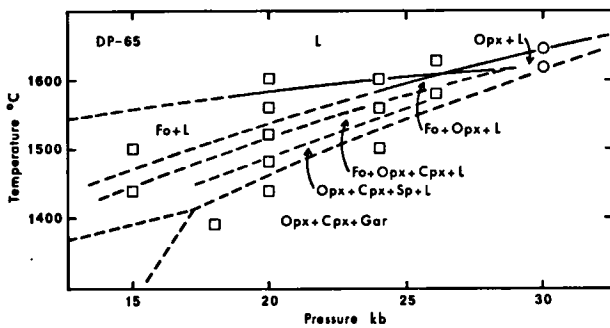
Fig. IV-4. PT-diagram for the composition diopside: pyrope = 1:1 (mol. ratios), after Kushiro (1965b).

solidus garnet-bearing assemblages occur. The role of forsterite at intermediate pressures up to 27 kb (Fig. IV-4) and the formation of garnet at the expense of spinel + liquid (Figs. IV-3 and IV-4) are mentioned.

When the actual composition of the veins (Table III-2) is compared with several diopside/pyrope ratios (Table IV-3) and mafic oxides are taken together, it is evident that no ratio shows a reasonable fit, and that molecular diopside/pyrope ratios between 1 and 1.5, as far as CaO and Al_2O_3 are concerned, show the best approximations.

Table IV-3. Weight percentages of oxides in the system diopside/pyrope.

diopside/pyrope

mol. ratio	weight ratio	SiO_2	MgO	Al_2O_3	CaO
1.5:1	45.5:55.5	49.6	24.8	14.0	11.6
1 :1	35 :65	48.5	25.9	16.5	9.1
1 :1.5	26.5:73.5	47.6	26.9	18.7	6.8
1 :2	21.5:78.5	47.1	27.4	20.0	5.5

Liquid B (φ) *of O'Hara* (1965, 1968)
An attempt was made to arrive at a more or less precise determination of the pressure range at which incipient melting occurred, and of the direction of possible fractionation pursuing the procedure advocated by O'Hara (1968): rock compositions have been calculated in the system $CaO-MgO-Al_2O_3-SiO_2$ (CMAS) and projected from or towards various points (mineral phases) onto certain planes.
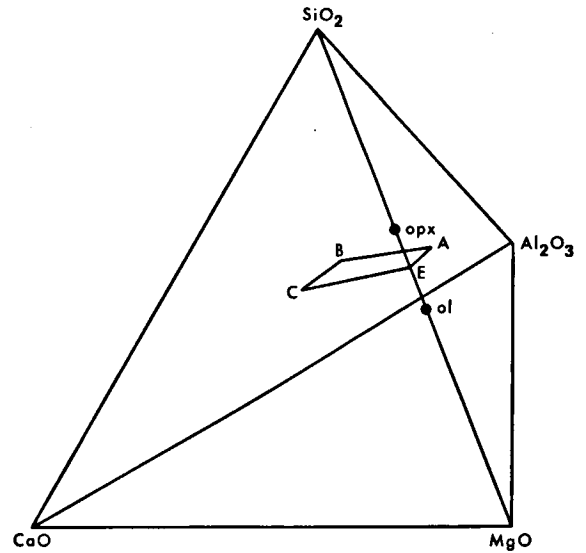
Fig. IV-5. Tetrahedron of $CaO-MgO-Al_2O_3-SiO_2$ (CMAS) showing the relationship between olivine (ol), orthopyroxene (opx) and the surface A-B-C-E of liquid compositions in equilibrium with olivine and orthopyroxene, after O'Hara (1968).

Within the tetrahedron CMAS the surface A-B-C-E (Fig. IV-5) represents possible liquid compositions in equilibrium with olivine and orthopyroxene.

On this surface B is the first liquid that will form on partial melting of any four-phase lherzolite; at about 20 kb its composition is hypersthene-normative and under 30 kb it becomes very rich in normative olivine obtaining a picritic character. Liquid B is in equilibrium with lherzolitic residua between 10 and 20 kb and with garnet-harzburgitic residua at high pressures. The line B-C on the surface A-B-C-E represents liquid compositions which are in equilibrium with olivine and two pyroxenes of variable alumina content; an alumina-rich phase is not present: all Al_2O_3 ($+ Fe_2O_3 + Cr_2O_3$) is present in pyroxenes.

Compositions of rocks from other localities are also plotted for comparative reasons.

Four subdivisions have been made:

1) Galician rocks (peridotites, pyroxenites, garnet-bearing assemblages, wehrlites and a gabbro from the Castriz area);
2) lherzolitic rocks with associated bands and/or veins from Beni Bouchera and Totalp;
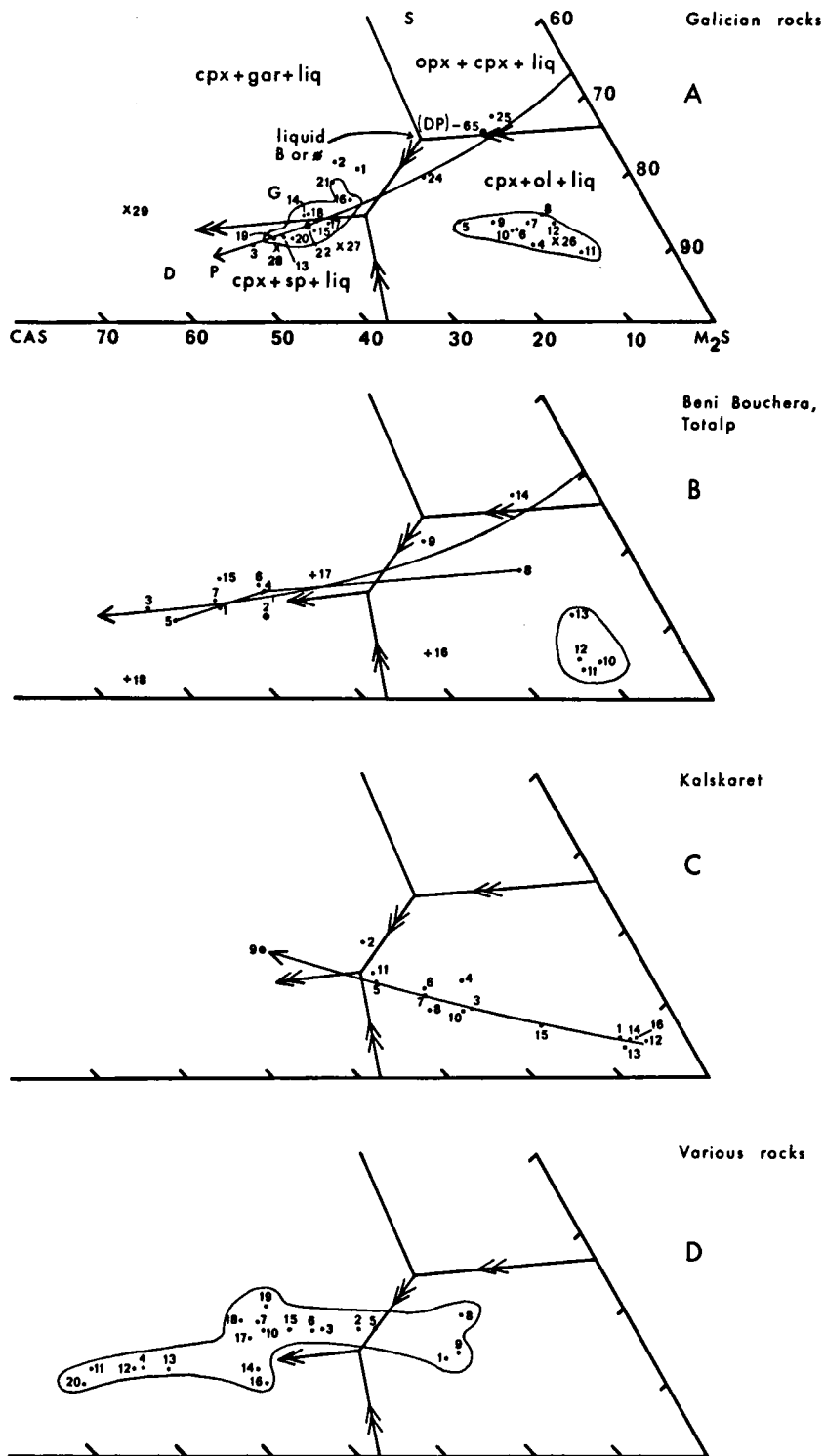
Fig. IV-6. Rock compositions plotted in the system CAS-M$_2$S-S (projected from or towards clinopyroxene CMS$_2$) and the postulated appearance of crystal-liquid relationships in this system under high pressures and anhydrous conditions, after O'Hara (1965).

Outlined areas represent peridotites (nrs. 4–12 and 26) and garnet-bearing veins (nrs. 13–22) in Fig. IV-6a, peridotites (nrs. 10–13) in Fig. IV 6b and all plotted rocks in Fig. IV-6d.

G, D and P (in Fig. IV-6a) are the projections of the averaged garnet, diopside and pargasite compositions, respectively. DP-65 is the projection of the composition diopside:pyrope = 1:1 (see Fig. IV-4).

Trend lines are indicated.

A list of the plotted rocks is given in Appendix 2.

3) the Kalskaret ultramafic rock series (garnet dunite to garnet websterite) in which, according to Carswell (1968b), a picritic liquid was more or less mechanically mixed with a residual host rock;

4) garnet peridotites, garnet pyroxenites and two kyanite eclogites from various localities.

In the various diagrams (Figs. A-IV-I, A-IV-2 and A-IV-3, in Appendix 2) several thermal divides and liquid control planes are indicated; the projection of liquid B at 15, 20 and 30 kb pressure is also given.

The projections of Galician rocks roughly indicate – accuracy of the analyses and reliability of this simplified process taken into consideration – generation of a liquid at high pressures. A few remarks about these figures are appropriate: 1) note and compare the positions of the average Cabo Ortegal garnet-bearing vein (point 22), the composition of a composite layer from Beni Bouchera (point 2) and the supposed liquid composition from Kalskaret (point 9) with regard to the liquid compositions of O'Hara (1968); 2) note the strongly linear trend in the Kalskaret series; 3) note the position of the average pargasite and garnet with regard to the composition of the Cabo Ortegal garnet-bearing veins.

The following discrepancies with O'Hara's procedure are mentioned:

1) the initial liquid is assumed to lie close to B, instead of at B;

2) lherzolitic residua are supposed to be present at higher pressures;

3) orthopyroxene forms the important liquidus phase instead of olivine at intermediate pressures.

A more interesting and valuable procedure consists of plotting the various analyses from the diopside point in the triangle M_2S-CAS-S (olivine-Ca-Tschermakite-molecule-quartz) and in making comparisons with the postulated appearance of crystal-liquid relationships under various pressures and temperatures (O'Hara, 1965). When these diagrams (Fig. IV-6) are inspected, the following remarks may be made:

1) Trends of the assumed lines of liquid descent of the complex veins from Beni Bouchera and the individual Cabo Ortegal veins show strong similarities. In the Beni Bouchera-Totalp diagram the line 8-4-5 represents compositions from one complex vein from Beni Bouchera. Totalp samples display a deviating pattern.

2) The linear trend in the Kalskaret series is well expressed. Attention is drawn to the composition of the liquid (point 9) in comparison with the average Cabo Ortegal garnet-bearing vein composition (point 22) and the composition of a whole composite vein from Beni Bouchera (point 2).

3) The outlined area in the diagram "Various rocks" roughly corresponds to that of the various trends.

4) The mineralogical features of the plotted Galician veins are best explained by a diagram between intermediate and high pressures: circumvention of

the Cpx + Gar + liq.-field, because of its shifting towards the CAS-corner, is assumed (Fig. IV-7).
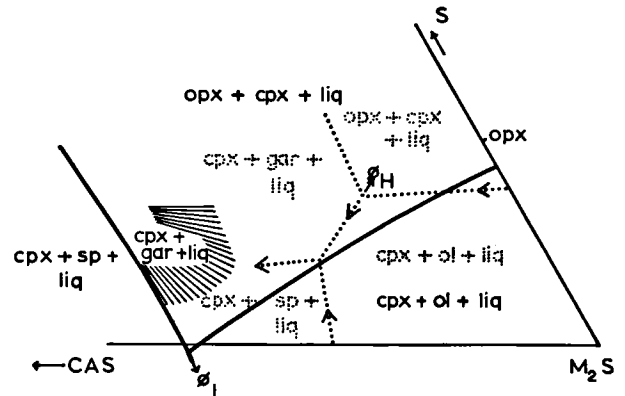
Fig. IV-7. Postulated appearance of crystal-liquid relationships in the system CAS-M_2S-S under intermediate and high pressures, after O'Hara (1965).
Stippled lines and names correspond to high-pressure phenomena. Heavy lines and names correspond to intermediate-pressure phenomena.
The assumed cpx+gar+liq field between intermediate and high pressures is indicated (hatched area) and the positions of the liquids under high ($\varnothing_H$) and intermediate ($\varnothing_I$) pressures are plotted.

The large extension of the Opx + Cpx + liq.-field and the place of liquids $\varnothing_H$ and $\varnothing_I$ (at high and intermediate pressures, respectively) are noted. Liquids (point 22 in Fig. IV-6a, point 2 in Fig. IV-6b) will largely travel in the Opx + Cpx + liq.-field, giving orthopyroxene-rich cumulates with fractionation (point 24 and 25 in Fig. IV-6a, point 8,9 and 14 in Fig. IV-6b) and going towards the CAS-corner, during which a supposed Cpx + Gar + liq.-field may be entered especially under the proper, metamorphic conditions (see also Fig. IV-3).

When mafic oxides are separated into Mg- and Fe + Mn-oxides and plotted with CaO into a triangle, distinct trends from ultramafic towards eclogitic assemblages become clear. When their constituent clinopyroxenes and garnets are also plotted and additional data (Al_2O_3 of rock and clinopyroxene, Na_2O of clinopyroxene and Cr_2O_3 of garnet) are given, several additional conclusions may be drawn (see Fig. IV-8 and notes ad Fig. IV-8 in Appendix 2).

Rock compositions with decreasing amounts of MgO generally show:

1) decreasing pyrope contents in garnets with more or less constant grossular contents;

2) decreasing Cr contents in garnets;

3) a clinopyroxene trend from diopside towards subcalcic augite;

4) an increase of Al_2O_3 in clinopyroxene;

5) rather constant, low jadeite components;
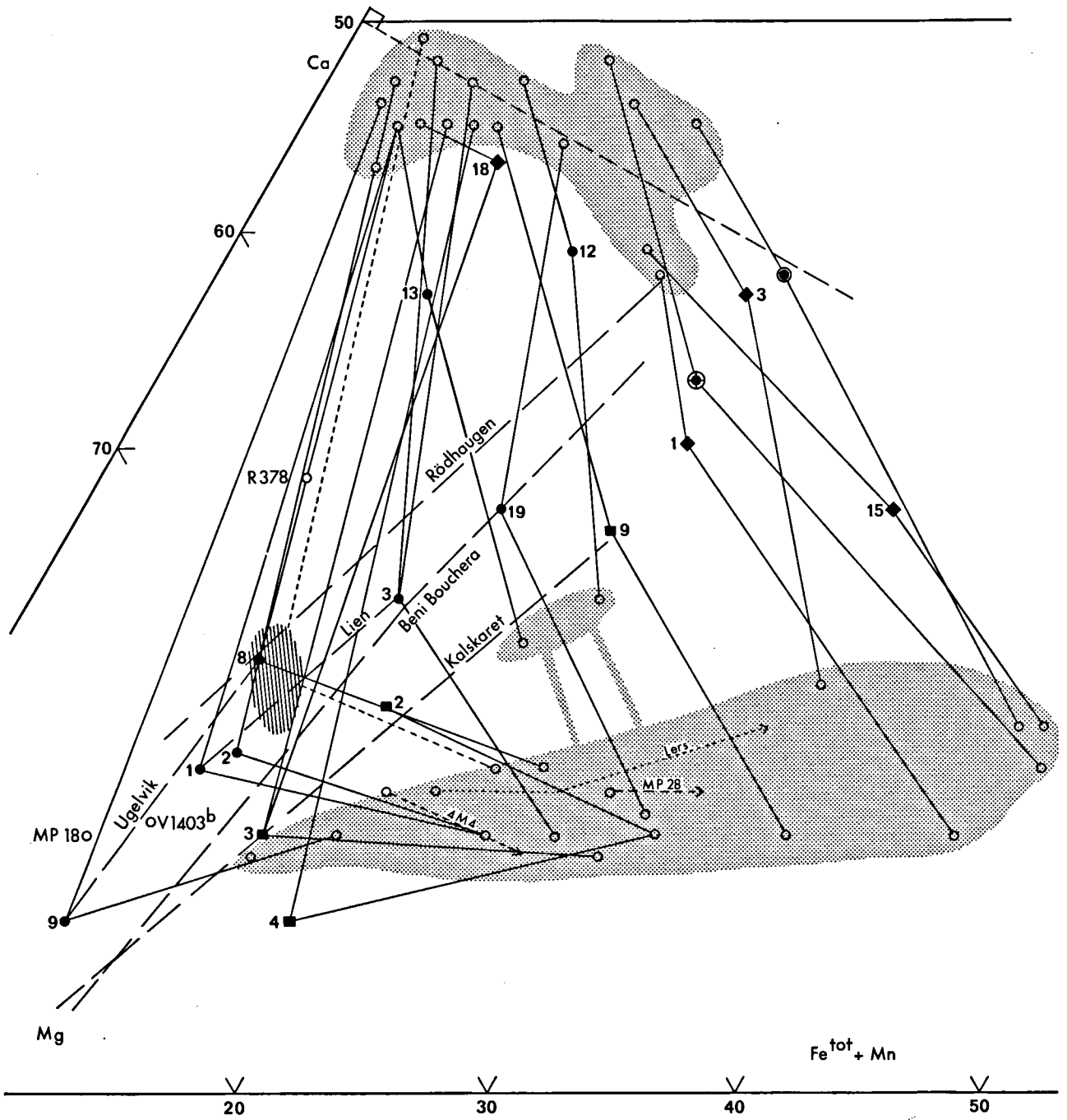
Fig. IV-8. Ca:Mg:Fe^{tot} + Mn diagram for coexisting garnet and clinopyroxene and their host rocks. Compare with Coleman et al. (1965, Fig. 11).

Full lines connect rock compositions with garnet and clinopyroxene compositions. Interrupted line connects garnet-bearing assemblages from Cabo Ortegal (hatched area) with mean clinopyroxene and garnet from these rocks. Some pyroxenites from Cabo Ortegal are plotted as open circles. Given numbers correspond to those used in Fig. IV-6 (see list in Appendix 2): Beni Bouchera and Totalp rocks ◆ , Kalskaret rocks ■ , Various rocks ● , garnet pyroxenite from Beni Bouchera (M 5-106, Kornprobst, 1966) ◉ , garnet-amphibole pyroxenite (Livingstone, 1967) ◉.

Heavy, interrupted lines indicate trend lines noted by Carswell (1968a) for Ugelvik, Lien, Kalskaret and Rödhaugen rocks, noted by Kornprobst (1969) for Beni Bouchera rocks. The zonal character of Galician garnet is indicated (with arrows); different garnet compositions in the composite dyke in the lherzolite of Lers are also given.

Shaded areas indicate all clinopyroxene compositions (above) and all garnet compositions (below).

Some additional data are given in Appendix 2: wt.% Al$_2$O$_3$ in rock, wt.% Al$_2$O$_3$ and wt.% Na$_2$O in clinopyroxene, wt.% Cr$_2$O$_3$ in garnet.

6) Ca/Mg + Fe ratios in clinopyroxene decrease; Ca/Ca + Mg ratios in clinopyroxene tend to increase slightly (cf. Peters, 1968).

Galician rocks nicely fit in this scheme: extremely low Na₂O contents are certainly due to the amphibolized character of the veins (Na₂O contents in clinopyroxenes from the spinel-garnet-pyroxenite band from the Castriz area are substantially higher).

EXAMPLES FROM OTHER LOCALITIES

Totalp, Switzerland (Peters, 1963; Peters & Niggli, 1965; Peters, 1968)

In a partly serpentinized porphyroclastic lherzolite bands of picotite pyroxenite (parallel to pyroxene-richer parts in the host lherzolite), veins and nodules of ceylonite pyroxenite, dykes of pyrope-ceylonite pyroxenite and lenses of spinel-free pyroxenites are found.

Minor olivine is present in the picotite (ortho)-pyroxenite which displays gradual transitions with the host rock. In ceylonite (clino)pyroxenites (orthopyroxene up to 33%, ceylonite up to 20%) ceylonite is found interstitially and exsolved from pyroxenes. A small amount of residual liquid gave rise to formation of small pyroxenes, ceylonite, brownish amphibole and phlogopite between the larger pyroxene individuals. In the pyrope-ceylonite pyroxenites pyrope occurs as large individual grains, often enclosing ceylonite, or as exsolution lamellae in both ortho- and clinopyroxene. Brownish amphibole is often encountered in fine-grained pyroxene aggregates. All transitions from pyrope-ceylonite- to ceylonite pyroxenite may be found. In all pyroxenites both Al-rich pyroxenes show exsolution lamellae of each other. In the spinel-free pyroxenites, in which both pyroxenes have lower Al₂O₃ contents, exsolution lamellae of enstatite in diopside are rather scarce.

In the opinion of Peters, a small amount of liquid, residual or anatectic, of a pyroxenitic composition intruded within an already solid, but still warm host rock without showing chilled margin effects.

Equilibrium temperatures vary between 900 °C (Ca/Ca + Mg ratios in clinopyroxenes) and 1400 °C (Mg/Fe distribution in clinopyroxene and orthopyroxene).

Peters (1968) considers equilibrium was reached in the upper mantle at a pressure range of 10–20 kb (derived from these temperatures and a supposed crystallization between the garnet-forming reactions, to the right of Fo/An = 1 and to the left of Fo/An = 2). He further assumes that the transition from spinel-towards garnet peridotites takes place at the rather low pressure of 20 kb (derived from Kushiro & Yoder, 1966).

He found no evidence of the lherzolite primarily having been a garnet-bearing rock.

Lers, French Pyrenees (Avé Lallemant, 1967)

In a generally medium-grained spinel lherzolite, in which harzburgitic varieties form continuous bands and coarse-grained (usually 2–4 cm ∅) layers of spinel

pyroxenite (mainly diopside, minor orthopyroxene and green spinel) occur abundantly, composite sills and dykes of garnet pyroxenite, dykes of garnet-plagioclase pyroxenite and a last generation of hornblendite veins are encountered.

The present author, disposing of a sample of a composite dyke of this lherzolite made a study of the variations in chemical compositions of the various minerals, the results of which are presented in Figs. III-1 and III-5. A gradual transition from orthopyroxenite + brown ceylonite, via websterite, clinopyroxenite + green spinel, pyrope-spinel clinopyroxenite towards pyrope clinopyroxenite is noted. Contrary to Peters' results (1968) a marked increase of sodium in the clinopyroxenes is found in this transition.

Having demonstrated a solid intrusion of this Pyrenean lherzolite, Avé Lallemant considers its spinel-pyroxenite layers and garnet pyroxenite dykes as original intergranular liquid ("partial fusion products or exsolution material from the high-pressure Mg/Si-spinels").

Beni Bouchera, Morocco (Kornprobst, 1966, 1969)

An isoclinally folded, layered spinel lherzolite with aluminous pyroxenes contains pyroxenite bands (3% of the total volume of the massif), which are often composite – varying from core to rim from orthopyroxenite, via websterite and garnet + spinel websterite towards garnet clinopyroxenite –, although bands of a single facies also occur (orthopyroxenites and garnet clinopyroxenites). Only a few petrographical phenomena are quoted: 1) the occurrence of two populations of garnet – large, possibly primary ones and small, exsolved and interstitial ones –; 2) an increase of minor amphibole towards the centre of the composite bands; 3) the occurrence of plagioclase, as exsolutions from clinopyroxenes and in the kelyphitized rims of garnet.

According to Kornprobst (1969) the origin of these rocks should be sought in the upper mantle, in which a pyrolitic diapir has risen adiabatically and intersected the solidus between 1400° and 1500 °C at about 25 kb.

A small amount of liquid, having a slightly picritic hypersthene-normative basaltic composition, originated while the residuum recrystallized in the Al-pyroxene peridotite field (with probably minor spinel). With further ascent the liquidus of the initial anatectic melt is crossed and aluminous pyroxenes start to crystallize, while the residual liquid, gaining a nepheline-normative alkali-basaltic composition, finally solidifies as a garnet-clinopyroxene assemblage. In a still later stage, during which aluminous pyroxenes increasingly exsolve spinel in the residual peridotite, some clinopyroxenes in the bands exsolve garnet and orthopyroxene. Finally the whole ultramafic mass has been emplaced into a granulite-facies environment, during which the last liquids were reinjected due to tectonic movements and subsequently the series was isoclinally folded. Contact metamorphic and partial anatexis phenomena are encountered in the rocks. Equilibrium temperatures indicate values between 1100° and 1200 °C at 15–20 kb for the final assemblage.

Kalskaret, South Norway (Carswell, 1968b)
Carswell describes two lens-shaped horizons of re-
markably fresh garnet peridotites occurring within
harzburgitic-dunitic rocks.

Within these horizons a transition is found from
garnet lherzolites, via garnet wehrlite to garnet
websterite, over a distance of several metres. A strong
linear trend between the compositions of the various
rocks having been proved, Carswell considers a limited
degree of mechanical mixing and segregation between
a picritic liquid (crystallized as a garnet websterite)
and a dunitic residuum the best explanation of the
intermediate compositions found. He states that this
process "superimposed upon the crystal-liquid mixing
process has been a factor involved in producing the
intermediate rock compositions which are difficult to
explain by the partial melting process alone".

Carswell pleads in favour of a crystallization under
eclogite-facies conditions within the upper mantle and
a recrystallization and reequilibration prior to or
during emplacement still under subsolidus eclogite-
facies conditions, perhaps as low as 600°–700 °C.

Indications of higher temperatures are deduced
from rare exsolution lamellae of garnet in clino-
pyroxene.

FINAL REMARKS

Although it is not the intention of the author to give a
general review of the common features of garnet
pyroxenites associated with ultramafic rocks and their
differences from true eclogites (omphacite + pyral-
mandine garnet), for which the reader is referred to
Smulikowski (1964), Ravier (1964), Coleman et al.
(1965) and O'Hara (1967b), some general remarks,
mainly concerning the chemical composition of rocks
and their constituent minerals will be given.

Besides the large variety of ariegitic rocks, noted by
O'Hara (1967b), there also proves to be a wide varia-
tion in garnet pyroxenites associated with ultramafic
rocks. Acceptation of the mechanism of initial melting
followed by fractional crystallization renders these
variations and trends easily understandable, while the
garnet- and spinel-free assemblages (e.g., plagioclase
pyroxenites and hornblendites from Lers, kyanite
eclogites from Alpe Arami (Möckel, 1969) and par-
gasitites from Cabo Ortegal) may be included in these
trends.

When the origin of basalts is sought in partial fusion
products of a parental, probably peridotitic rock and
with the basalt-eclogite transformation (Green &
Ringwood, 1967c) in mind the chemical distinction
between garnet pyroxenites and eclogites may be
difficult, although their mode of occurrence is funda-
mentally different. With regard to possible differences
in modes of emplacement, O'Hara & Mercy (1963)
state that "it must be concluded that most eclogites
which occur as lenses in metamorphic terrains have
been introduced there as crystalline masses by tectonic
action". Comparable considerations relative to the
emplacement of alpinetype peridotites have been
brought forward by de Roever (1957). The suggestion

of den Tex (1965) to discuss these rocks in terms of
their metamorphic lineages also shows that a clear
genetic distinction between garnet pyroxenites and
eclogites should be difficult to make in certain cases.
Ravier's statement (1964) is in conflict with this
concept: "Elles (les ariégites) sont, peut-être, des té-
moins du manteau supérieur et il semble bien qu'elles
n'aient subi aucune évolution "crustale". Les éclogites,
au contraire, sont des roches metamorphiques". Ravier
does not exclude, however, the possibility that ariegites
may be transformed into eclogites.

The marked difference between residual lherzolites
with their partial melting products (the orthopyrox-
enite-websterite-garnet ± spinel clinopyroxenite suite)
and residual garnet-free or still garnet-bearing peri-
dotites with their garnet-bearing partial melting
products might be explained by assuming different
depths of melting and segregation processes inducing
different compositions of the initial liquids and differ-
ent residual rocks.

Also, of course, their metamorphic history is at
stake.

The low equilibration temperatures proposed for
Swiss and Norwegian garnet peridotites against signi-
ficantly higher temperatures (at lower pressures) for
Pyrenean (and presumably for all lherzolites) suggest
an evolutionary path for garnet peridotites – at the
high P-side of the transition from spinel- to garnet
peridotite – from the solidus (about 1500 °C and 30 kb
pressures) towards lower T-conditions (maybe along
the Precambrian shield geotherm), while during the
ascent of lherzolitic rocks with their melting products
(maybe along the oceanic geotherm) a variety of reac-
tions may take place in these melting products (e.g.,
incoming of spinel, amphibole and the formation of
garnet at the expense of pyroxenes), (see Fig. IV-9).

PETROGENESIS OF THE LHERZOLITIC PERIDO-
TITES AND ASSOCIATED VEINS AND BANDS

Introduction
After data having been gathered about mineral sta-
bility ranges, temperatures and pressures, conditions
and results of partial melting, a genetic model is ten-
tatively proposed. This model has been set up for the
Cabo Ortegal peridotite, while deviating characteris-
tics of Mellid and Castriz peridotites are separately
mentioned.

Order of events
A pyrolitic diapir, rising upwards – probably from the
low-velocity zone – intersects its dry solidus and a
small amount of picritic liquid originates. With regard
to the composition of this liquid, to its crystallization
products and to the mineralogical character of the
residual host rock, an intersection within the garnet
pyrolite field (1450°–1550 °C, 25–30 kb) and a re-
crystallization under pyroxene pyrolite conditions
(1400°–1500 °C, 20–25 kb) appear to give the best fit
with experimental data (see Fig. IV-9: fields Ia and
Ib).
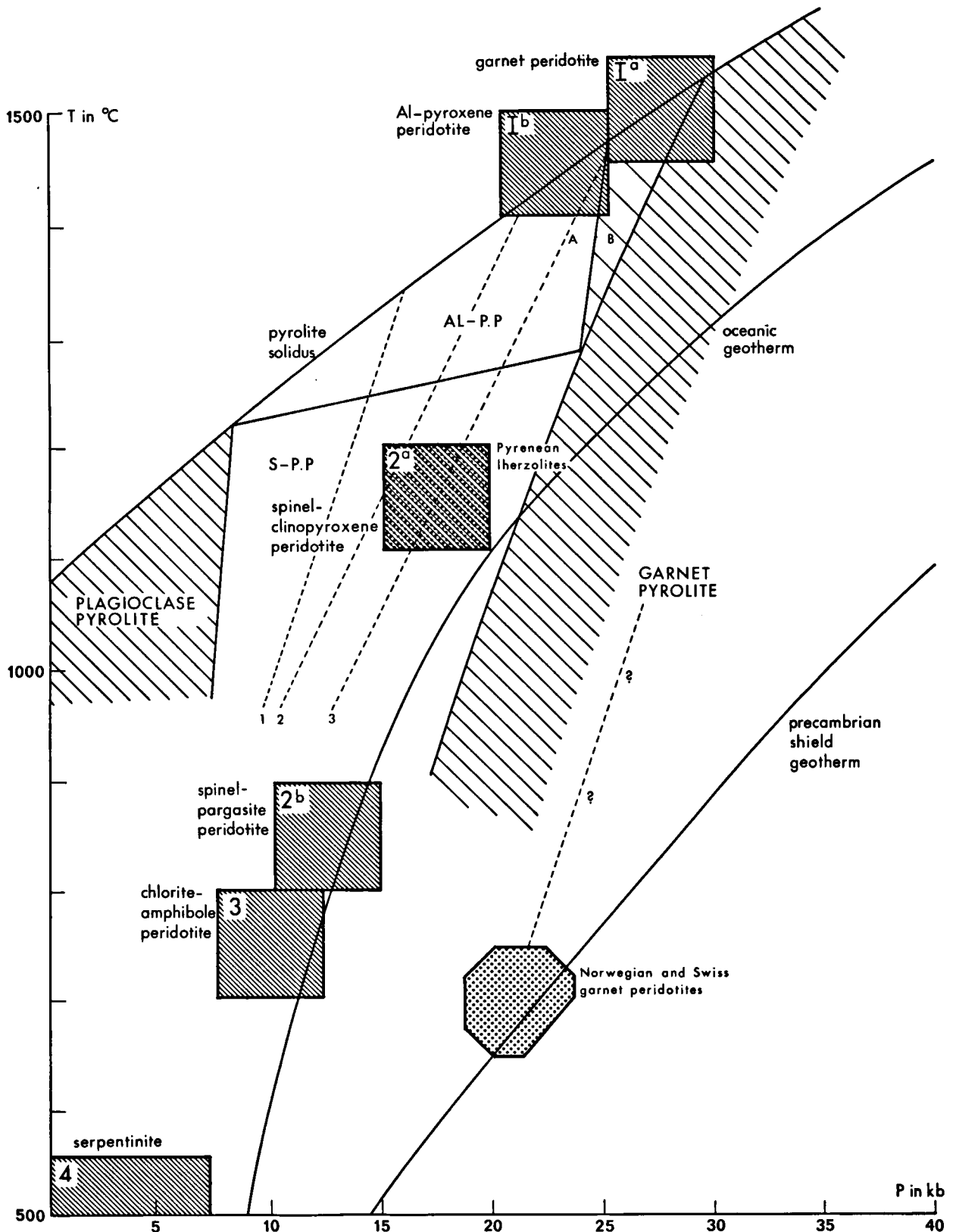
Fig. IV-9. The proposed evolutionary path of the Cabo Ortegal peridotite in the pyrolite PT-diagram.
AL-P.P   = aluminous pyroxene pyrolite
S-P.P   = spinel-pyroxene pyrolite
A and B   = garnet boundaries in pyrolites I + II and III, respectively
1, 2 and 3 = garnet transitions in the systems Fo/An = 1, Fo/An = 2 and Fo + Al-Di + Sp, respectively
Data are derived from Green & Ringwood (1967b), Kushiro & Yoder (1966), MacGregor (1965a) and O'Hara (1967a).

The initial liquid became trapped and, as the interval between liquidus and solidus of a picrite under these conditions is small, quickly solidified into pyroxenitic veins and bands. However, it should be noted that, according to Mottana (1967), the solidus of an ariegitic rock is situated at appreciably lower temperatures. Fractional crystallization resulted in increasingly Al-rich orthopyroxene-, orthopyroxene-clinopyroxene- and clinopyroxene-orthopyroxene assemblages.

With further ascent Al-rich pyroxenes exsolved spinel in both host rocks and pyroxenites. Primary spinel probably was present in minor amounts. Presumably spinel was also formed by olivine-consuming reactions such as $Ol + Al\text{-}Cpx \leftrightarrows Cpx + Opx + Sp$ and $Ol + Al\text{-}Opx \leftrightarrows Opx + Sp$ (MacGregor, 1965b). With these reactions the spinel lherzolite field was entered.

With a further rise of the diapir and maybe an increase of the P/T ratio the garnet stability field was reached by the mafic assemblages: spinel and pyroxenes were no longer in stable association and garnet was formed. Alumina was extracted from spinel, leaving behind a more Cr-rich spinel; titanium could not be incorporated in the garnet molecule so that ilmenite and högbomite were formed, while trails of tiny inclusions in many garnets probably represent nondigested Ti-bearing minerals. A Ti-bearing clinopyroxene is still present in the spinel-garnet-clinopyroxene band from the Castriz area $(TiO_2\ 1.3\%)$; in this sample no ilmenite or högbomite were found. This field represents the stage at which the ultramafic rocks were emplaced and equilibrium conditions were obtained at about $1100°–1200°C$ and 15–20 kb pressure (see Fig. IV-9: field 2a).

Since all first-cycle recrystallization processes in the Galician ultramafic rocks took place under similarly catazonal conditions as the associated crustal rocks, which include granulites and eclogites, an emplacement of hot, solid ultramafites during catazonal metamorphism is preferred over an emplacement before these high PT-conditions prevailed in the crustal rocks. The lack of contact metamorphism with crustal rocks including eclogites, which, according to Vogel (1967), equilibrated at $630°–900°C$ under 14–19 kb pressure, may be due to insufficient temperature differences or to a regional overprint of Hercynian age.

During a hydrous recrystallization and mylonitization phase the formation of aluminous amphibole was the most characteristic mineralogical feature. It was probably formed in the peridotites according to the reaction $Ol + Al\text{-}Cpx + Sp \leftrightarrows Al\text{-}Amf$ (Boyd, 1959) or by replacement by clinopyroxene. The spinel-clinopyroxene peridotite assemblage $(Ol + Opx + Cpx + Sp)$ was replaced by a spinel-pargasite peridotite assemblage $(Ol + Opx + Amf + Sp \pm Cpx)$.

In some veins, however, abundant hydration did not take place: in the spinel clinopyroxenite vein, R 378, brownish pargasite is present only in minor amounts, while also in some, generally thicker, garnet-bearing veins the amount of clinopyroxene is still surprisingly high. This may be explained by assuming

that hydration was mainly effective along planes of internal movement, amphibolizing thin bands but preserving the anhydrous character of the discordant and generally thicker veins. The mineral assemblage itself may also contribute to this feature: pyroxenes in the host peridotite might become more easily amphibolized than pyroxenes in the pyroxenites.

The peculiar position of the spinel clinopyroxenite, sample R 378, may be explained only by assuming that a small amount of reinjected liquid – injected before the hydration phase – could not enter the garnet stability field anymore under subsolidus conditions. The difference in chemical composition of the interstitial brownish amphibole encountered in this vein – higher amounts of alkalies and TiO_2 compared with the greenish amphibole usually found in the Cabo Ortegal peridotites – may be due to different PT-conditions.

Summarizing, it may be stated that emplacement in the lower crust under catazonal conditions was followed by a hydrous phase of catazonal retrogradation. With regard to the coexistence of amphibole and garnet in the garnet-bearing assemblages temperatures of $800°–900°C$ and pressures of 10–15 kb prevailed during this phase (see Fig. IV-9: field 2b). According to Vogel (1967) these events occurred during a Precambrian orogenic cycle.

A later recrystallization occurred during the Hercynian orogeny. Temperatures and pressures – derived from distribution coefficients – indicate PT-conditions of $700°–750°C$ and 8–12 kb pressure, under hydrous conditions. According to Koning (pers. comm., 1970), these values are rather high for Hercynian Galicia. Moderately aluminous pyroxenes recrystallized into low-alumina pyroxenes, amphiboles became somewhat impoverished in Al_2O_3, while aluminous chlorite was formed, e.g., by hydration of spinel (see Fig. IV-9: field 3). Garnet – already metastable within the catazonal retrogradation phase – was not stable in this phase and altered into spinel + amphibole.

During subsequent serpentinization processes at temperatures below $550°C$ orthopyroxene altered into bastite and abundant serpentine minerals were produced. Consequently, according to O'Hara (1967a), the host rocks successively went through the chlorite-amphibole peridotite-, the bastite-peridotite- and the serpentinite-facies (Fig. IV-9: field 4).

In the spinel-pargasite peridotite of the Mellid area the scarcity of spinel inclusions in garnet may point to a reaction in which the spinel-garnet transition nearly ran to completion (due to an earlier entry or to a further penetration into the garnet stability field, compared with the Cabo Ortegal peridotites). With regard to PT-estimates and the occasionally observed hypidiomorphic habit of the Mellid garnets, the first possibility of a somewhat earlier entry seems preferable. Also compositional differences in amphiboles from the two areas (contents of Na_2O and TiO_2) may indicate somewhat higher equilibration temperatures and pressures for the Mellid assemblage. The preservation of high temperature and pressure indications at Mellid

is probably caused by a less hydrated second Pre-cambrian phase in combination with lower PT-conditions during the Hercynian cycle.

In the few samples studied from the Castriz spinel-clinopyroxene peridotite amphibole was only present in minor amounts. In these rather anhydrous samples initially high temperature indications were preserved. The prehydration mineralogy of the garnet-bearing veins and bands is nicely expressed in the spinel-garnet-clinopyroxenite bands encountered in this peridotite.

SPINEL-HORNBLENDE PERIDOTITE FROM THE SANTIAGO AREA

Conclusions from this small ultramafic body occurring in garnet amphibolites must of necessity be scarce. According to van Zuuren (1969), the rock was em-placed before a first pre-Hercynian metamorphic phase of high to intermediate pressure amphibolite-facies conditions, although in some metabasites granulite-facies conditions were encountered.

Chemically the rock resembles a largely recrystalli-zed, metamorphic wehrlite, in which Ti-bearing aluminous clinopyroxene has been replaced by com-mon hornblende + aluminous spinel + ilmenite.

It is difficult to determine whether intermediate assemblages were formed, such as spinel + pyroxenes or spinel + pargasite.

The abundant presence of exsolved spinel in ortho-pyroxene and common hornblende points in this direction, but it must be admitted that strong indi-cations of significantly higher metamorphic conditions than those actually visible – i.e., high grade parts of the amphibolite facies, with temperatures of about 600°–700 °C and 5–8 kb pressure, according to van Zuuren (1969) – are not present. During the Hercynian orogenic cycle minor chlorite was formed.

CHLORITE-AMPHIBOLE PERIDOTITE OF MELLID

When discussing the history of the Cabo Ortegal peridotitic rocks, it has been argued that porphyro-blastesis of spinel plays an important, if not vital role in the metamorphic evolution of the ultramafic rocks.

The former presence of spinel porphyroblasts, even when highly serpentinized, is often recognized in ultramafic rocks in the form of chlorite clusters around opaque spinels. On the basis of distinct presence or absence of such porphyroblasts conclusions may be drawn about the metamorphic history of the ultra-mafic rock in question.

As evidence of this phenomenon is lacking the author concludes that granulite-facies-conditions never affec-ted this peridotite. The assumption seems warranted, therefore, that this rock did not undergo the regionally prevailing pre-Hercynian granulite-facies conditions and that they were emplaced not long before or during the Hercynian orogeny, by which they were trans-formed into chlorite-amphibole peridotites.

CASTRIZ ROCKS

Warnaars (1967) having exhaustively studied the ultramafic rocks that occur in the Castriz area the present author, who did not make field observations in this area and only disposed of several rock samples, does not feel the need to reiterate all his results. Only the most important features will be mentioned.

The main rock type encountered in the several scattered occurrences is a wehrlite, consisting pre-dominantly of clinopyroxene and olivine, while plagio-clase-bearing assemblages are found as layers parallel to the regional schistosity. Textural and mineralogical evidence, as well as temperature and pressure esti-mates, distinctly point to an igneous assemblage, which is only slightly modified by recrystallization. The origin of these rocks is tentatively sought in a peridotitic rock. Although Warnaars states that "their is no resemblance to the ultramafic magma series in the sense of Hess nor to alpine-type peridotites in general", a tectonic emplacement of partial melting products of a parental peridotite at low pressures into basaltic rocks might be envisaged. Under low pressures the clinopyroxene-olivine field is greatly enlarged and liquids crystallize following the olivine-clinopyroxene-plagioclase sequence (O'Hara, 1965). It may be possible that its emplacement was lubricated by small amounts of residual liquids, which were rich in CaO and Al_2O_3 (the trend towards the CAS-corner men-tioned above) and when fractionated, became under-saturated in silica. There is no need to introduce contamination processes for the explanation of the calco-aluminous character of the spinel-amphibole wehrlites, which might be considered as wehrlites + residual liquids. The occurrence of patchy amphi-bolites – also rich in calcium and alumina – around the ultramafic bodies is noteworthy. It is tentatively suggested that the emplacement at low pressures of still hot, but largely solid ultramafic bodies - lubri-cated by Ca- and Al-rich residual liquids – induced contact metamorphic and metasomatic phenomena in the immediate host rocks, which were not erased by subsequent metamorphic phases.

Regarding these metamorphic phases there appears to exist a correlation with phenomena described from the Lizard complex: an anhydrous recrystallized core with hydrous recrystallized margins. Marginal hy-dration might also in this case be consistent with marginal cooling and thus be an effect of lower temper-ature rather than higher water pressures (Green, 1964). In the anhydrous assemblages spinel-orthopyroxene symplektites were formed in plagioclase-bearing as-semblages and aluminous pyroxenes reacted with olivine to give Al-poor pyroxenes and spinel, while common hornblende and spinel in the spinel-amphi-bole wehrlites represent the hydrous metamorphic assemblage.

With regard to the development of spinel-ortho-pyroxene symplektites recrystallization took place within the low-pressure part of the spinel-lherzolite facies of O'Hara (1967a) – the Seiland subfacies with the diopside + enstatite + anorthite + spinel associa-tion in basic assemblages – with a slight increase of the P/T ratio. The common occurrence of brown amphi-bole in or near these symplektites points to higher

water pressures. Temperatures of 1000°–1100 °C and pressures of 11–12 kb are assumed by Warnaars for this phase in the still hot ultramafic bodies; these estimates are probably too high because of the common occurrence of amphibole. Temperatures of about 900 °C under 10 kb pressure are better estimates.

On the other hand, temperatures in the spinel-amphibole wehrlites (and in all rocks occurring at the margin of the ultramafic bodies) were probably significantly lower and more in accord with country rock temperatures. The spinel-amphibole aggregates in these wehrlites originally mainly consisted of plagioclase with minor clinopyroxene, in the opinion of the present author. A slight increase of the P/T ratio under hydrous conditions may lead to the observed phenomena: orthopyroxene rims around olivine (due to the unstable coexistence of olivine and plagioclase under these PT-conditions), rims of brownish amphibole around clinopyroxene and abundant exsolution of spinel in clinopyroxene, porphyroblastesis of green spinel and development of common hornblende around spinel. Although it might be suggested that the alteration of the original assemblage took place in two stages – development of a spinel-pyroxene association followed by large-scale amphibolization – no sufficient evidence was found to warrant this suggestion.

Warnaars noted one catazonal phase with hornblende-clinopyroxene-almandine-subfacies conditions in the mafic country rocks. However, as the chemical composition of the spinel-amphibole wehrlites might be compared with the garnet-bearing assemblages from Cabo Ortegal, the absence of garnet and also maybe of pargasite indicates lower PT-conditions for these rocks: a recrystallization under low pressure granulite-facies conditions seems more likely.

These events took place during a pre-Hercynian orogenic cycle.

Mesozonal conditions prevailed during a Hercynian cycle, in which a further amphibolization occurred: clinopyroxene was replaced by tremolite and orthopyroxene by cummingtonite. Spinel-amphibole peridotites were altered into chlorite-amphibole peridotites with chromite. The country rocks underwent albite-epidote-amphibolite-facies conditions.

CONCLUSIONS

The present investigation shows that mineral analyses are a useful aid in unravelling the metamorphic history of ultramafic rocks, especially when compositional differences are indicative of changing PT-conditions. These conditions apply particularly to pyroxenes (Al_2O_3 contents, Mg/Fe ratios), amphiboles (contents of Al_2O_3, TiO_2 and alkalies) and garnets (pyrope contents and zonary character). A sound knowledge of the stability ranges of these minerals in ultramafic assemblages is, however, required for a petrological interpretation of these compositional differences. Although many experimental investigations concerning ultramafic mineral assemblages were already carried out during the last decade, the need for more detailed information is clearly felt: the relation between the appearance of garnet and aluminous amphibole and the whole-rock composition, as well as the conduct of natural ultramafic assemblages under intermediate to high pressures and hydrous conditions are still insufficiently understood.

The use of distribution coefficients between coexisting minerals as geothermometers and/or geobarometers may seem appealing, nevertheless many objections may be raised against it. These objections deal mainly with the validity of these temperature and pressure derivations and the conditions of equilibration. The calculated values should be supported by petrographical evidence.

The electron microprobe proves to be an indispensable tool in determining chemical differences between more generations of a single mineral species (pyroxenes and amphiboles) and zonary textures in garnets. This technique will, in future, largely replace more conventional analytical methods for the determination of the major elements in minerals.

Further, it is concluded that a chemical approach to the petrology of ultramafites, although providing many useful data, does not by itself solve all problems concerning genesis, emplacement and metamorphism; in combination with results obtained from petrofabric analysis and a thorough study of the country rocks a more satisfactory hypothesis may be expected.

SAMENVATTING

De onderzochte ultramafische gesteenten komen op verschillende plaatsen voor in een gordel van metabasieten van vermoedelijk Precambrische ouderdom in West-Galicië, Spanje. Verschillende typen worden aangetroffen: spinel-clinopyroxeen-, spinel-pargasiet-, spinel-hoornblende- en chloriet-amfibool-peridotieten, wehrlieten, spinel-amfibool- en plagioklaas-wehrlieten. Veel gesteenten zijn gedeeltelijk of geheel geserpentiniseerd.

In de spinel-clinopyroxeen-peridotieten komen banden, in de spinel-pargasiet-peridotieten banden, aders en lensen voor van granaat ± spinel-pyroxeniet en -pargasiet, terwijl spinel-pyroxenieten incidenteel gevonden worden in de spinel-pargasiet-peridotiet van Cabo Ortegal. Verondersteld wordt dat deze pyroxenieten en pargasitieten gekristalliseerd zijn uit een partiële smelt van een mantelperidotiet. Deze smelt heeft een picritische samenstelling en kristalliseert als

een Al-rijke pyroxeen associatie, waarin granaat ge-
vormd wordt onder subsolidus omstandigheden ten
koste van spinel en pyroxeen.

Plaatsname van deze katazonale gesteenten ge-
schiedde tijdens een Precambrische orogenese onder
hoge-druk granulietfacies omstandigheden. De be-
rekende evenwichtskondities zijn 1100°–1200°C bij
15–20 kb druk. Door katazonale retrogradatie worden
deze spinel-clinopyroxeen-peridotieten omgezet in
spinel-pargasiet-peridotieten (800°–900°C bij 10–15 kb
druk). Waarschijnlijk is granaat in metastabiel even-
wicht met pargasiet en ontstaat in deze fase het zo-
naire karakter van de granaat. Al-rijke chloriet wordt
gevormd tijdens de Hercynische orogenese onder
mesozonale omstandigheden. Granaat zet dan om in
spinel-amfibool-kelyfiet en de nieuwgevormde py-
roxenen en amfibolen hebben lagere Al-percentages.
Een hydrothermale aktiviteit aan het einde van de
Hercynische orogenese veroorzaakte de serpentinisatie
van deze peridotieten.

De spinel-hoornblende-peridotiet heeft waarschijn-
lijk geen hoge-druk granulietmetamorfose meegemaakt
tijdens de Precambrische orogene hoofdfase.

De chloriet-amfibool-peridotiet heeft vermoedelijk
een vroeg-Paleozoische ouderdom.

De wehrlieten worden beschouwd als partiële
smelten van een peridotiet, die onder lage druk ge-
kristalliseerd zijn, terwijl de spinel-amfibool-wehrlieten
gehydrateerde plagioklaas-wehrlieten zijn.

Chemische gesteente-analysen van peridotieten en
pyroxenieten worden gegeven. De neutronen-aktive-
ringsanalyse is toegepast bij de bepaling van enke-
le sporenelementen. Elektronenmikrosonde-analysen
worden gegeven van olivijnen, pyroxenen, granaten,
amfibolen, spinellen, chlorieten, högbomieten en il-
menieten. De mineraalsamenstellingen worden ver-
geleken met gesteente-analysen en verdelingskoëffi-
ciënten zijn berekend waaruit temperatuur- en druk-
indikatoren zijn afgeleid. De konklusie is gewettigd
dat de chemische benaderingswijze van de petrologie
van ultramafieten, hoewel zij veel nuttige gegevens
verschaft, niet alle problemen rond hun genese, plaats-
name en metamorfose oplost; in kombinatie met
maakselanalytische resultaten en een gedegen studie
van de geässocieerde gesteenten mag een meer be-
vredigende hypothese verwacht worden.

REFERENCES

Abelson, P. H., ed., 1959. Researches in geochemistry. Vol. 1. New York, Wiley, 511 pp.

Avé Lallemant, H. G., 1967. Structural and petrofabric analysis of an "Alpine-type" peridotite: the lherzolite of the French Pyrenees. Leidse Geol. Med., 42, pp. 1–57.

Bartholomé, P., 1961. Co-existing pyroxenes in igneous and metamorphic rocks. Geol. Mag., 98, pp. 346–348.

—, 1962. Iron-magnesium ratio in associated pyroxenes and olivines. Geol. Soc. Am. Buddington vol., pp. 1–20.

Behr, H. J., et al., 1965. Die Granulite von Zöblitz im Erzgebirge als Beispiel für Granulitbildung in tiefreichenden Scherhorizonten. Krystallinikum, 3, pp. 7–29.

Bethe, H. A., 1930. Zur Theorie des Durchgangs schneller Korpuskularstrahlen durch Materie. Ann. Phys., 5, pp. 325–400.

Binns, R. A., 1962. Metamorphic pyroxenes from the Broken Hill district, New South Wales. Min. Mag., 35, pp. 306–326.

Bishop, H. E., 1968. The absorption and atomic number corrections in electronprobe X-ray microanalysis. Brit. Jour. Appl. Phys. (J. Phys. D), (2) 1, pp. 673–684.

Borg, I. Y., 1967. On conventional calculations of amphibole formulae from chemical analyses with inaccurate H_2O (+) and F determinations. Min. Mag., 36, pp. 583–590.

Boyd, F. R., 1959. Hydrothermal investigations of amphiboles. In: Abelson (1959), pp. 377–396.

Boyd, F. R. & Schairer, J. F., 1964. The system $MgSiO_3$-$CaMgSi_2O_6$. Jour. Petr., 5, pp. 275–309.

Brown, G., 1961. The X-ray identification and crystal structures of clay minerals. London, Min. Soc., 544 pp.

Bultitude, R. J. & Green, D. H., 1968. Experimental study at high pressures on the origin of olivine nephelinite and olivine melilite nephelinite magmas. Earth Planet. Sci. Lett., 3, pp. 325–337.

Cardoso, M. G. I. & Parga-Pondal, I., 1951. Kotschubeita de la Sierra de la Capelada, Cabo Ortegal, Galicia (España). Notas comuns. inst. geol. minero Esp., 24, pp. 93–100.

Carswell, D. A., 1968a. Possible primary upper mantle peridotite in Norwegian basal gneiss. Lithos, 1, pp. 322–355.

—, 1968b. Picritic magma – residual dunite relationships in garnet peridotite at Kalskaret near Tafjord, South Norway. Contr. Min. Petr., 19, pp. 97–124.

Carte géologique du nord-ouest de la péninsule ibérique (1967). Published by the Geological Survey of Portugal, Lisbon.

Coleman, R. G. et al., 1965. Eclogites and eclogites: their differences and similarities. Bull. Geol. Soc. Am., 76, pp. 483–508.

Davis, B. T. C. & Boyd, F. R., 1966. The join $Mg_2Si_2O_6$-$CaMgSi_2O_6$ at 30 kilobars pressure and its application to pyroxenes from kimberlites. Jour. Geophys. Res., 71, pp. 3567–3576.

Deer, W. A., Howie, R. A. & Zussman, J., 1963. Rock-forming minerals. Vol. 2: Chain silicates. London, Longmans, 372 pp.

Duncumb, P. & Reed, S. J. B., 1968. The calculation of stopping power and backscatter effects in electron probe microanalysis. In: Heinrich (1968), pp. 133–154.

— & Shields, P. K., 1966. Effect of critical excitation potential on the absorption correction. In: McKinley et al. (1966), pp. 284–295.

Fiala, J., 1965. Pyrope of some garnet peridotites of the Czech Massif. Krystallinikum, 3, pp. 55–74.

—, 1966. The distribution of elements in mineral phases of some garnet peridotites from the Bohemian massif. Krystallinikum, 4, pp. 31–53.

Frey, F. A., 1969. Rare earth abundances in a high-temperature peridotite intrusion. Geochim. Cosmochim. Acta, 33, pp. 1429–1447.

Frietsch, R., 1957. Determination of the composition of garnets without chemical analysis. Geol. Fören. Förh., 79, pp. 43–51.

Gilbert, M. C., 1968. Reconnaissance study of the stability of amphiboles at high pressures. Carnegie Inst. Wash. Yearb., 67, pp. 167–170.

Girod, M., 1967. Données pétrographiques sur des pyroxénolites à grenat en enclaves dans des basaltes du Hoggar (Sahara central). Bull. Soc. fr. Min. Crist., 90, pp. 202–213.

Green, D. H., 1964. The petrogenesis of the high-temperature peridotite intrusion in the Lizard area, Cornwall. Jour. Petr., 5, pp. 134–188.

—, 1966. The origin of the "eclogites" from Salt Lake Crater, Hawaii. Earth Planet. Sci. Lett., 1, pp. 414–420.

—, 1969. The origin of basaltic and nephelinitic magmas in the Earth's mantle. Tectonophys., 7, pp. 409–422.

— & Ringwood, A. E., 1967a. The genesis of basaltic magmas. Contr. Min. Petr., 15, pp. 103–190.

—, 1967b. The stability fields of aluminous pyroxene peridotite and garnet peridotite and their relevance in upper mantle structure. Earth Planet. Sci. Lett., 3, pp. 151–160.

—, 1967c. An experimental investigation of the gabbro to eclogite transformation and its petrological applications. Geochim. Cosmochim. Acta, 31, pp. 767–833.

—, 1969. The origin of basalt magmas. In: Hart (1969), p. 489–495.

Hart, P. J., ed., 1969. The earth's crust and upper mantle. Geophysical monograph 13. Richmond (Virg.), William Byrd Press, 735 pp.

Heinrich, K. F. J., 1966. X-ray absorption uncertainty. In: McKinley et al. (1966), pp. 296–377.

—, 1967. The absorption correction model for microprobe analysis. Abs. 2nd natl. conf. Electron Microprobe Analysis, Boston, Mass. Paper 7.

Heinrich, K. F. J., ed., 1968. Quantitative electron probe microanalysis. Natl. Bur. Stand. Sp. Publ. 298. Washington, U.S. Government Printing Office, 299 pp.

Hostetler, P. B. et al., 1966. Brucite in Alpine serpentinites. Am. Min., 51, pp. 75–98.

Ito, K. & Kennedy, G. C., 1967. Melting and phase relations in a natural peridotite to 40 kilobars. Am. Jour. Sci., 265, pp. 519–538.

Jackson, E. D., 1966. "Eclogite" in Hawaiian basalts. U.S. Geol. Surv. Prof. Paper 550-D, pp. 151–157.

Kappel, F., 1967. Die Eklogite Meidling im Tal und Mitterbachgraben im niederösterreichischen Moldanubikum südlich der Donau. N. Jahrb. Min. Abh., 107, pp. 266–298.

Keil, K., 1967. The electron microprobe X-ray analyzer and its application in mineralogy. Fortschr. Min., 44, pp. 4–66.

Kieft, C. & Maaskant, P., 1969. Quantitative microprobe-analyses of silicates: a comparison of different correction methods. Abs. conf. Roy. Micr. Soc. Roy. Min. Soc., Manchester, 1969.

Koning, H., 1966. Les types des roches basiques et ultrabasiques qu'on rencontre dans la partie occidentale de la Galice (Espagne). Leidse Geol. Med., 36, pp. 235–242.

Kornprobst, J., 1966. A propos des péridotites du massif des Beni Bouchera (Rif septentrional – Maroc). Bull. Soc. fr. Min. Crist., 89, pp. 399–404.

—, 1969. Le massif ultrabasique des Beni Bouchera (Rif Interne, Maroc): Etude des péridotites de haute température et de haute pression, et des pyroxenolites, à grenat ou sans grenat, qui leur sont associées. Contr. Min. Petr., 23, pp. 283–322.

Kretz, R., 1961. Some applications of thermodynamics to coexisting minerals of variable compositions. Examples: orthopyroxene-clinopyroxene and orthopyroxene-garnet. Jour. Geol., 69, pp. 361–387.

—, 1963. Distribution of magnesium and iron between orthopyroxene and calcic pyroxene in natural mineral assemblages. Jour. Geol., 71, pp. 773–785.

Kushiro, I., 1962. Clinopyroxene solid solutions. Pt. 1. The $CaAl_2SiO_6$ component. Jap. Jour. Geol. Geog., 33, pp. 213–220.

—, 1965a. Clinopyroxene solid solutions at high pressures. Carnegie Inst. Wash. Yearb., 64, pp. 112–117.

—, 1965b. The liquid relations in the systems forsterite-$CaAl_2SiO_6$-silica and forsterite-nepheline-silica at high pressures. Carnegie Inst. Wash. Yearb., 64, pp. 103–109.

—, 1968. Compositions of magmas formed by partial zone melting of the earth's upper mantle. Jour. Geophys. Res., 73, pp. 619–634.

—, 1969. Discussion of the paper "The origin of basaltic and nephelinitic magmas in the earth's mantle" by D. H. Green. Tectonophys., 7, pp. 427–436.

— & Yoder, H. S., Jr., 1966. Anorthite-forsterite and anorthite-enstatite reactions and their bearing on the basalt-eclogite transformation. Jour. Petr., 7, pp. 337–362.

— et al., 1968. Melting of a peridotite nodule at high pressures and high water pressures. Jour. Geophys. Res., 73, pp. 6023–6029.

Lambert, I. B. & Wyllie, P. J., 1968. Stability of hornblende and a model for the low velocity zone. Nature, 219, p. 5160.

Leake, B. E., 1968. A catalog of analysed calciferous and subcalciferous amphiboles together with their nomenclature and associated minerals. Geol. Soc. Am. Sp. Paper 98.

Livingstone, A., 1967. A garnet peridotite and a garnet-amphibole pyroxenite from South Harris, and their bearing on the South Harris eclogite facies status. Min. Mag., 36, pp. 380–388.

Long, J. V. P., 1967. Electron probe microanalysis. In: Zussman (1967), pp. 215–260.

MacGregor, I. D., 1964. The reaction 4 enstatite + spinel ⇌ forsterite + pyrope. Carnegie Inst. Wash. Yearb., 63, p. 157.

—, 1965a. Stability fields of spinel and garnet peridotites in the synthetic system MgO-CaO-Al_2O_3-SiO_2. Carnegie Inst. Wash. Yearb., 64, pp. 126–134.

—, 1965b. Aluminous diopsides in the three-phase assemblage diopside solid solution + forsterite + spinel. Carnegie Inst. Wash. Yearb., 64, pp. 134–135.

—, 1967. Mineralogy of model mantle compositions. In: Wyllie (1967), pp. 382–393.

Mackenzie, D. B., 1960. High-temperature alpine-type peridotite from Venezuela. Bull. Geol. Soc. Am., 71, pp. 303–318.

McKie, D., 1963. The högbomite polytypes. Min. Mag., 33, pp. 563–580.

McKinley, T. D. et al., eds., 1966. The electron microprobe. New York, Wiley, 1035 pp.

Mercy, E. L. P. & O'Hara, M. J., 1965. Chemistry of some garnet-bearing rocks from South Norwegian peridotites.

Norsk Geol. Tidsskr., 45, pp. 323–332.

Miyashiro, A., 1966. Some aspects of peridotite and serpentinite in orogenic belts. Jap. Jour. Geol. Geog., 37, pp. 45–61.

Möckel, J. R., 1969. Structural petrology of the garnet-peridotite of Alpe Arami (Ticino, Switzerland). Leidse Geol. Med., 42, pp. 61–130.

Monchoux, P. & Besson, M., 1969. Sur les compositions chimiques des minéraux des lherzolites pyrénéennes et leur signification génétique. Bull. Soc. fr. Min. Crist., 92, pp. 289–298.

Mottana, A. et al., 1967. Experimental studies on ariegites. Can. Min., 19, p. 302.

Naldrett, A. J. & Kullerud, G., 1967. Investigations of the nickel-copper ore and adjacent rocks of the Strathcona Mine, Sudbury District, Ontario. Carnegie Inst. Wash. Yearb., 65, pp. 302–320.

O'Hara, M. J., 1963. The join diopside-pyrope at 30 kilobars. Carnegie Inst. Wash. Yearb., 62, pp. 116–118.

—, 1965. Primary magmas and the origin of basalts. Scot. Jour. Geol., 1, pp. 19–40.

—, 1967a. Mineral facies in ultrabasic rocks. In: Wyllie (1967), pp. 7–18.

—, 1967b. Mineral parageneses in ultrabasic rocks. In: Wyllie (1967), pp. 393–403.

—, 1968. The bearing of phase equilibria studies in synthetic and natural systems on the origin and evolution of basic and ultrabasic rocks. Earth-Sci. Rev., 4, pp. 69–133.

— & Mercy, E. L. P., 1963. Petrology and petrogenesis of some garnetiferous peridotites. Trans. Roy. Soc. Edinburgh, 65, pp. 251–314.

—, 1966. Garnet-peridotite and eclogite from Bellinzona, Switzerland. Earth Planet. Sci. Lett., 1, pp. 295–300.

— & Yoder, H. S., Jr., 1967. Formation and fractionation of basic magmas at high pressures. Scot. Jour. Geol., 3, pp. 67–117.

Oosterom, M. G. & Das, H. A., 1969. Neutron activation analysis of Vourinos and Othrys ultramafic rocks and serpentinites; with special reference to alkali contents. Proc. Kon. Ned. Akad. Wetensch., Series B, 72, pp. 175–191.

Page, N. J., 1967. Serpentinization considered as a constant volume metasomatic process: a discussion. Am. Min., 52, pp. 545–549.

Paraskevopoulos, G. M., 1969. Rodingite in Serpentiniten von NW-Thessalien, Griechenland. N. Jahrb. Min. Abh., 112, pp. 47–62.

Parga-Pondal, I., 1956. Nota explicativa del mapa geológico de la parte NO de la provincia de La Coruña. Leidse Geol. Med., 21, pp. 468–484.

Pattee, H. H. et al., eds., 1963. X-ray optics and X-ray microanalysis. Vol. 3. New York, Academic Press.

Peters, T., 1963. Mineralogie und Petrographie des Totalpserpentins bei Davos. Schweiz. Min. Petr. Mitt., 43, pp. 529–685.

—, 1968. Distribution of Mg, Fe, Al, Ca and Na in coexisting olivine, orthopyroxene and clinopyroxene in the Totalp serpentinite (Davos, Switzerland) and in the alpine metamorphosed Malenco serpentinite (N. Italy). Contr. Min. Petr., 18, pp. 65–75.

— & Niggli, E., 1964. Spinellführende Pyroxenite ("Ariégite") in den Lherzolitkörpern von Lherz und Umgebung (Ariège, Pyrenäen) und der Totalp (Graubünden, Schweiz), ein Vergleich. Schweiz. Min. Petr. Mitt., 44, pp. 513–517.

Philibert, J., 1963. A method for calculating the absorption correction in electronprobe microanalysis. In: Pattee et al. (1963), pp. 379–392.

Phillips, R., 1963. The recalculation of amphibole analyses. Min. Mag., 33, pp. 701–711.

—, 1966. Amphibole compositional space. Min. Mag., 35, pp. 945–952.

Prinz, M. & Nehru, C. E., 1969. Comments on "Kaersutite from San Carlos, Arizona, with comments on the paragenesis of this mineral" by Brian Mason. Min. Mag., 37, pp. 333–338.

Ravier, J., 1964. Ariégites et éclogites. Bull. Soc. fr. Min. Crist., 87, pp. 212–215.

Reed, S. J. B., 1964. Some aspects of X-ray microanalysis in mineralogy. Ph. D. Thesis. University of Cambridge.

—, 1965. Characteristic fluorescence corrections in electronprobe microanalysis. Brit. Jour. Appl. Phys., 16, pp. 913–926.

Ringwood, A. E., 1969. Composition and evolution of the upper mantle. In: Hart (1969), pp. 1–17.

— et al., 1964. Petrological constitution of the upper mantle. Carnegie Inst. Wash. Yearb., 63, pp. 147–152.

Roever, W. P. de, 1957. Sind die Alpinotypen Peridotitmassen vielleicht tektonisch verfrachtete Bruchstücke der Peridotitschale? Geol. Rundschau, 46, pp. 137–146.

Romijn, E., 1959. Petrografische kartering van het westelijk gedeelte van Cabo Ortegal (Galicië, Sp.). Unpublished M. Sc. Thesis. University of Leyden.

Rost, F., 1961. Zur Stellung der Granatultrabasite des Sächsischen Grundgebirges. Freiberger Forschungsh., C 119, pp. 119–134.

—, 1968. Ueber die Fazieseinstufung orogenotyper Peridotite und ihre Beziehungen zur Peridotitschale des Erdmantels. Internat. Geol. Cong., Rept. 23th Sess. Prague 1968, pp. 187–196.

Scherpenzeel, E. van, 1969. Petrografie en mineralogie van een gebied rondom Mellid (Galicië, NW Spanje). Unpublished M. Sc. Thesis. University of Leyden.

Shapiro, L., 1967. Rapid analysis of rocks and minerals by single solution method. Jour. Surv. Res., 575B, pp. D187–D191.

— & Brannock, W. W., 1962. Rapid analysis of silicate, carbonate and phosphate rocks. Geol. Surv. Bull., 1144-A.

Smith, J. V., 1965. X-ray emission microanalysis of rockforming minerals. I: Experimental techniques. Jour. Geol., 73, pp. 830–864.

Smulikowski, K., 1964. Le probléme des éclogites. Geol. Sudet., 1, pp. 13–52.

Sørensen, H., 1967. Metamorphic and metasomatic processes in the formation of ultramafic rocks. In: Wyllie (1967), pp. 204–212.

Springer, G., 1967a. Die Berechnung von Korrekturen für die quantitative Elektronenstrahl-Mikroanalyse. Fortschr. Min., 45, pp. 103–124.

—, 1967b. Investigations into the atomic number effect in electronprobe microanalysis. N. Jahrb. Min. Mon. h., 20, pp. 304–317.

—, 1967c. The correction for continuous fluorescence in electronprobe microanalysis. N. Jahrb. Min. Abh., 106, pp. 241–256.

Streckeisen, A. L., 1967. Classification and nomenclature of igneous rocks. N. Jahrb. Min. Abh., 107, pp. 104–214.

Stueber, A. M. & Goles, G. G., 1967. Abundances of Na, Mn, Cr, Sc and Co in ultramafic rocks. Geochim. Cosmochim. Acta, 31, pp. 75–93.

Sweatman, T. R. & Long, J. V. P., 1969. Quantitative electron-probe microanalysis of rock-forming minerals. Jour. Petr., 10, pp. 332–379.

Tex, E. den, 1965. Metamorphic lineages of orogenic plutonism. Geol. Mijnb., 44, pp. 105–132.

—, 1966. Aperçu pétrologique et structural de la Galice cristalline. Leidse Geol. Med., 36, pp. 211–222.

—, 1969. Origin of ultramafic rocks, their tectonic setting and history: a contribution to the discussion of the paper "The origin of ultramafic and ultrabasic rocks" by P. J. Wyllie. Tectonophys., 7, pp. 457–488.

Thayer, T. P., 1966. Serpentinization considered as a constant volume metasomatic process. Am. Min., 51, pp. 685–710.

Tongeren, G. van, 1970. Petrografie van het gebied om Agualada (La Coruña, NW Spanje). Unpublished M. Sc. Thesis. University of Leyden.

Vogel, D. E., 1967. Petrology of an eclogite- and pyrigarnitebearing polymetamorphic rock complex at Cabo Ortegal, NW Spain. Leidse Geol. Med., 40, pp. 121–213.

Warnaars, F. W., 1967. Petrography of a peridotite-, amphibolite and gabbro-bearing polyorogenic terrain NW of Santiago de Compostela (Spain). Ph. D. Thesis. University of Leyden. 208 pp.

Whittaker, E. J. W., 1968. Classification of the amphiboles. Pap. Proc. 5th Gen. Meeting I. M. A. Cambridge, 1966, pp. 232–242.

Winchell, H., 1958. The composition and physical properties of garnet. Am. Min., 43, pp. 595–600.

Winchell, A. N. & Winchell, H., 1959. Elements of optical mineralogy. Pt. 2, description of minerals. 4th ed., New York, Wiley, 551 pp.

Winkler, H. G. F., 1967. Die Genese der metamorphen Gesteine. Berlin, Springer Verlag, 2nd ed., 237 pp.

Wyllie, P. J. ed., 1967. Ultramafic and related rocks. New York, Wiley, 464 pp.

—, 1969. The origin of ultramafic and ultrabasic rocks. Tectonophys., 7, pp. 437–455.

Ziebold, T. O., 1967. Precision and sensitivity in electron microprobe analysis. Analyt. Chem., 39, pp. 858–861.

Zussman, J., ed., 1967. Physical methods in determinative mineralogy. London, Academic Press, 514 pp.

Zuuren, A. van, 1969. Structural petrology of an area near Santiago de Compostela (NW Spain). Leidse Geol. Med., 45, pp. 1–71.

APPENDIX 1

TABLES

Table III-1. Chemical analyses peridotitic rocks.

	1	2	3	4	5	6	7	8	9	10
SiO_2	44.3	40.2	41.8	40.1	39.8	39.6	44.8	42.0	40.9	
TiO_2	.02	.11	.02	.14	.11	.11	.12	.12	.08	
Al_2O_3	3.3	2.7	4.1	5.3	1.4	2.3	5.1	3.1	2.5	
Fe_2O_3	1.9	8.4	4.1	5.7	5.9	5.9	1.9	5.6	3.9	
FeO	6.1	.90	3.2	2.5	3.2	2.8	6.8	3.8	4.3	
MnO	.13	.14	.13	.18	.12	.12	.18	.12	.08	
MgO	40.8	34.4	34.9	31.3	36.1	34.8	37.0	35.1	36.6	
CaO	2.3	2.0	3.0	2.6	1.9	2.5	3.2	2.5	2.0	
Na_2O	.10	.20	.10	.40	.20	.28	.27	.30	.10	
K_2O	–	.05	–	.05	.07	.06	–	–	.04	
P_2O_5	.03	.02	–	–	.03	.02	–	.01	.06	
CO_2	.33	.46	.33	.25	n.d.	n.d.	.15	.62	n.d.	
H_2O	1.6	10.7	9.4	12.2	10.7	11.1	.90	7.4	8.4	
Cr_2O_3	n.d.	n.d.	n.d.	n.d.	.17	.20	n.d.	n.d.	.57	
NiO	n.d.	n.d.	n.d.	n.d.	n.d.	n.d.	n.d.	n.d.	.30	
	100.91	100.28	101.08	100.72	99.70	99.79	100.42	100.67	99.83	

Recalculated on a water-free basis:

	1	2	3	4	5	6	7	8	9	10
SiO_2	44.9	45.6	46.0	45.7	45.1	45.0	45.2	45.6	45.0	45.34
TiO_2	.02	.12	.02	.16	.12	.12	.12	.13	.09	.10
Al_2O_3	3.3	3.0	4.5	6.0	1.6	2.6	5.1	3.4	2.8	3.59
FeO	7.9	9.6	7.5	8.7	9.5	9.2	8.5	9.6	8.6	8.79
MnO	.13	.16	.14	.21	.14	.14	.18	.13	.09	.15
MgO	41.3	39.0	38.3	35.7	40.8	39.5	37.3	38.1	40.2	38.91
CaO	2.3	2.3	3.3	3.0	2.2	2.8	3.2	2.7	2.2	2.67
Na_2O	.10	.23	.10	.46	.23	.32	.27	.33	.11	.24
K_2O	–	.06	–	.05	.08	.07	–	–	.04	.03
P_2O_5	.03	.02	–	–	.03	.02	–	.01		.02
Cr_2O_3					.19	.22			.63	n.d.
NiO									.33	n.d.
	99.98	100.09	99.86	99.98	99.99	99.99	99.87	100.00	100.16	99.84

Analysts: Miss M. van Wijk and Mr. L. F. M. Belfroid

n.d.	not determined
tr	trace
*)	total Fe as FeO
**)	recalculated to 100 % anhydrous

1.	FCM 1	largely recrystallized spinel-pargasite peridotite
2.	R 70	partly serpentinized spinel-pargasite peridotite
3.	MP 16	item
4.	V 1405b	item, with streaks of pargasitite
5.	R 31	item
6.	R 20	item, with streaks of orthopyroxene-chlorite pargasitite
7.	1 M 9	foliated Mellid spinel-pargasite peridotite
8.	4 M 1	item
9.	FW 928	Castriz spinel-clinopyroxene peridotite
10.		average of 1–9 on a water-free basis
11.		standard deviation
12.	V 3	chlorite-bearing serpentinite
13.	2 M 2	item, from the chlorite-amphibole peridotite of the Mellid area
14.	6 M 2	item
15-16.		pyroxene pyrolites (Ringwood et al., 1964)
17-18.		garnet pyrolites (Ringwood et al., 1964)
19.		pyrolite I (Green & Ringwood, 1967b)
20.		pyrolite II (Green & Ringwood, 1967b)
21.		pyrolite III (Green & Ringwood, 1967b)
22.		model mantle composition, derived from chondritic abundances (Ringwood, 1969)

11	12	13	14	15	16	17	18	19	20	21	22
	39.9	39.9	41.1	44.69	44.77	45.58	43.22	43.20	43.95	45.20	43.25
	–	.01	–	.08	.19	.15	–	.58	.57	.71	
	3.1	1.3	1.7	3.19	4.16	2.41	3.51	4.01	3.88	3.54	3.90
	5.4	6.3	5.2	.09	*)	.27	*)	.35	.75	.48	*)
	2.9	2.0	3.4	7.54	8.21	6.41	9.52	7.88	7.50	8.04	9.25
	.18	.09	.13	.14	.11	.12	.23	.13	.13	.14	
	35.7	36.0	36.3	39.80	39.22	42.60	39.69	39.54	39.00	37.48	38.10
	.80	.10	1.4	2.97	2.42	2.10	3.25	2.67	2.60	3.08	3.22
	.05	.02	–	.18	.22	.24	.45	.61	.60	.57	1.78
	.05	–	–	.02	.05	–		.22	.22	.13	
	.05	–	–	.04	.01	.03	.13				
	.25	.25	.49	.17			**)				
	10.1	12.4	11.0	.43	**)	**)	**)				
	n.d.	n.d.	n.d.	.45	.40	.09	tr	.42	.41	.43	
	n.d.	n.d.	n.d.	.26	.24	n.d.	tr	.39	.39	.20	
	98.48	98.37	100.72	100.05	100.00	100.00	100.00	100.00	100.00	100.00	99.50

11	12	13	14
.39	45.6	46.8	46.3
.05	–	.01	–
1.38	3.5	1.6	1.9
.78	8.8	9.1	9.2
.03	.21	.10	.15
1.78	40.7	42.2	40.9
.44	.91	.11	1.6
.12	.06	.02	–
.03	.06	–	–
.02	.06	–	–
	99.90	99.94	100.05

nrs. 1–6 and 12 represent analyses from Cabo Ortegal rocks
nrs. 5 and 6 are derived from Vogel (1967)
nr. 9 is derived from Warnaars (1967)

Table III-2. Chemical analyses of garnet-bearing veins from Cabo Ortegal.

	1	2	3	4	5	6	7	8	9	10
SiO_2	38.7	39.8	40.4	42.0	42.5	42.6	42.6	44.0	44.5	41.91
TiO_2	2.0	1.5	.54	.90	.60	.13	.70	.57	.50	.84
Al_2O_3	14.5	15.4	14.3	12.1	14.3	13.5	13.5	12.6	10.4	13.39
Fe_2O_3	3.2	1.9	2.3	3.3	2.5	2.1	2.0	3.1	2.0	2.49
FeO	4.6	7.7	4.7	3.4	3.9	2.4	5.4	3.1	4.1	4.36
MnO	.23	.34	.33	.11	.22	.10	.26	.17	.24	.22
MgO	22.1	21.8	23.3	22.4	22.2	23.3	21.5	21.6	22.9	22.32
CaO	7.3	4.3	8.1	8.5	9.1	8.1	8.5	9.7	10.2	8.19
Na_2O	.90	.05	.20	1.3	.35	.95	.60	1.5	.15	.66
K_2O	.20	<.05	<.05	.20	.10	.30	.05	–	.01	.11
P_2O_5	.10	.11	–	.05	–	.10	–	.04	.03	.05
CO_2	.18	.25	.20	.42	.20	.23	.24	.15	.21	.23
H_2O	4.5	4.2	5.4	4.7	5.2	6.2	4.4	3.7	1.26	4.39
	98.51	97.40	99.82	99.38	101.17	100.01	99.75	100.23	96.50	99.16

Analysts: Miss M. van Wijk and Mr. L. F. M. Belfroid

n.d.   not determined

estimated amounts of garnet, pyroxenes + amphibole + spinel and serpentine veinlets in the analysed hand-specimen:

	1	2	3	4	5	6	7	8	9
garnet	20	80	40	10	30	<1	50	<5	30
pyroxenes amphibole spinel	70	10	40	80	60	90	40	90	60
serpentine	10	10	20	10	10	10	10	5	10

1. L 6
2. L 3
3. MP 10
4. L 4
5. MP 14
6. PC 5
7. L 14
8. MP 28
9. V 1403AH
10. average of nrs. 1–9
11. standard deviation
12. nr. 10 minus 5% serpentine
13. nr. 10 minus 10% serpentine
14. R 70: spinel-garnet pyroxenite (after Vogel, 1967)

1	12	13	14
92	42.2	42.1	43.4
57	.89	.94	.52
51	14.2	15.0	12.3
56	2.6	2.8	3.1
52	4.6	4.9	5.3
09	.23	.25	.22
67	21.4	20.2	19.8
70	8.7	9.2	11.8
51	.70	.74	.47
10	.12	.12	.08
05	.05	.06	–
08	.24	.26	n.d.
90	4.0	3.5	2.4
	99.93	100.07	99.39

Table III-3. Chemical analyses of pyroxenite bands and veins and some rocks from the Castriz area.

	1	2	3	4	5	6	7	8
SiO_2	51.9	52.0	52.5	47.5	43.4	44.1	41.6	47.7
TiO_2	.16	.20	.02	.10	.75	.64	.65	.67
Al_2O_3	5.4	5.7	3.3	7.9	13.1	6.4	13.4	13.5
Fe_2O_3	2.1	1.7	1.4	3.0	2.5	6.3	3.3	2.4
FeO	3.4	3.5	3.4	3.5	2.7	4.7	4.6	4.1
MnO	.16	.13	.15	.12	.14	.05	.04	.04
MgO	21.3	20.1	28.9	28.0	20.4	22.7	21.2	13.1
CaO	14.4	13.3	6.0	6.7	13.0	11.8	10.2	15.6
Na_2O	.63	1.1	.20	.15	.75	.59	.98	1.5
K_2O	–	–	–	.05	.01	–	–	–
P_2O_5	–	.04	.53	.06	–	.02	.02	.02
CO_2	.20	.33	.11	.18	.12	n.d.	n.d.	n.d.
H_2O	.68	1.0	3.2	3.2	3.2	2.5	3.2	1.0
Cr_2O_3	n.d.	n.d.	n.d.	n.d.	n.d.	.70	.33	.10
NiO	n.d.	n.d.	n.d.	n.d.	n.d.	.14	.11	.03
	100.33	99.10	99.71	100.46	100.07	100.64	99.63	99.76

Analysts: Miss M. van Wijk and Mr. L. F. M. Belfroid

n.d. not determined

1. MP 20   amphibolized pyroxenite band
2. MP 21   item
3. MP 18   composite band (external zones of chlorite orthopyroxenite, central zone of amphibolized pyroxenite)
4. V 1403b   brown ceylonite orthopyroxenite
5. R 378   spinel sensu stricto clinopyroxenite
6. FW 769   wehrlite
7. FW 753   spinel-amphibole wehrlite
8. FW 848   olivine gabbro

nrs. 1–5 represent analyses from Cabo Ortegal rocks
nrs. 6–8 represent analyses from the Castriz area (after Warnaars, 1967)

Table III-4. Conventional chemical and electron microprobe analyses of a spinel-pargasite peridotite (FCM 1) and a garnet bearing vein (MP 10).

	FCM 1		MP 10	
	conventional chemical	electron microprobe	conventional chemical	electron microprobe
SiO_2	44.3	43.6	40.4	42.2
TiO_2	.02	.06	.54	.34
Al_2O_3	3.3	2.6	14.3	11.5
Fe_2O_3	1.9	} 7.7	2.3	} 5.9
FeO	6.1		4.7	
MnO	.13	.13	.33	.27
MgO	40.8	40.3	23.3	24.9
CaO	2.3	2.5	8.1	7.7
Na_2O	.10	.16	.20	.15
K_2O	–	.08	<.05	.04
Cr_2O_3	n.d.	.36	n.d.	.18
NiO	n.d.	.28	n.d.	.06

n.d. not determined

Table III-5. Neutron activation analyses of peridotites, garnet-bearing veins and pyroxenites.

		Co (ppm)	Sc (ppm)	Na$_2$O (wt.%)	Na$_2$O "wet" (wt.%)	MnO (wt.%)	MnO "wet" (wt.%)	Cr$_2$O$_3$ (wt.%)	Eu (rel.)	Ce (ppm)
I	FCM 1	124	9	.14	.10	.11	.13	.69	9	2
	R 70	130	10	.28	.20	.12	.14	.79	2	7.5
	MP 16	145	13	.15	.10	.10	.13	.95	<1	1
	V 1405B	136	11	.39	.40	.09	.18	.55	8	37
	1 M 9	143	12	.28	.27	.12	.18	.88	<1	30
	4 M 1	145	13	.38	.30	.11	.12	1.05	6	<1
	V 3	133	11	.09	.05	.10	.18	.67	<1	<1
	2 M 2	188	12	.01	.02	.08	.09	1.33	<1	4.5
	6 M 2	133	9	–	.03	.11	.13	.96	<1	13.5
II	L 6	91	49	.88	.90	.15	.23	.48	26	<1
	L 3	70	34					.44	6	9
	MP 10	65	49	.16	.20	.25	.33	.39	<1	–
	L 4	89	29	1.31	1.25	.12	.11	.31	27	1.5
	MP 14	70	46					.18	<1	<1
	PC 5	56	30					.20	38	150
	L 14	77	31	.54	.60	.21	.26	.34	14	<1
	MP 28	79	48	1.42	1.45	.11	.17	.18	14	11.5
	V 1403AH	61	45					.35	21	1
III	MP 20	86	45	.58	.63	.11	.16	2.06	<1	12.5
	MP 21	72	28	1.38	1.10	.12	.13	1.50	40	<1
	MP 18	102	20	.30	.20	.11	.15	.58	12	25
	V 1403b	68	20					1.53	<1	9
	R 378	83	45	.63	.75	.10	.14	.37	19	50

I   peridotitic rocks (see Table III-1)
II garnet-bearing veins (see Table III-2)
III pyroxenites (see Table III-3)

Table III-6. Electron microprobe analyses of olivines.

	1	2	3	4	5	6	7	8	9	10
SiO_2	40.8	40.5	40.6	40.5	40.1	38.9	40.65	40.7	40.0	40.3
MgO	49.1 ± .5	46.4	49.2	47.2	46.0	39.3	48.85	47.4	45.5	46.1
FeO	9.7 ± .6	12.4	9.7	11.6	13.4	20.8	9.75	11.7	14.1	14.1
MnO	.2	.3	.1	.2	.2	.3	.08	.1	.2	.1
NiO	.4	.1	.4	.3	.2	.2	.27	.3	.3	.2
	100.2	99.7	100.0	99.8	99.9	99.5	99.60	100.2	100.1	100.9

numbers of cations on basis of 4 O:

	1	2	3	4	5	6	7	8	9	10
Si	1.00	1.01	1.00	1.00	1.00	1.01	1.00	1.01	1.00	1.0
Mg	1.79	1.72	1.80	1.74	1.71	1.52	1.79	1.75	1.70	1.7
Fe	.20	.26	.20	.24	.28	.45	.20	.24	.29	.2
Mn	.004	.005	.003	.004	.003	.006	–	.003	.005	.0
Ni	.009	.003	.008	.006	.003	.004	.01	.007	.007	.0
$\dfrac{100\,Mg}{Mg + Fe}$	90.0	86.9	90.0	87.9	85.9	77.2	90.0	88.0	85.5	85.5

Olivines from Cabo Ortegal rocks:
1. average and range of 4 olivines from spinel-pargasite peridotites and brown ceylonite orthopyroxenites
2. amphibolized pyroxenite band (MP 20)
Olivines from the Mellid area:
3. spinel-pargasite peridotite (1 M 3)
4. item (5 M 2)
5. chlorite-amphibole peridotite (96-D2-5)
Olivines from the Santiago area:
6. spinel-hornblende peridotite (95-A4-51)
Olivines from the Castriz area:
7. spinel-clinopyroxene peridotite (FW 928)
8. pyroxenitic part in spinel-clinopyroxene peridotite (FW 928)
9. amphibole peridotite (FW 894)
10. item (FW 894)
11. item (FW 898)
12. wehrlite (FW 897)
13. item (FW 769)
14. olivine gabbro (FW 850a)
15. item (FW 848)

nrs. 7, 10, 13 and 15 represent analyses from Warnaars (1967)

11	12	13	14	15
40.3	40.2	39.90	39.5	38.75
46.0	44.4	44.55	39.8	39.40
13.5	15.6	16.05	21.6	22.20
.2	.2	.25	.3	.20
.2	.2	.20	.3	.08
100.2	100.6	100.95	101.5	100.63
1.00	1.01	1.00	1.01	1.00
1.71	1.66	1.66	1.51	1.51
.28	.33	.33	.46	.48
.005	.004	.01	.006	.01
.007	.004	.01	.007	—
85.9	83.5	83.5	76.7	75.9

Table III-7. Electron microprobe analyses of orthopyroxenes.

	1	2	3	4	5	6	7	8	9
SiO_2	56.0 (55.3–56.5)	56.5	52.9	54.6	56.0	53.1	58.1	54.9	55.3
TiO_2	–	–	–	–	–	.1	–	–	–
Al_2O_3	3.3 (3.1– 4.3)	2.2	5.8	4.2	3.4	5.5	.8	3.2	2.4
MgO	33.4 (33.2–33.6)	33.9	33.3	33.5	33.8	31.9	33.5	32.3	28.9
FeO	6.7 (6.4– 7.0)	6.7	6.7	6.6	6.5	8.0	7.9	8.1	13.1
MnO	.2	.2	.2	.2	.2	.2	.3	.1	.3
CaO	.2 (.1– .2)	.2	.3	.3	.3	.8	.3	.3	.2
Cr_2O_3	.2 (.0– .4)	.2	.5	.4	.3	–	.1	.2	–
NiO	–	.1	.1	.1	–	–	–	–	–
	100.0	100.0	99.8	99.9	100.5	99.6	101.0	99.1	100.2

numbers of cations on basis of 6 O:

	1	2	3	4	5	6	7	8	9
Si	1.93	1.95	1.84	1.89	1.92	1.86	1.99	1.93	1.95
Al	.13	.09	.24	.17	.14	.23	.03	.13	.10
Ti	–	–	–	–	–	.003	–	–	–
Mg	1.72	1.75	1.73	1.73	1.73	1.66	1.71	1.69	1.52
Fe	.19	.19	.19	.19	.19	.23	.23	.24	.39
Mn	.006	.006	.006	.006	.006	.006	.008	.003	.01
Ca	.007	.007	.011	.011	.011	.03	.01	.011	.01
Cr	.005	.005	.014	.011	.008	–	.002	.006	–
Ni	–	.003	.003	.003	–	–	–	–	–

$\dfrac{100\ Mg}{Mg + Fe}$	90.1	90.2	90.1	90.1	90.1	87.8	88.1	87.6	79.5

Orthopyroxenes from Cabo Ortegal rocks:
1.   average and range of 4 orthopyroxenes from spinel-pargasite peridotites (R 302b, R 42, R 139 and R 51)
2.   spinel-pargasite peridotite (FCM 1)
3.   brown ceylonite orthopyroxenite (V 1403b)
4.   item
5.   item
6.   spinel sensu stricto clinopyroxenite (R 378)
7.   amphibolized pyroxenite band (MP 20)
   Orthopyroxenes from the Mellid area:
8.   spinel-pargasite peridotite (5 M 2)
   Orthopyroxenes from the Santiago area:
9.   spinel-hornblende peridotite (95-A4-51)
Orthopyroxenes from the Castriz area:
10.   spinel-clinopyroxene peridotite (FW 928)
11.   item
12.   wehrlite (FW 897)
13.   item (FW 769)
14.   olivine gabbro (FW 850a)
15.   item (FW 848)

nrs. 10, 11, 13 and 15 represent analyses from Warnaars (1967); he noted .05 and .30% Na_2O in nrs. 13 and 15, respectively

10	11	12	13	14	15
55.00	56.80	54.7	55.00	53.9	53.30
.08	.08	.2	.18	.2	.21
5.20	1.55	3.0	2.95	4.2	3.75
31.90	33.60	31.1	30.80	27.9	28.25
6.50	6.70	9.9	11.05	13.5	14.23
.07	.07	.2	.23	.3	.20
.55	.20	.3	.30	.4	.35
.29	.03	.3	.08	–	.03
.06	.07	–	.03	–	.06
99.65	99.10	99.7	100.62	100.4	100.38

1.90	1.97	1.93	1.93	1.91	1.89
.21	.06	.12	.12	.18	.16
.002	.002	.004	.01	.004	.004
1.65	1.74	1.63	1.61	1.48	1.49
.19	.20	.29	.32	.40	.42
.002	.002	.007	.01	.008	.005
.02	.01	.01	.01	.02	.01
.01	.002	.007	–	–	–
.002	.002	–	–	–	.002
89.8	89.7	84.9	83.2	78.8	78.0

Table III-8. Electron microprobe analyses of clinopyroxenes.

	1		2	3	4	5	6	7	8	9
SiO$_2$	53.8	(53.1–55.5)	50.8	50.8	51.8	52.3	53.8	55.5	52.2	52.6
TiO$_2$	.2		.9	.3	.2	.2	.1	–	.2	.2
Al$_2$O$_3$	1.9	(1.2– 2.7)	6.5	5.5	4.1	3.9	2.1	.4	3.8	3.2
MgO	17.4	(16.8–18.2)	15.4	17.5	16.9	16.4	17.2	17.3	16.8	16.2
FeO	2.0	(1.8– 2.3)	2.5	2.1	2.1	2.0	2.0	2.3	2.6	3.0
MnO	.1		.1	.1	.1	.1	.1	.1	.1	.1
CaO	24.5	(24.3–25.1)	22.8	22.9	23.3	23.8	24.3	24.3	23.8	23.4
Na$_2$O	.1		.9	.3	.3	.3	.3	.2	.4	.4
Cr$_2$O$_3$	.1	(.1– .4)	.2	.7	.7	.4	.3	.1	.4	–
NiO	–		–	.1	.1	–	–	–	–	–
	100.1		100.1	100.3	99.6	99.4	100.2	100.2	100.3	99.1

numbers of cations on basis of 6 O:

Si	1.95		1.83	1.84	1.90	1.92	1.96	2.01	1.90	1.93
Al	.08		.31	.23	.18	.17	.09	.02	.16	.14
Ti	.005		.02	.006	.004	.004	.002	–	.006	.006
Mg	.94		.80	.95	.93	.90	.93	.93	.91	.88
Fe	.06		.08	.06	.07	.06	.06	.07	.08	.09
Mn	.003		.003	.002	.002	.002	.002	.004	.003	.003
Ca	.95		.87	.89	.92	.94	.94	.94	.93	.92
Na	.01		.09	.02	.02	.02	.02	.01	.03	.03
Cr	.003		.006	.02	.02	.015	.01	.004	.01	–
Ni	–		–	.002	.002	–	–	–	–	–

$\dfrac{100\ Mg}{Mg + Fe}$

94.0	90.9	94.1	93.0	93.8	93.9	93.0	91.9	90.7

Clinopyroxenes from Cabo Ortegal rocks:
1. average and range of 10 clinopyroxenes from spinel-pargasite peridotites and garnet-bearing veins
2. spinel sensu stricto clinopyroxenite (R 378)
3. brown ceylonite orthopyroxenite (V 1403b)
4. item
5. item
6. item
7. amphibolized pyroxenite band (MP 20)
Clinopyroxenes from the Mellid area:
8. spinel-pargasite peridotite (1 M 3)
9. item (5 M 2)
Clinopyroxenes from the Castriz area:
10. spinel-clinopyroxene peridotite (FW 928)
11. item
12. pyroxenitic part of spinel-clinopyroxene peridotite (FW 928)
13. item
14. item
15. wehrlite (FW 897)
16. item (FW 769)
17. olivine gabbro (FW 850a)
18. item
19. item (FW 848)
20. spinel-garnet clinopyroxenite band (B 439a)

nrs. 10, 11, 16 and 19 represent analyses from Warnaars (1967)

10	11	12	13	14	15	16	17	18	19	20
53.50	53.75	49.5	50.8	50.7	51.5	51.80	48.7	51.4	50.75	50.0
.18	.13	.7	.7	.7	1.1	.92	2.1	.9	.95	1.3
4.60	2.60	8.6	7.1	6.0	5.7	4.45	9.0	6.3	6.20	7.2
16.60	16.55	14.0	14.6	15.0	14.9	15.10	13.0	13.9	13.60	13.7
2.70	2.75	3.6	3.4	3.6	3.5	3.80	4.9	4.8	5.25	3.8
.05	.06	.1	.1	.1	.1	.04	.1	.1	.10	–
22.70	23.65	22.9	22.6	22.8	22.1	23.10	21.5	22.0	22.40	22.2
.40	.50	.9	.9	.7	1.1	.60	1.3	1.0	1.25	1.1
.47	.19	.1	.1	.1	.7	.37	–	–	.08	–
–	.03	–	--	–	–	.01	–	–	–	–
101.20	100.21	100.4	100.3	99.7	100.7	100.19	100.6	100.4	100.58	99.3

10	11	12	13	14	15	16	17	18	19	20
1.91	1.95	1.80	1.84	1.86	1.87	1.89	1.78	1.87	1.85	1.84
.19	.11	.37	.30	.26	.24	.19	.39	.27	.26	.31
.006	.005	.02	.02	.02	.03	.03	.06	.03	.03	.04
.895	.89	.76	.79	.82	.81	.82	.71	.75	.74	.75
.08	.09	.11	.10	.11	.11	.11	.15	.15	.16	.12
–	–	.003	.003	.003	.004	–	.003	.003	–	–
.87	.92	.89	.88	.90	.86	.90	.84	.86	.87	.88
.03	.035	.06	.06	.05	.08	.04	.09	.07	.09	.08
.014	.01	.003	.003	.003	.02	.01	–	–	–	–
–	–	–	–	–	–	–	–	–	–	–
91.6	91.3	87.4	88.8	88.2	88.1	87.6	82.5	83.3	82.2	86.2

Table III-9. Electron microprobe analyses of garnets.

	1	2	3	4	5	6	7	8	9	10
SiO_2	42.5	41.8	42.1	40.7	42.0	41.5	42.2	n.d.	n.d.	n.d.
Al_2O_3	23.0	22.8	23.6	24.0	23.9	24.1	23.6	23.5	24.3	n.d.
MgO	17.5	17.3	17.5	17.2	16.3	16.2	18.3	17.5	18.1	15.1
FeO	10.1	10.5	9.7	11.6	11.2	12.0	10.1	10.0	10.5	13.5
MnO	.6	.6	.5	1.0	.8	1.0	.5	.7	.6	1.6
CaO	6.3	6.1	5.9	5.1	6.4	5.8	5.7	6.1	5.9	5.4
Cr_2O_3	1.1	.7	.2	.6	.3	.2	.1	.6	.2	n.d.
	101.1	99.8	99.5	100.2	100.9	100.8	100.5			

numbers of cations on basis of 12 O:

	1	2	3	4	5	6	7	8	9	10
Si	3.02	3.01	3.02	2.94	3.00	2.98	3.00	*)	*)	**)
Al	1.93	1.94	2.00	2.04	2.01	2.03	1.98	1.97	1.99	
Cr	.06	.04	.01	.03	.02	.01	–	.03	.01	
Mg	1.85	1.86	1.87	1.85	1.74	1.72	1.94	1.85	1.87	1.65
Fe	.61	.63	.58	.70	.67	.71	.60	.65	.61	.83
Mn	.03	.04	.03	.06	.05	.06	.03	.04	.04	.10
Ca	.48	.47	.44	.39	.49	.47	.44	.46	.44	.42
	2.97	3.00	2.92	3.00	2.95	2.96	3.01	3.00	2.96	3.00

molecular ratios of most important garnet end members:

	1	2	3	4	5	6	7	8	9	10
pyrope	62.3	62.0	64.0	61.7	59.0	58.1	64.5	61.7	63.2	55.0
almandine	20.5	21.0	19.9	23.3	22.7	24.0	19.9	21.7	20.6	27.7
spessartine	1.0	1.3	1.0	2.0	1.7	2.0	1.0	1.3	1.3	3.3
grossular	16.2	15.7	15.1	13.0	16.6	15.9	14.6	15.3	14.9	14.0

n.d.   not determined
*)   numbers of cations are based on $Al + Cr = 2.00$
**)   numbers of cations are based on $Mg + Fe + Ca + Mn = 3.00$

Garnets from Cabo Ortegal rocks (garnet-bearing veins/bands in spinel-pargasite peridotite):
Major constituents of veins/bands are mentioned
1.   FCM 1   enclosed as eyes in spinel-pargasite peridotite
2.   V 1403a   clinopyroxene, garnet around green and brown spinel
3.   R 1   mainly garnet
4.   R 302b   clinopyroxene, garnet
5.   R 139   amphibole, remnants of garnet
6.   R 351   amphibole, garnet around green spinel
7.   R 351   amphibole, garnet around green spinel
7.   MP 14   amphibole, garnet around green spinel (+ högbomite)
8.   MP 10   clinopyroxene, garnet (near border of vein)
9.   MP 10   item (centre of vein)
10.   MP 28   amphibole, garnet around green spinel
11.   MP 28   item
12.   MP 28   item
Garnets from the Mellid area (garnet-bearing eyes and lenses in spinel-pargasite peridotite):
13.   5 M 2
14.   4 M 4
15.   4 M 4
16.   4 M 4
17.   3 M 1
Garnets from the Castriz area (spinel-garnet clinopyroxene band in peridotite):
18.   B 439a   clinopyroxene, garnet around green spinel

11	12	13	14	15	16	17	18
n.d.	n.d.	41.7	n.d.	n.d.	n.d.	n.d.	41.6
n.d.	n.d.	23.1	n.d.	n.d.	n.d.	23.8	23.3
16.1	14.8	18.1	19.2	18.2	17.4	19.1	16.7
12.6	14.0	10.6	9.1	10.3	12.1	8.7	12.9
1.2	1.6	.7	.5	.8	1.2	.5	.5
5.4	5.4	5.5	5.9	5.1	4.2	6.0	5.5
n.d.	n.d.	.2	n.d.	n.d.	n.d.	n.d.	—
		99.9					100.5

11	12	13	14	15	16	17	18
**)	**)	2.99	**)	**)	**)	*)	3.00
		1.95				2.00	1.98
		.01					—
1.74	1.62	1.92	2.00	1.95	1.88	2.03	1.80
.76	.86	.63	.53	.62	.73	.52	.78
.07	.10	.04	.03	.05	.07	.03	.03
.42	.42	.42	.43	.39	.33	.46	.43
2.99	3.00	3.01	2.99	3.01	3.01	3.04	3.04

11	12	13	14	15	16	17	18
58.2	54.0	63.8	66.9	64.8	62.5	66.8	59.2
25.4	28.7	20.9	17.7	20.6	24.2	17.1	25.6
2.3	3.3	1.3	1.0	1.6	2.3	1.0	1.0
14.0	14.0	14.0	14.4	13.0	11.0	15.1	14.1

Table III-10. Electron microprobe analyses of amphiboles.

	1	2	3	4	5	6	7	8
SiO_2	45.0 (43.4–46.1)	45.5	41.4	51.8	43.4 (43.1–43.7)	51.8	50.1	42.0
Al_2O_3	13.5 (11.1–15.7)	13.7	16.7	7.0	14.6 (14.3–14.9)	5.7	8.3	14.1
TiO_2	.6 (.4– .9)	.5	1.1	.2	.9 (.6– 1.4)	.1	.4	4.6
MgO	17.7 (16.4–19.0)	18.3	17.4	19.9	17.5 (17.2–17.7)	21.1	18.7	15.7
Fe_2O_3	4.3	3.4	4.6	2.8	3.7	4.4	4.8	–
FeO	.5 (4.1– 5.1)	–	–	1.5	.9 (4.0– 4.5)	–	1.0	5.1
MnO	.1	–	.1	.1	.1	.1	.1	.1
CaO	12.5 (12.0–12.7)	12.5	11.9	12.4	12.2 (11.9–12.3)	12.6	12.4	11.7
Na_2O	1.8 (1.4– 2.0)	1.7	3.4	1.3	2.9 (2.8– 3.0)	1.4	.8	3.0
K_2O	.5 (.2– .6)	.9	.5	.2	.4 (.2– .6)	.1	.2	.2
Cr_2O_3	.5 (.0– 1.1)	1.2	.1	.4	.6 (.1– .9)	.3	.2	1.0
NiO	–	–	–	–	.1	.1	–	.1
	97.0	97.7	97.2	97.6	97.3	97.7	97.0	97.6

numbers of cations on basis of 23 O:

	a	b	a	b	a	b	a	b	a	b	a	b	a	b	a
Si	6.37	6.32	6.37	6.33	5.88	5.78	7.19	7.21	6.16	6.11	7.18	7.20	7.02	7.03	6.02
Al^{IV}	1.63	1.68	1.63	1.67	2.12	2.22	.81	.79	1.84	1.89	.82	.80	.98	.97	1.98
Al^{VI}	.62	.75	.63	.74	.68	.85	.34	.42	.60	.72	.11	.22	.39	.52	.40
Ti	.06	.07	.05	.06	.12	.13	.02	.02	.10	.10	.01	.01	.04	.04	.50
Cr	.06	.06	.13	.14	.01	.01	.04	.05	.07	.07	.03	.04	.02	.02	.11
Fe^{3+}	.46		.36		.50		.30		.40		.46		.50		–
Fe^{2+}	.06	.50	–	.35	–	.48	.17	.46	.11	.49	–	.45	.12	.60	.61
Mg	3.73	3.60	3.82	3.70	3.68	3.52	4.12	4.05	3.70	3.59	4.36	4.25	3.91	3.80	3.35
Mn	.01	.01	–	–	.01	.01	.01	.01	.01	.01	.01	.01	.01	.01	.01
Ni	–	–	–	–	–	–	–	–	.01	.01	.01	.01	–	–	.01
Y site	5.00	4.99	4.99	4.99	5.00	5.00	5.00	5.01	5.00	4.99	4.99	4.99	4.99	4.99	4.99
original Y excess		.13		.11		.16		.09		.11		.15		.14	.00
Ca	1.90	2.05	1.88	2.00	1.81	1.99	1.85	1.94	1.86	1.98	1.87	2.04	1.85	2.03	1.80
Na	.49	.53	.46	.49	.94	1.03	.35	.37	.80	.85	.38	.41	.23	.24	.83
K	.09	.10	.16	.17	.09	.10	.04	.04	.07	.08	.02	.02	.04	.04	.04

$\dfrac{100\ Mg}{Mg + Fe}$	87.8	91.4	88.0	89.8	87.9	90.5	86.3	84.4

a)   all $Mg + Fe + Mn + Ni$ in Y site
b)   recalculated after subtraction of cummingtonite molecule (= excess of $Mg + Fe + Mn + Ni$ in Y site)

Amphiboles from Cabo Ortegal rocks:
1.   average and range of 13 amphiboles from spinel-pargasite peridotites and garnet-bearing veins/bands
2.   spinel-pargasite peridotite (FCM 1)
3.   spinel sensu stricto clinopyroxenite (R 378)
4.   amphibolized pyroxenite (MP 20)
Amphiboles from the Mellid area:
5.   average and range of 3 amphiboles from spinel-pargasite peridotites
6.   chlorite-amphibole peridotite (96-D2-5)
Amphiboles from the Santiago area:
7.   spinel-hornblende peridotite (95-A4-51)
Amphiboles from the Castriz area:
8.   wehrlite (FW 897)
9.   item (FW 898)
10.   amphibole peridotite (FW 894)
11.   olivine gabbro (FW 850a)
12.   item

9	10	11	12
41.0	47.9	43.0	55.7
13.2	7.4	16.3	.5
4.5	.4	2.1	–
16.0	20.3	14.2	20.1
1.1	4.7	–	5.0
4.7	–	7.0	3.3
.1	.1	.1	.1
11.2	12.0	11.7	12.6
3.7	2.8	2.9	.1
.3	–	.7	–
.9	.7	–	–
–	.1	–	–
96.7	96.4	98.0	97.4

a	b	a	b	a	a	b
5.97	5.95	6.81	6.80	6.15	7.80	7.88
2.03	2.05	1.19	1.20	1.85	.08	.09
.23	.26	.05	.16	.90	–	–
.49	.50	.04	.05	.23	–	–
.10	.11	.08	.09	–	–	–
.12		.50		–	.52	–
.57	.69	–	.49	.84	.39	.90
3.47	3.44	4.30	4.19	3.03	4.19	4.12
.01	.01	.01	.01	.01	.01	.01
–	–	.01	.01	–	–	–
4.99	5.01	4.99	5.00	5.01	5.11	5.01
	.04		.16	.00		.15
1.75	1.78	1.83	1.99	1.79	1.89	2.06
1.04	1.07	.77	.84	.80	.03	.03
.06	.06	–	–	.13	–	–
83.4		89.6		78.2	82.2	

Table III-11. Electron microprobe analyses of chlorites, högbomites and ilmenites.

	chlorites					högbomites			ilmenites	
	1	2	3	4		5	6		7	8
SiO_2	30.8	29.1	29.5	31.1		–	–		–	–
TiO_2	.1	.1	.1	.1		8.2	7.2		52.3	54.1
Al_2O_3	20.8	20.8	19.9	17.6		60.7	61.2		.2	n.d.
Fe_2O_3									3.2*	
FeO	3.5	3.7	3.6	3.4		10.7	13.3		35.3	42.2
MnO	–	–	n.d.	n.d.		.1	.1		1.0	.6
MgO	32.6	31.9	32.4	32.6		17.1	16.8		7.9	3.0
Cr_2O_3	.2	.1	1.0	.1		2.1	.6		.3	n.d.
NiO	–	.2	n.d.	n.d.		.3	.5		n.d.	n.d.
	88.0	85.9	86.5	84.9		99.2	99.7		100.2	99.9

numbers of cations on basis of

	14 O					8 O			3 O	
Si	2.86	2.79	2.80	2.97						
Al^{IV}	1.14	1.21	1.20	1.03						
Al^{VI}	1.13	1.13	1.03	.95	Al	3.65	3.69			
Ti	.005	.005	.005	.005	Ti	.31	.28	Ti	.94	1.00
Cr	.02	.01	.11	.01	Cr	.08	.02	Fe^{3+}	.06	
Fe	.27	.30	.28	.35	Fe	.46	.57	Fe^{2+}	.71	0.87
Mg	4.49	4.53	4.57	4.64	Mn	.004	.004	Mn	.02	.01
Ni		.015			Mg	1.30	1.28	Mg	.27	.11
					Ni	.01	.02			
	9.915	9.99	9.995	9.955		5.814	5.864		2.00	1.99

* Fe_2O_3 calculated
n.d. not determined

Chlorites   – – $(Mg_{6-x-y}Fe^{2+}{}_yAl_x)(Si_{4-x}Al_x)O_{10}(OH)_8$:
1–2. garnet-bearing veins from Cabo Ortegal (R 139 and MP 14, respectively)
3–4. spinel-pargasite peridotites from Cabo Ortegal (BU 2 and HK 18, respectively)

Högbomites   – – $R^{2+}{}_{1.0–1.6}Ti^4{}_{.2–.4}R^{3+}{}_{3.7–4.3}O_{7.6–8.0}(OH)_{0–0.4}$:
5–6. garnet-bearing veins from Cabo Ortegal (R 1 and MP 14, respectively)

Ilmenites   – – $(Mg, Fe^{2+}, Mn, Ni)(Ti, Fe^{3+}, Al, Cr)O_3$:
7. garnet-bearing vein from Cabo Ortegal (R 139)
8. spinel-hornblende peridotite from the Santiago area (95-A4-51)

APPENDIX 2

FIGURES
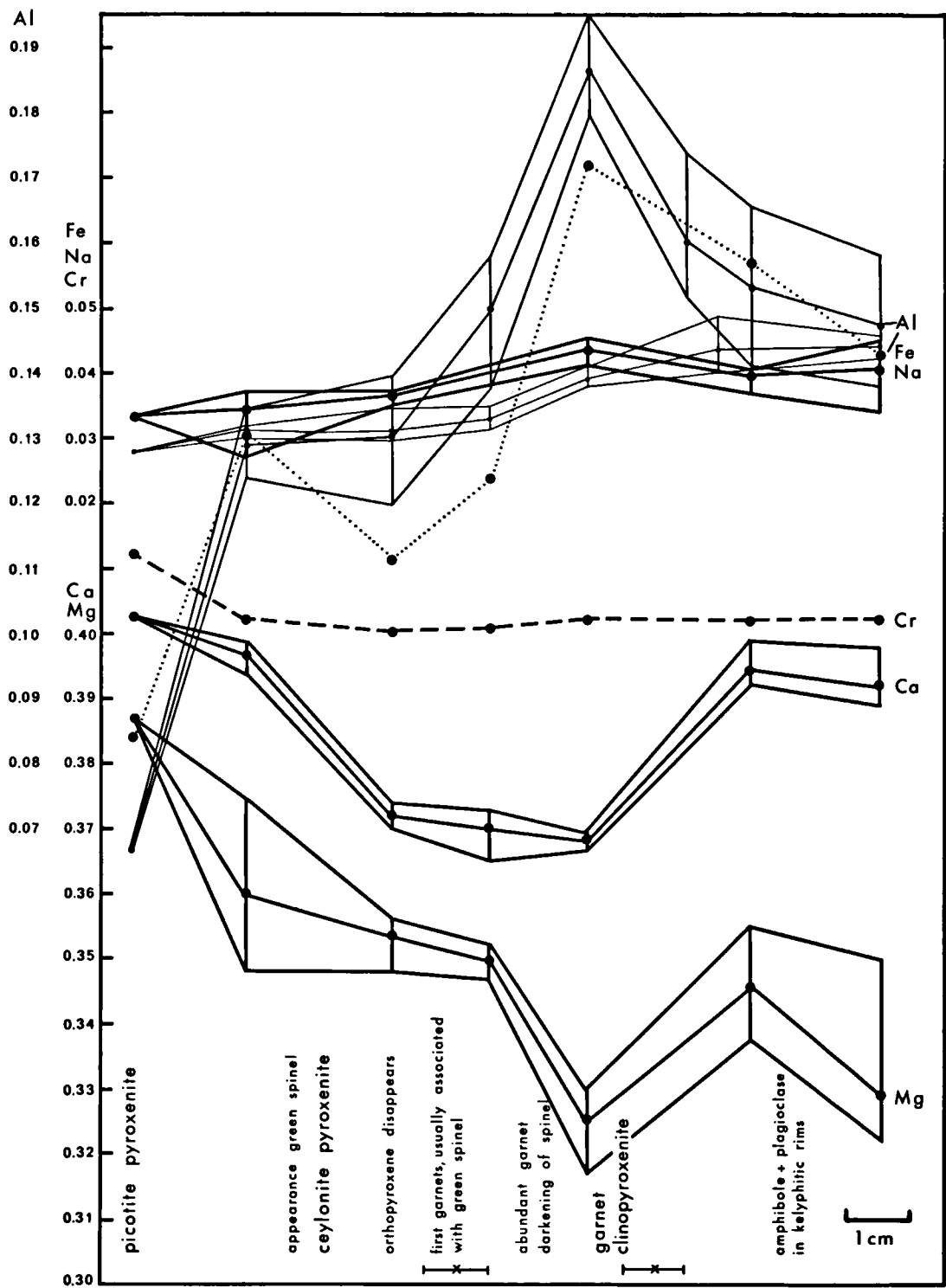
Fig. III-1. Atomic proportions of clinopyroxenes from a composite dyke in the lherzolite of Lers (sample AL-L-54).
Three grains were usually measured at approximately equal distances along the profile in the vein; average and range of the compositions are given.
Alumina has been measured twice.
Compositions of the various spinels occurring in this dyke are plotted in Fig. III-5.
The position of the analysed garnets is indicated (|⊸×⊸|) on the horizontal scale.
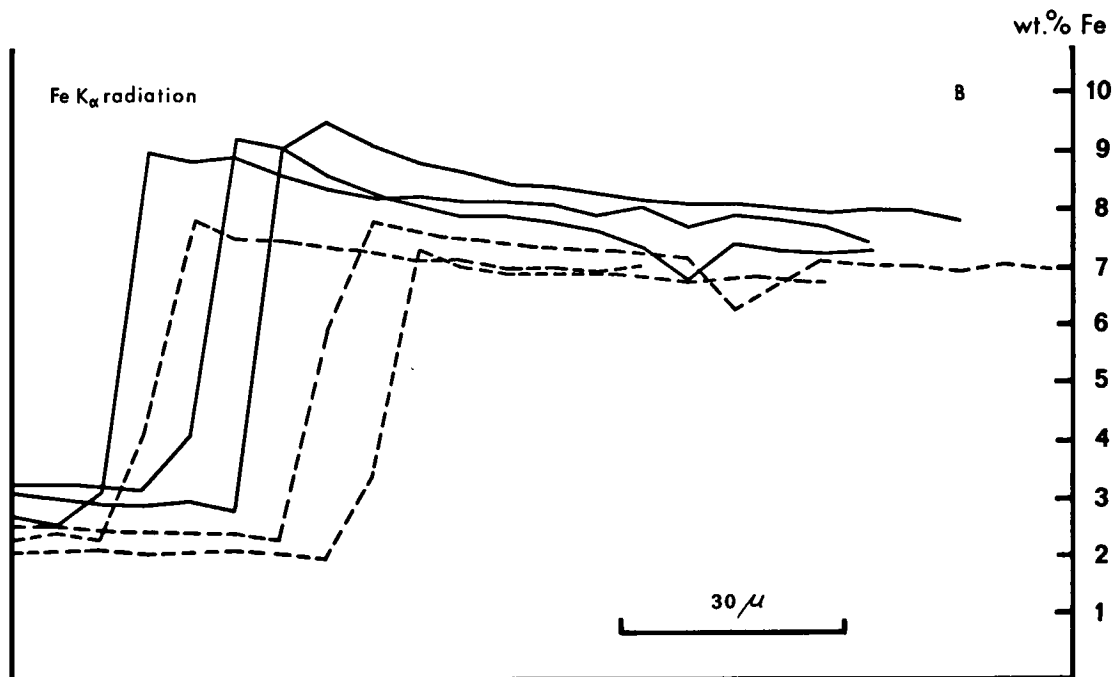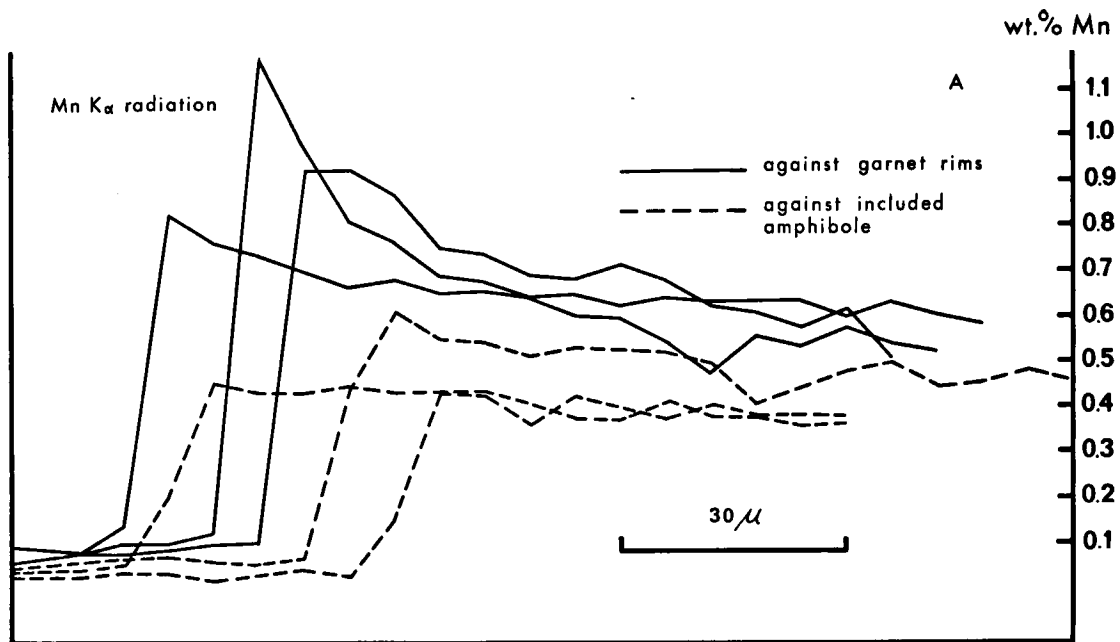
Fig. III-2. Step-scanning profiles across garnet borders, sample 4 M 4 – spinel-pargasite peridotite from the Mellid area with garnet-bearing bands.
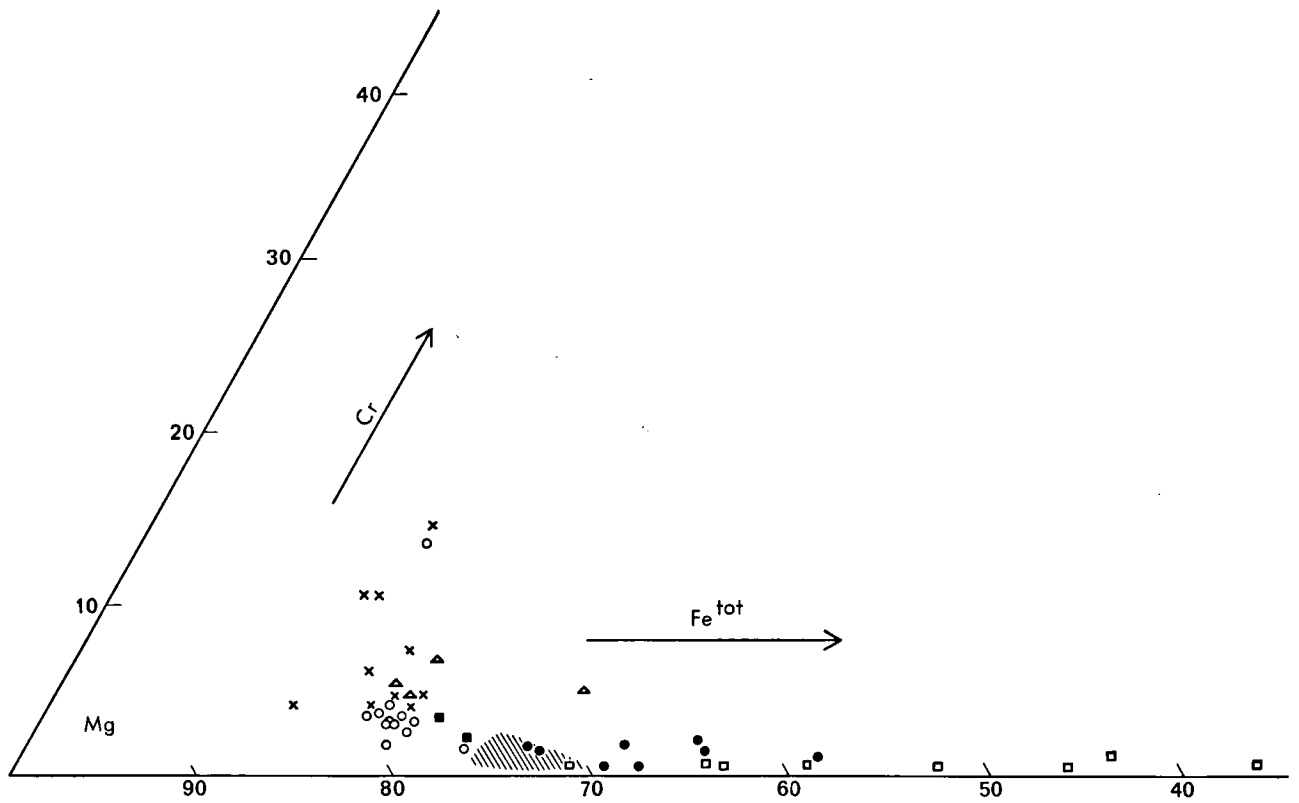
Fig. III-3. Mg:Fe^{tot}:Cr plot of garnet compositions (after Carswell, 1968a).

hatched area — Galician garnet-bearing assemblages
triangles — Ugelvik garnet peridotites
open circles — Bohemian garnet peridotites
solid circles — Kalskaret and Almklovdalen garnet peridotites
solid squares — Bellinzona garnet peridotites
open squares — Eclogite nodules from kimberlite pipes
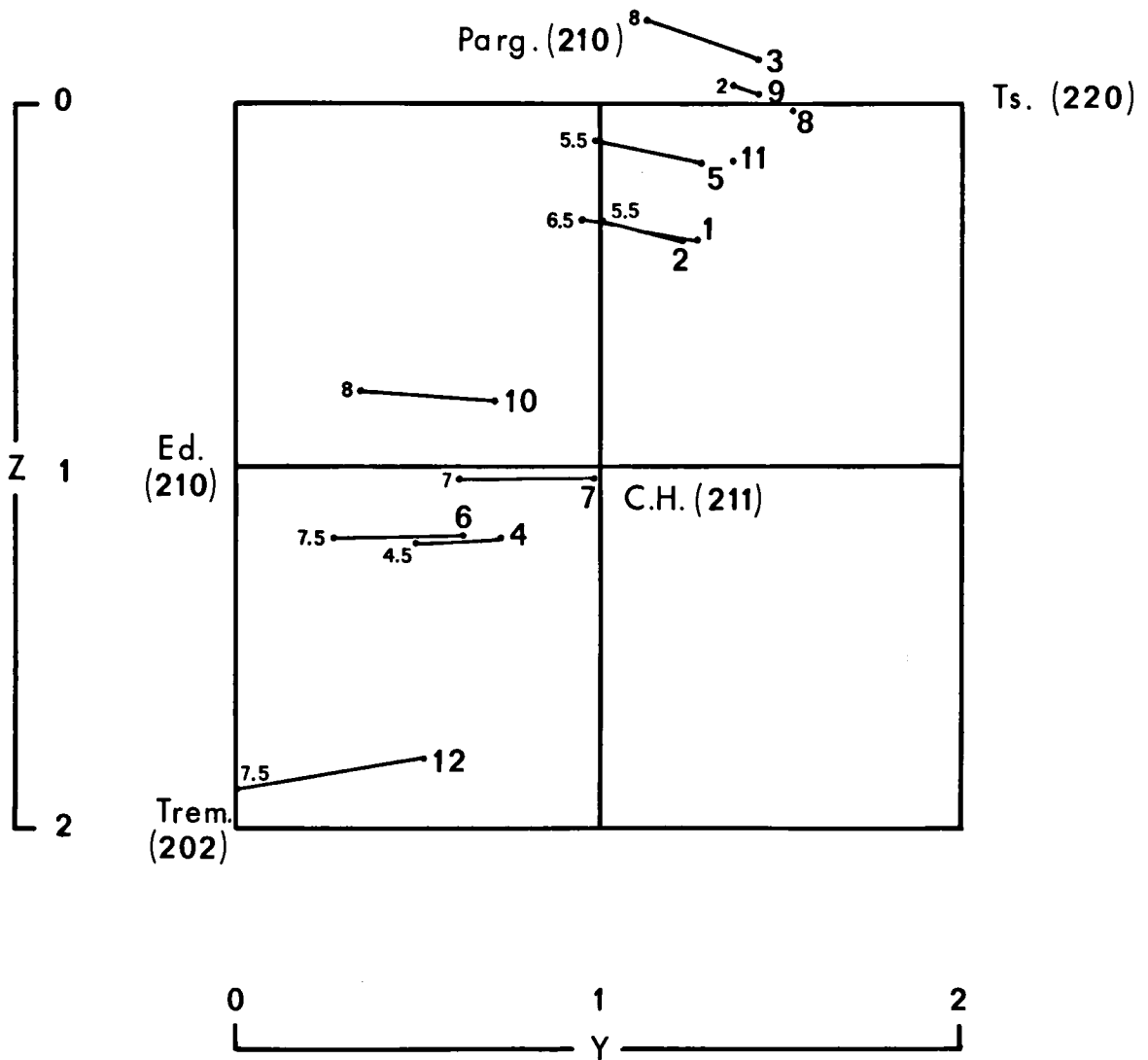
Fig. III-4. yz coordinates of analysed amphiboles (Table III-10), after Whittaker (1968).
y = number of $Al^{VI} + Fe^{3+} + Cr + 2 Ti$
z = number of Si in excess of 6.00
lines connect amphibole analyses calculated according to method 1 (left) and method 2 (right); amounts of cummingtonite molecule are given at the left end.

spinel chrom-spinel

light-
green

light-
brown

$\bullet$ Mg/Mg+Fe^{2+}
$\bullet$ Mg/Mg+Fe^{tot}

0.75

ceylonite picotite

brown

bg

dark-
green

pleonaste chrom-pleonaste

0.50

(bg) brownish green to
(gb) greenish brown

0.25

0 0.25 0.50 0.75

$\bullet$ Cr+Fe^{3+}/Cr+Fe^{3+}+Al
$\bullet$ Cr/Cr+Al
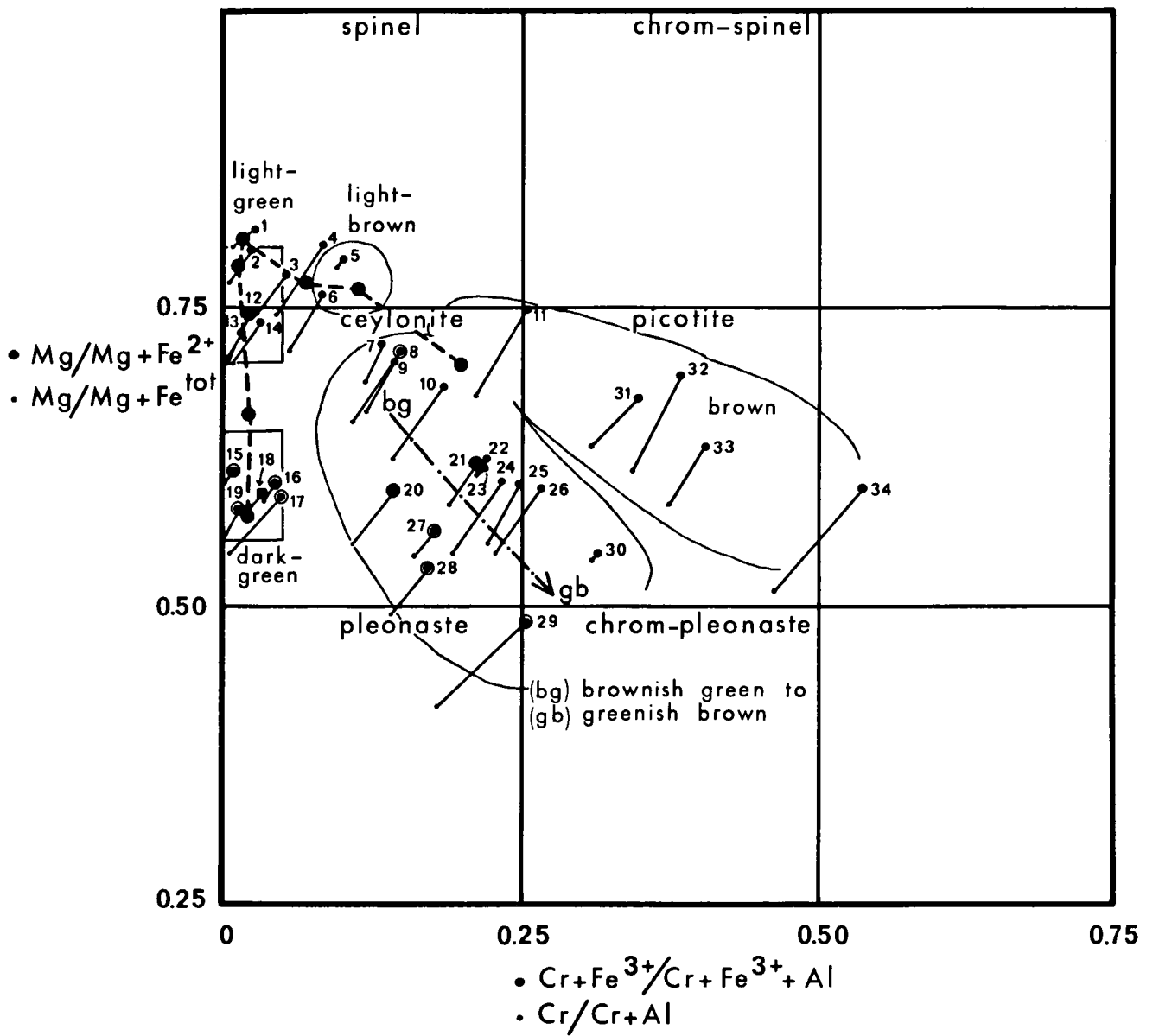
Fig. III-5. Plot of spinel compositions.
Spinels from Cabo Ortegal rocks:
spinel-pargasite peridotites: 10, 24, 26, 31, 33, 34
garnet-bearing veins: 1, 4, 9, 11, 13, 14, 22, 23, 25, 30, 32
spinel sensu stricto clinopyroxenite: 2,3
brown ceylonite orthopyroxenite: 7
Spinels from the Mellid area:
garnet-bearing bands: 5,6
Spinels from the Santiago area:
spinel-hornblende peridotite: 18
Spinels from the Castriz area:
spinel-clinopyroxene peridotite: 8
wehrlites: 15, 16, 20, 21, 27, 28, 29
gabbros: 17, 19
spinel-garnet clinopyroxenite band: 12
variations in spinel compositions in composite dyke in lherzolite of Lers:

olivine-garnet peridotite-liquid
control line in advanced
partial melting

plane of critical under-
saturation of silica
or olivine-gabbro
thermal divide

garnet-pyroxene
plane or eclogite
divide

Galician rocks

A

Beni Bouchera,
Totalp

B

Kalskaret

C

Various rocks

D

Fig. A-IV-1. Rock compositions plotted in the system C_3A-M-S (projected from or towards clinopyroxene CMS_2), after O'Hara (1968).

Heavy lines with dots indicate liquid B compositions: from left to right, at 15, 20 and 30 kb, respectively.

Outlined areas represent peridotites (nrs. 4–12 and 26) and garnet-bearing veins (nrs. 13–22) in Fig. A-IV-1a, peridotites (nrs. 10–13) in Fig. A-IV-1b.

G, D and P (in Fig. A-IV-1a) are the projections of the averaged garnet, diopside and pargasite compositions, respectively.

Fig. A-IV-2. Rock compositions plotted in the system C_2S_3-M_2S-A_2S_3 (projected from or towards orthopyroxene MS), after O'Hara (1968).

Heavy lines with dots indicate liquid B compositions: from above to below, at 15, 20 and 30 kb, respectively.

Outlined areas represent peridotites (nrs. 4–12 and 26) and garnet-bearing veins (nrs. 13-22) in Fig. A-IV-2a, peridotites (nrs. 10–13) in Fig. A-IV-2b.

G, D and P (in Fig. A-IV-2a) are the projections of the averaged garnet, diopside and pargasite compositions, respectively.
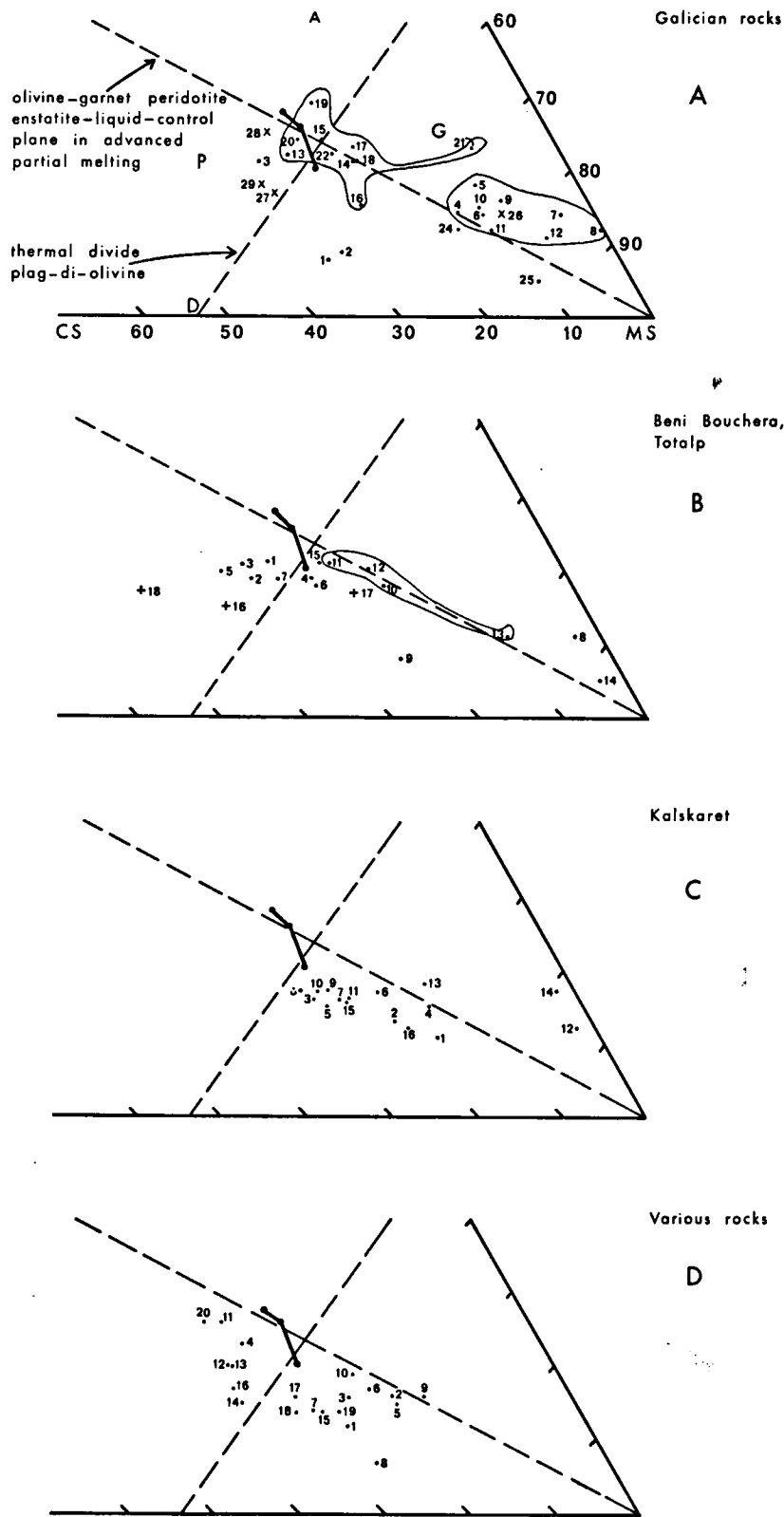
Fig. A-IV-3. Rock compositions plotted in the system CS-MS-A (projected from or towards olivine M_2S), after O'Hara (1968). Heavy lines with dots indicate liquid B compositions: from above to below, at 15, 20 and 30 kb, respectively.
Outlined areas represent peridotites (nrs. 4–12 and 26) and garnet-bearing veins (nrs. 13–22) in Fig. A-IV-3a, peridotites (nrs. 10–13) in Fig. A-IV-3b.
G, D and P (in Fig. A-IV-3a) are the projections of the averaged garnet, diopside and pargasite compositions, respectively.

List of rocks plotted in Figs. IV-6, IV-8, A-IV-1, A-IV-2 and A-IV-3.

Galician rocks (Analyses and rock names given in Tables III-1, III-2 and III-3)
1. MP 20
2. MP 21
3. R 378
4. 1 M 9
5. V 1405b
6. MP 16
7. V 3
8. 2 M 2
9. R 70
10. 4 M 1
11. FCM 1
12. 6 M 2
13. MP 28
14. MP 14
15. PC 5
16. V 1403AH
17. MP 10
18. L 14
19. L 6
20. L 4
21. L 3
22. average garnet-bearing vein
24. V 1403b
25. MP 18

Castriz rocks:
×26. FW 928
×27. FW 769
×29. FW 753
×29. FW 848

Beni Bouchera and Totalp rocks
1. M 6-79   garnet pyroxenite
2. M 7-58   composite layer of pyroxenite ± garnet
3. M 5-43   garnet pyroxenite
4. M 7-70   composite layer (middle section: websterite)
5. M 7-70   composite layer (central section: garnet pyroxenite)

6. M 6-129   garnet websterite
7. M 5-40   kelyphitized garnet pyroxenite
8. M 7-70   composite layer (external section: ortho-pyroxenite)
9. M 5-103   websterite
10. M 5-97   peridotite
11. M 5-102   peridotite
12. M 6-228   serpentinized peridotite
13. M 6-128   peridotite
14. M 6-78   enstatitite (calculated)
15. M 5-367   garnet pyroxenite
+16. TP 332   picotite pyroxenite
+17. TP 338   ceylonite pyroxenite
+18. TP 458   pyrope-ceylonite pyroxenite

nrs. 1–15 represent samples from Beni Bouchera (Kornprobst, 1969)
nrs. 16–18 are samples from Totalp (Peters, 1963)
rock names are copied from the authors; the term pyroxéno-lite (used by Kornprobst, 1969) has been replaced by pyroxenite

Kalskaret rocks
1. N 21   garnet dunite
2. N 23   garnet websterite
3. N 26   garnet wehrlite
4. T 96   garnet lherzolite
5. T 97   garnet wehrlite
6. T 150   amphibolized garnet peridotite
7. T 151   garnet lherzolite
8. T 152   garnet wehrlite
9. T 153   garnet websterite (assumed liquid composition)
10. T 154   garnet wehrlite
11. T 155   amphibolized garnet peridotite
12. T 156   dunite
13. T 200   peridotite
14. T 268   dunite
15. T 100   altered garnet? periodtite
16. T 162   amphibolized garnet peridotite

nrs. 1–3 are derived from Mercy & O'Hara (1965), nrs. 4–16 from Carswell (1968b).

Various rocks

	name	locality	reference
1. N 69	garnet lherzolite	Lien	Mercy & O'Hara (1965)
2. N 70	garnet lherzolite	Lien	Mercy & O'Hara (1965)
3. N 71	garnet websterite	Lien	Mercy & O'Hara (1965)
4. N 75	garnet-Cr-diopside rock	Rödhaugen	Mercy & O'Hara (1965)
5. N 76	garnet lherzolite	Rödhaugen	Mercy & O'Hara (1965)
6. N 77	garnet-olivine websterite	Rödhaugen	Mercy & O'Hara (1965)
7. –	Rödhaugen eclogite (calculated)	Rödhaugen	Mercy & O'Hara (1965)
8. U 6	garnet peridotite	Ugelvik	Carswell (1968a)
9. U 8	garnet peridotite	Ugelvik	Carswell (1968a)
10. IV	eclogite in peridotite	Alpe Arami	O'Hara & Mercy (1966)
11. V	kyanite eclogite	Alpe Arami	O'Hara & Mercy (1966)
12. –	eclogite	Mitterbachgraben	Kappel (1967)
13. –	eclogite	Meidling im Tal	Kappel (1967)
14. 1	'eclogite' (calculated)	Salt Lake Crater	Jackson (1966)
15. 3	'eclogite'	Salt Lake Crater	Jackson (1966)
16. C	garnet pyroxenite	Salt Lake Crater	Green (1966)
17. 1	'eclogite'	Salt Lake Crater	Ravier (1964)
18. 2	ariegite	Lers	Ravier (1964)
19. 1	garnet-spinel pyroxenite	Hoggar	Girod (1967)
20. VI	kyanite eclogite	Alpe Arami	O'Hara & Mercy (1966)

1) Samples 1–9 represent Norwegian rocks.
2) The kyanite eclogites, nrs. 11 and 20, occur at the margins of the Alpe Arami garnet peridotite; due to poor exposures their association with the ultramafic rocks is not clear.
3) Eclogites 12 and 13 occur as lenses within serpentinized garnet peridotites. Garnets are pyrope-rich (54–59%), clinopyroxenes contain small alkali-pyroxene components. Kappel admits that these rocks should be called garnet pyroxenites;

on historical reasons the name eclogite was, however, maintained.
4) The eclogites from Salt Lake Crater should be called garnet pyroxenites, as has been argued by Green (1966) and Ravier (1964); they are found as xenoliths in Hawaiian basalts.
5) The garnet-spinel pyroxenite, nr. 19, is found as enclaves in alkali basalts in the volcanic area of Atakor (Hoggar, Central Sahara); the French term pyroxénolite has been replaced by pyroxenite.

Notes ad Fig. IV-8.
Some data about rocks and minerals plotted in Fig. IV-8.

Rock	100 Mg/ Mg + Ca + Fe + Mn	wt.% Al_2O_3 rock	wt.% Al_2O_3 clinopyroxene	wt.% Na_2O clinopyroxene	wt.% Cr_2O_3 garnet
V 9	83	6.27	3.26	2.28	2.32
K 4	74	6.44	3.08	1.84	0.84
V 1	74	6.68	2.15	1.34	2.15
K 3	73	5.81	2.71	1.50	0.91
V 2	72	10.65	2.69	1.20	0.95
V 8	69	3.70	0.95	0.56	2.30
Gal	69	13.39	1.90	0.10	0.40
K 2	65	8.55	2.43	1.05	0.39
V 3	62	12.23	1.66	1.01	0.32
V 19	56	8.08	6.54	1.14	0.29
V 13	54	16.48	10.01	1.58	n.d.
K 9	52	11.58	2.94	2.15	–
BB 18	48	11.9	9.6–5.5	1.3–1.0	–
V 12	47	16.65	9.33	1.98	n.d.
BB 1	47	15.25	4.88	1.58	0.88
SH	45	10.88	6.20	1.55	0.39
BB 3	41	15.38	7.08	1.74	0.33
BB 15	40	15.19	5.01	1.28	0.33
BBx	39	11.65	8.52	2.02	0.15

APPENDIX 3

PLATES

Ia. Garnet-bearing veins at the Limo.

Ib. Isoclinal folding in the spinel-pargasite peridotite from the Mellid area.

PLATE I

IIa. Garnets in the spinel-pargasite peridotite from the Mellid area (parallel to the foliation).

IIb. Garnet eye in the spinel-pargasite peridotite from the Mellid area (perpendicular to the foliation).

PLATE II
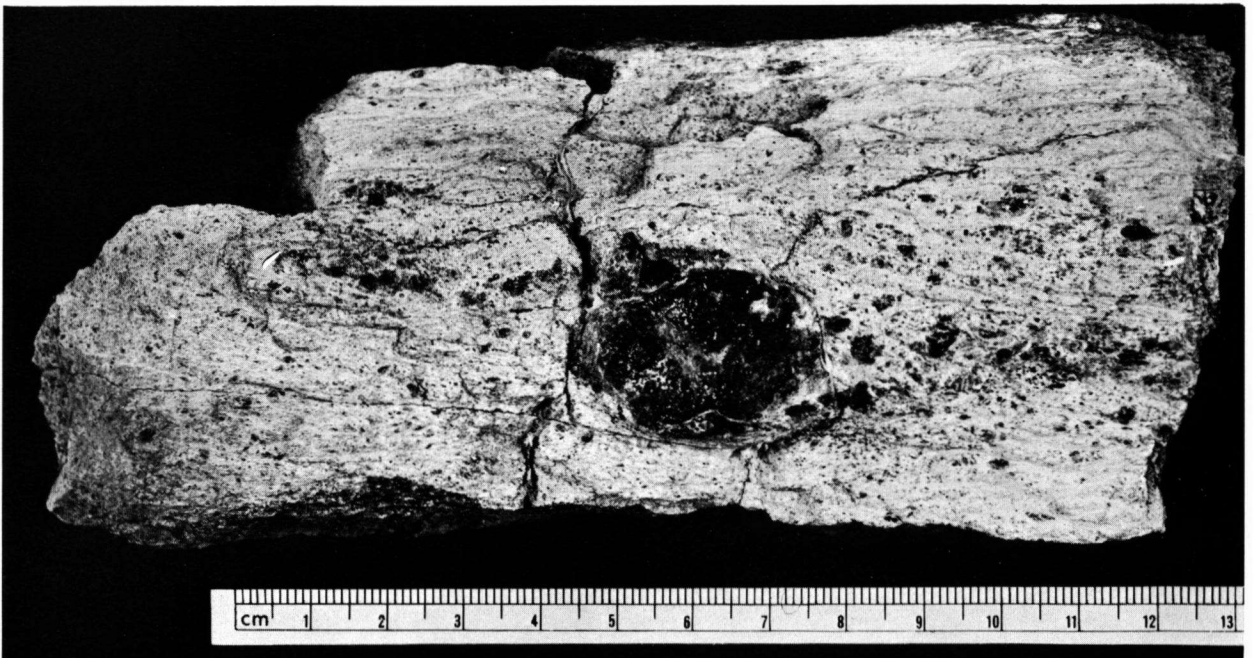
IIIa. Intersecting garnet-bearing veins from Cabo Ortegal.

IIIb. Spinel-pargasite peridotite with garnet eye from the Mellid area. Thin section 1 M 3.

IIIc. Backscattered electron picture of a spinel-pyroxene kelyphite between garnet and aluminous orthopyroxene. Brightness is directly proportional to the mean atomic number of the various mineral phases. The picture is somewhat disturbed by electronic noise. Thin section 4 M 3.
g = garnet
c = clinopyroxene
o = orthopyroxene

IIId. Ca X-ray emission picture of the area in Plate IIIc. A grain of apatite is present at the garnet border.

PLATE III
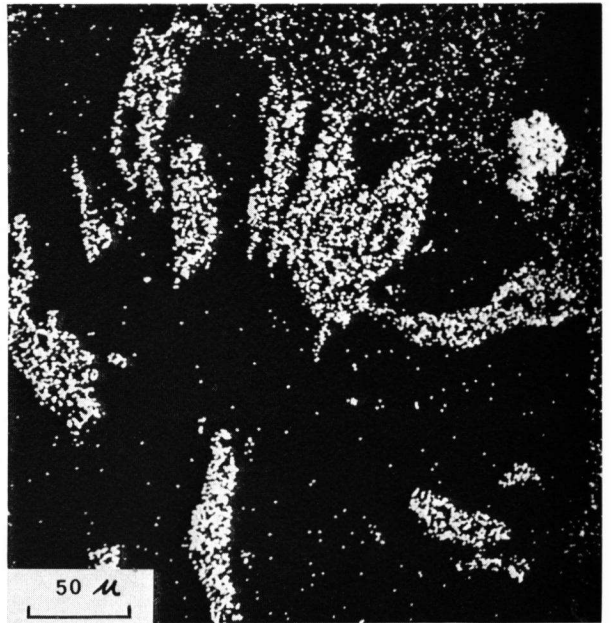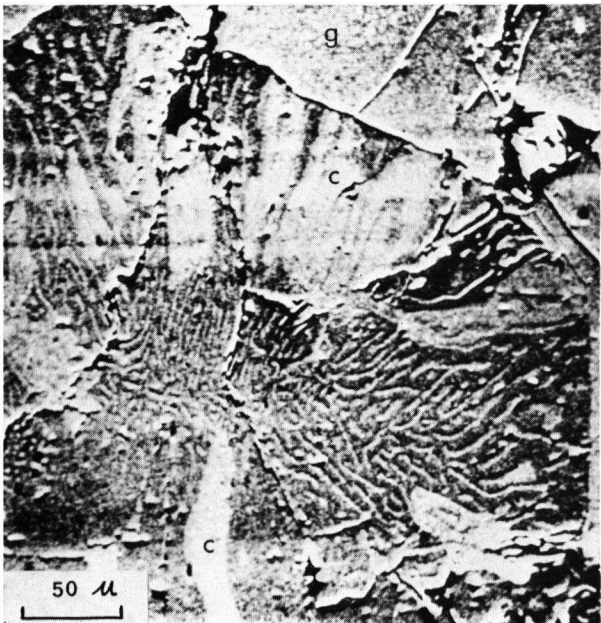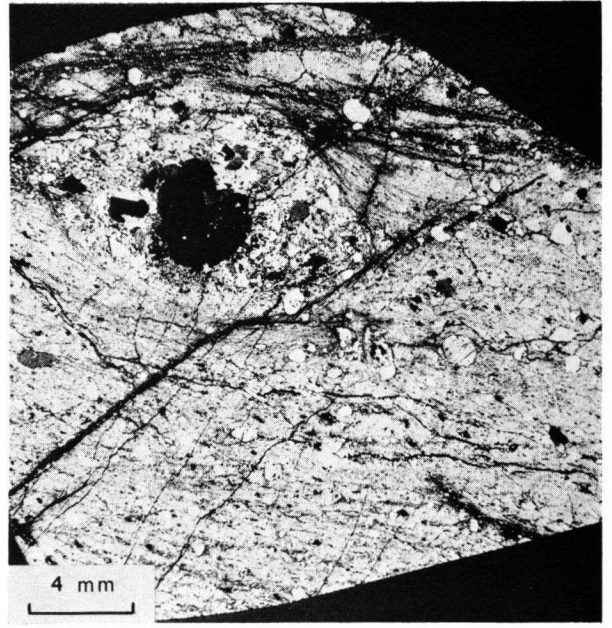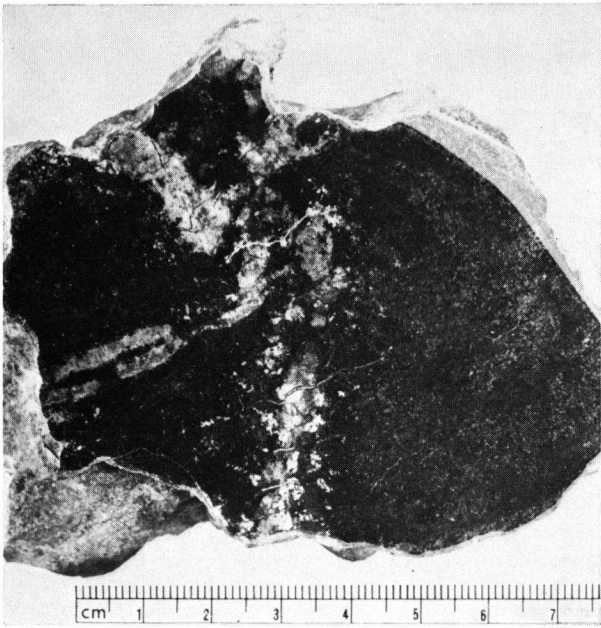
IVa. Backscattered electron picture of a complex spinel-pyroxene kelyphite between garnet and olivine.
Brightness is directly proportional to the mean atomic number of the various mineral phases. The picture is somewhat disturbed by electronic noise. Thin section 5 M 2.
g = garnet
c = clinopyroxene
a = amphibole
ol = olivine

IVb. Ca X-ray emission picture of the area in Plate IVa. The difference in Ca content between amphibole and clinopyroxene is evident.

PLATE IV

100 𝓊

100 𝓊
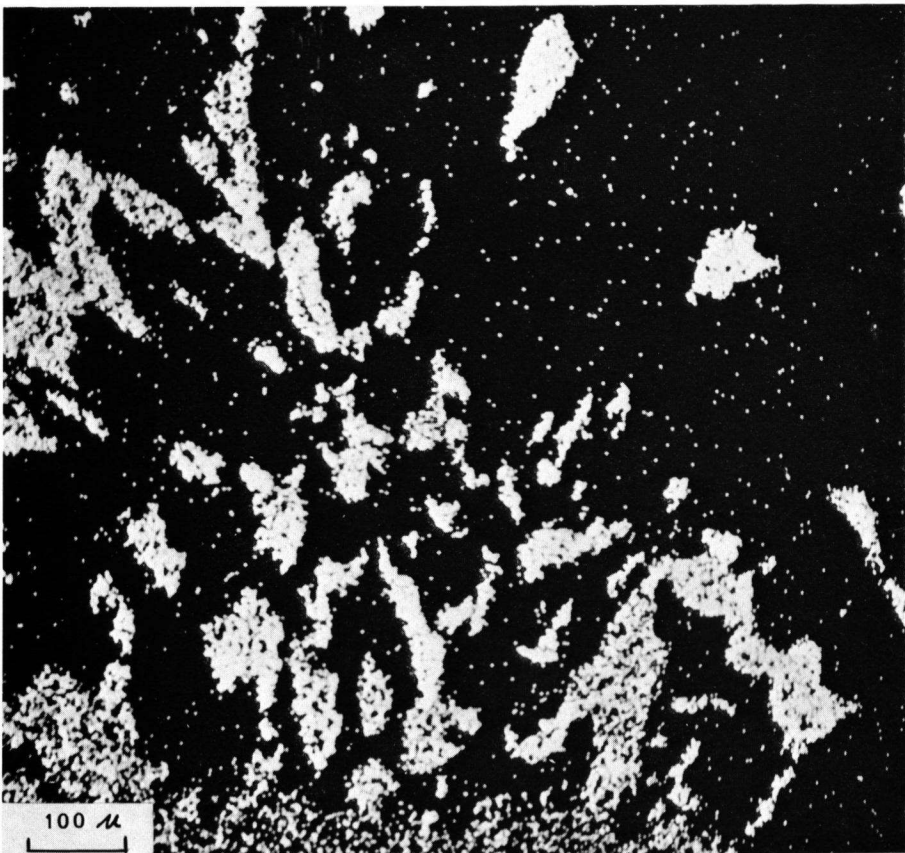
Va. Backscattered electron picture of the left top corner of Plate IVa.
o = orthopyroxene
c = clinopyroxene
s = spinel

Vb. Spinel-amphibole kelyphite. Thin section BU 3.
g = garnet
o = orthopyroxene
s = spinel

Vc. Al X-ray emission picture of the area in Plate Vb.

Vd. Ca X-ray emission picture of the area in Plate Vb.

PLATE V
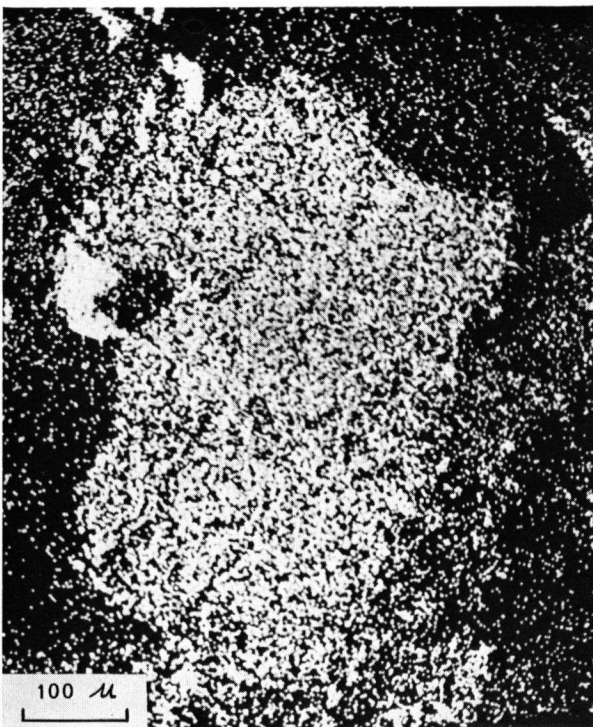
VIa. Högbomite around spinel, included in garnet. Thin
section MP 14.
g = garnet
s = spinel
a = amphibole
c = chlorite
h = högbomite

VIb. Continuous scanning profiles for Mg, Fe, Mn and Ca
radiation across a remnant of garnet included in amphibole.
Thin section MP 28.
Contents of these elements are given in Table III-9.

PLATE VI

200 μ

Mg

Fe

Mn

Ca

10 μ